Charles University

Faculty of Science

Department of Physiology

Study programme: Animal physiology

Nikhil Ahuja

Hippocampal neuronal representation of a moving object in a novel spatial avoidance task

Hipokampální neuronální reprezentace pohybujícího se objektu v nové úloze vyhýbání se prostoru

Doctoral thesis

Supervisor: Professor Aleš Stuchlík, Ph.D.

Consultant: Dr. Eduard Kelemen, Ph.D.

Prague, 2021

Prohlášení autora

Prohlašuji, že tato práce je mojí prací provedenou pod vedením prof. Aleše Stuchlíka a Dr. Eduarda Kelemena. Tato práce neobsahuje moji předchozí práci ani práci jiných lidí bez jejich uvedení. Řádně jsem uvedl a citoval všechny zdroje a literaturu použitou k přípravě této práce. Tato práce ani její podstatná část nebyla předložena k získání tohoto nebo jiného akademického titulu.

V Praze ……

Nikhil Ahuja

Prohlášení spoluautora

Jménem všech spoluautorů tímto prohlašuji, že Nikhil Ahuja zásadně přispěl k přípravě článků a souvisejícího materiálu, který je nedílnou součástí této práce. Samostatně provedl experimenty uvedené v této práci a uvedl výzkumné články, kde je uveden jako první autor, vzniklé pod mým vedením a vedením Dr. Eduarda Kelemena. Významně také přispěl u výzkumných článků, ve kterých byl jedním ze spoluautorů.

V Praze ……

Aleš Stuchlík, Ph.D.

Acknowledgment

First and foremost, I would like to thank my parents, Mr. Anil Ahuja and Mrs. Veena Ahuja for their love and support throughout my Ph.D. studies. They always encouraged me to work hard, especially, when things did not go well and pushed me further to excel. One phrase I will always remember from my mother is “this journey could be long and arduous but you should never give up and complete it.” I would like to thank my wife, Shiyana who became a part of my life during the last years of my Ph.D. studies. Nevertheless without her help and understanding I would not be here. I would further like to thank my younger sister, Pritika, for her love and help that always made me feel that I was not far away from my family.

Since the start of my Masters, I was always fascinated by how neurons communicate in the brain. Thanks to my classmate and a long-time friend, Ali Danish Zaidi, and my senior Apoorv Sharma who introduced me to the amazing world of neuroscience. During my early college years, I was fascinated by learning and memory, which led me to read and explore long-term potentiation studies. This is when I first got to know about electrophysiology. During my short stay at the National Brain Research Center, Manesar, India, I learnt about place cells. I still remember how I felt when I got to know about this phenomenon. It was a wow moment and I asked myself how much more clearly we know of a phenomenon where we know exactly what the electrical activity in the brain is coding. It was this day when I decided that I would do my doctoral study on place cells. I believe my desire to work on place cells brought me to Prague.

It’s true that time flies when you enjoy what you do and know that your every step is taking you closer to your goal, that’s what I felt during the journey of my Ph.D. research work at the Institute of Physiology, Prague. For this, I would like to acknowledge my indebtedness and render my warmest thanks to my supervisors, Prof. Ales Stuchlik and Dr. Eduard Kelemen (Edo) for making this research work so much enjoyable under their friendly guidance and for their invaluable expert advice throughout all stages of the work. Their leadership qualities and positive outlook towards life have always motivated me and given me strength and temperament to deal with intricacies both at the professional and personal front. During my studies I have worked in close collaboration with Edo who agreed to mentor me on my electrophysiology study. I have learnt a lot from him and his experiences. I always felt lucky to have Ales and Edo together as my supervisors. Ales is an expert in animal behavior studies and Edo is an expert in electrophysiology studies. My Ph.D. study was based on both animal behavior and electrophysiology. My doctoral study required experience in both areas, so I always felt that I had the best of both worlds.

With a sense of regard and reverence I take this opportunity to express my deep sense of gratitude and heartfelt thanks to Dr. Karel Jezek, Biomedical Center, Pilsen, and Dr. Premsyl Jiruska who helped me in getting started with electrophysiology. I had a great learning experience with both of them. With Dr. Jiruska’s lab it continued well until the end of my Ph.D. which helped me to successfully execute my research work. I would like to thank lab members Jan Kudlacek and Jan Chvojka and other members of the epileptology lab. I would also like to thank Frantisek Zitricky from Dr. Karel Jezek’s lab in Pilsen for discussions about our lab life, work and weekend trips in the Czech Republic.

The most enjoyable part of my Ph.D. study has been meeting a wonderful group of fellow researchers. Firstly I would like to extend my appreciation to all the members of our research team and especially David, Enrico, Stepan, Honza, Jindra, Marketa, and Mrs. Markova. I would like to thank Misha, our animal house manager, for her assistance through the period of my Ph.D. I am also thankful to Helena, Dominika and Hanka for helping me orient around things when I first came to Prague.

My colleagues and friends outside our lab, including Prasoon, Shivam, Pasha, Jeet, Smriti, and friends from University of Delhi were always there when I needed them for any advice or help so I cannot thank them enough. I am also very thankful to the IT support team, Martin Andrew, Vaclav and Tomas, who were very helpful whenever we had a related issue.

Laboratory animals offer us the gift of knowledge. It's my moral obligation to appreciate every part of their sacrifice to unearth the facts which helped lay the necessary foundation for this research work.

This work was supported by the Czech Science Foundation (GACR) grants 17-04047S, 19-03016S, 20-00939S, and Czech Health Research Council (AZV) grant 17-30833A.

Again I would like to thank everybody who was an important part in the completion of this research work. Thank you all.

Date: **Nikhil Ahuja**

Abstract

In real world environments, animals need to organize their behavior relative to other moving animals or objects; when hunting a predator, when migrating in groups or during various social interactions. In all of these situations, the animal needs to orient relative to another moving animal/object. To understand the role of the hippocampus in this ability we adopted a two-step approach. We developed a task that would mimic important elements of this behavior in the laboratory. The task required the rats to assess not only their distance from the moving object but also their position relative to the object. We further studied how neurons in the hippocampal CA1 subfield encode the subject, the moving object and the environment in the behavioral paradigm and how do these representations interact among themselves.

In rats, we aimed to characterize spatial behaviors relative to moving objects and to explore the cognitive mechanisms controlling these behaviors. Three groups of animals were trained to avoid a mild foot-shock delivered in one of three positions: either in front, on the left side, or the right side of a moving robot. Using different variations of the task, we also probed whether avoidance was simply due to increased noise level or size of the retinal image or appearance of the robot.

As the hippocampus is believed to be the anatomical site combining what and where information about an experience. It has been hypothesized that what and where information reaches the hippocampus primarily via lateral entorhinal cortex (LEC) and medial entorhinal cortex (MEC), respectively (Hargreaves et al., 2005). It is also known that the distal region of the hippocampal CA1 subfield primarily receives direct inputs from LEC and the proximal region receives input from MEC (Witter et al., 2000). We thus hypothesized that input about what part of our behavioral paradigm, in this case, the moving robot, should be represented in the distal CA1. We, therefore, targeted our electrodes to this area in the hippocampus.

The main conclusions from these experiments are as follows:

1) Rats recognize geometrical spatial relationships relative to a moving object. We found that rats can learn to avoid the front or either side of a moving object.

2) This ability is not solely dependent upon retinal size, noise levels, or prominent visual marks on the object. By using an all-white version of the moving robot we observed that rats can perform similarly as with the black and white moving object.

3) Electrophysiology recording from trained and untrained rats indicated that the animal represented both the position of the rat in the room as well as a spatial relationship between the rat and robot, we observed different responses in the recorded cells. However, they did not cluster into different classes of cells.

4) Analysis of spatial parameters, like coherence and spatial information suggested subtle differences between spatial activity in trained and untrained rats.

Abstrakt

V reálném prostředí musí zvířata přizpůsobovat své chování jiným pohybujícím se zvířatům nebo předmětům; při lovu dravce, při migraci ve skupinách nebo při různých sociálních interakcích. Ve všech těchto situacích se zvíře musí orientovat vzhledem k jinému pohybujícímu se zvířeti/předmětu. Při studiu role hipokampu v těchto procesech jsme postupovali ve dvou krocích. Vyvinuli jsme behaviorální úlohu reflektující klíčové prvky tohoto chování v laboratorních podmínkách. Řešení úlohy vyžadovalo, aby testovaný potkan vyhodnotil nejen svoji vzdálenost od pohybujícího se objektu, ale také svoji polohu vzhledem k tomuto objektu. Dále jsme studovali, jak neurony v hipokampální oblasti CA1 v tomto behaviorálním paradigmatu kódují subjekt, pohybující se objekt a okolní prostředí a jak tyto reprezentace mezi sebou interagují.

Zaměřili jsme se na charakterizaci prostorového chování potkanů ve vztahu k pohybujícím se objektům a na prozkoumání kognitivních mechanismů regulujících toto chování. Tři skupiny zvířat byly natrénovány, aby se vyhýbaly mírnému elektrickému stimulu, který byl aplikován v jedné ze tří oblastí vůči pohybujícímu se robotovi: před robotem, po jeho levé nebo pravé straně. Pomocí různých modifikací úlohy jsme také zkoumali, zda k vyhýbání docházelo na základě vnímání zvýšené úrovně hluku, velikosti sítnicového obrazu nebo vzhledu robota.

Hipokampus je považován za anatomickou strukturu kombinující informace “co” a “kde” o konkrétní události. Byla vyslovena hypotéza, že informace “co” a “kde” vstupují do hipokampu primárně prostřednictvím laterální entorinální kůry (LEC), respektive mediální entorinální kůry (MEC) (Hargreaves et al., 2005). Je také známo, že distální část hipokampální oblasti CA1 primárně přijímá přímé vstupy z LEC a proximální oblast přijímá vstupy z MEC (Witter et al., 2000). Předpokládali jsme tedy, že informace “co”, v našem případě pohybující se robot, by měla být reprezentována v distální části CA1. Zaměřili jsme proto nahrávací elektrody na tuto oblast v hipokampu.

Hlavní závěry z těchto experimentů jsou následující:
1) Potkani rozpoznávají geometrické prostorové vztahy vzhledem k pohybujícímu se objektu. Prokázali jsme, že potkani se mohou naučit vyhýbat se přední nebo vybrané boční straně pohybujícího se předmětu.

2) Tato schopnost není závislá pouze na velikosti sítnicového obrazu, hladině hluku nebo výrazných vizuálních značkách na objektu. Prokázali jsme, že při použití bílé verze

pohybujícího se robota bez vizuálních značek potkani mohou úlohu řešit podobně jako při použití černobílého pohybujícího se objektu.

3) Nahrávání neurálních dat u trénovaných a netrénovaných potkanů naznačilo, že zvíře si utvořilo reprezentaci jak své vlastní polohy v místnosti, tak prostorového vztahu mezi sebou a robotem. Pozorovali jsme odlišné odpovědi mezi nahrávanými buňkami. Tyto buňky se však neshlukovaly do odlišných klastrů.

4) Analýza prostorových parametrů, jako jsou koherence a prostorové informace, naznačila mírné rozdíly mezi prostorovou aktivitou u trénovaných a netrénovaných potkanů.

Table of contents

List of figures and tables

Figures

Tables

List of Abbreviations

3D	3-dimensional
ACC	Anterior cingulate cortex
AVpr1b	Vasopressin 1b receptor
B&W	Black and white
CA	Cornu Ammonis
CDN	Car-dependent navigation
CMOR	Crossmodal object recognition
CSC	Complex spike cell
DG	Dentate gyrus
dLS	Dorsal lateral septum
EC	Entorhinal cortex
EEG	Electroencephalograph
Info	Information
ITT	Inferior temporal
LEC	Lateral entorhinal cortex
LFP	Local field potential
LIA	Large irregular amplitude
Max	Maximum dwell time (in behavioural heatmaps; B&W)
Max	Maximum firing rate (in spike ratemaps; colored)
ms	Milliseconds
mPFC	Medial prefrontal cortex
PF	Place field
PFC	Prefrontal cortex
PPC	Posterior parietal cortex
PRC	Perirhinal cortex
SIA	Small irregular activity
MEC	Medial entorhinal cortex
LS	Lateral septum
LV	Landmark vector
SEM	Standard error of mean
vCA1	Ventral CA1
vLS	Ventral lateral septum
VMHvl	Ventrolateral subnucleus of the ventromedial hypothalamus

List of publications

Doctoral thesis-related publications

Ahuja, N.*, Lobellová, V., Stuchlík, A., Kelemen, E. (2020). Navigation in a Space With Moving Objects: Rats Can Avoid Specific Locations Defined With Respect to a Moving Robot.

Frontiers in Behavioral Neuroscience. doi: 10.3389/fnbeh.2020.576350. IF = 2.512

*Contributed as the first author and was involved in study design, performed experiments, analysis and writing the paper

Svoboda, J., Lobellová, V., Popelíková, A., Ahuja, N.*, Kelemen, E., Stuchlík, A. (2017). Transient inactivation of the anterior cingulate cortex in rats disrupts avoidance of a dynamic object. Neurobiology of Learning and Memory. 139, 144-148. IF= 2.768

*Contributed as a co-author, assisted in the experiments

Other publications

Szczurowska, E., Ahuja, N.*, Jiruška, P., Kelemen, E., Stuchlík, A. (2018). Impairment of neural coordination in hippocampal neuronal ensembles after a psychotomimetic dose of dizocilpine. Progress in Neuro-psychopharmacology and Biological Psychiatry. 81, 275-283. IF= 4.361

*Contributed as a shared first author, performed experiments, analysis and edited the paper

Introduction

1.1 Hippocampal neuroanatomy

The hippocampus is a brain structure involved in many processes including spatial memory and navigation. Principal cells in the hippocampus have been found to encode a repertoire of variables, including spatial position (J. O'Keefe & Dostrovsky, 1971), time (MacDonald et al., 2011), the position of other moving objects (Danjo et al., 2018; Omer et al., 2018), etc. The hippocampus and its related structures are included under the umbrella term the hippocampal information. It includes CA1, CA2, CA3, dentate gyrus, subiculum, parasubiculum, presubiculum, entorhinal cortex (EC). In rodents, the hippocampus resembles a seahorse or banana-shaped structure. It extends from the midline close to the septal nuclei and runs as a C-shaped structure over and up to the back of the thalamus. The longitudinal axis is referred to as the septotemporal axis. It has been named Cornu Ammonis (CA) or Ammon's horn after an Egyptian mythological figure, hence the name of the subfields of the hippocampus CA1, CA2 and CA3. The CA regions are each composed of layers, stratum oriens, stratum pyramidale, stratum radiatum and stratum lacunosum moleculare (Tzakis & Holahan, 2019).

Unlike neocortex, the typical organizational feature within the hippocampal formation is its unidirectionality i.e. connections are not reciprocal. The main input to the hippocampus is from the superficial layers of the EC and the main output structure is the subiculum. The basic intrahippocampal circuitry is trisynaptic, consisting of three pathways, perforant pathway, mossy fibers and Schaffer collaterals. The perforant pathway consists of unidirectional projections from superficial layer II of the EC to the dentate gyrus (DG) and CA3 and layer III to CA1 and subiculum (figure 1.1A). The granule cells in the DG project to CA3 to form the mossy fiber pathway. The cells in CA3 project to CA1, which makes up the Schaffer collateral pathway (figure 1.1A and B).

The major fiber systems in the hippocampal formation are angular bundle, temporoammonic alvear pathway, fimbria-fornix and hippocampal commissures. The main route taken by projections from the ventrally situated EC to all septotemporal levels of the hippocampal subfields and DG is the angular bundle. At the temporal level, most of the EC projections to CA1 are through the perforant pathway. However, at the septal level, most of the EC projections to CA1 come via alvear pathway. The fimbria-fornix pathway comprises the projection and to and from the subcortical targets. They both carry projections from the hippocampus and subiculum. The fornix primarily carries projections

from the septal third. The commissural fiber is the third major fiber system in the hippocampal formation. This system carries fiber to the contralateral hippocampal formation.

The principal cell layer in the CA1 is the pyramidal layer. A relatively cell-free layer containing basal dendrites and lying deeper to the pyramidal layer is stratum oriens. This layer also contains various types of interneurons and some Schaffer collateral connections. Most of the CA3 to CA1 Schaffer collateral connections are located in the stratum radiatum, a superficial layer just above the pyramidal layer. Projections from the entorhinal cortex terminate just a layer above the radiatum, in stratum lacunosum moleculare. Both stratum moleculare and radiatum contain various types of interneurons (Cembrowski et al., 2016; Klausberger & Somogyi, 2008). The DG consists of three layers, molecular, granular and polymorphic cell layers. The molecular layer is a relatively cell-free layer and lies closest to the hippocampal fissure. The granular layer lies deeper to the molecular layer and contains granule cells, principal cells in the DG. The molecular and granule cell layers enclose the polymorphic cell layer. The most common cell type in the polymorphic layer is the mossy cell.

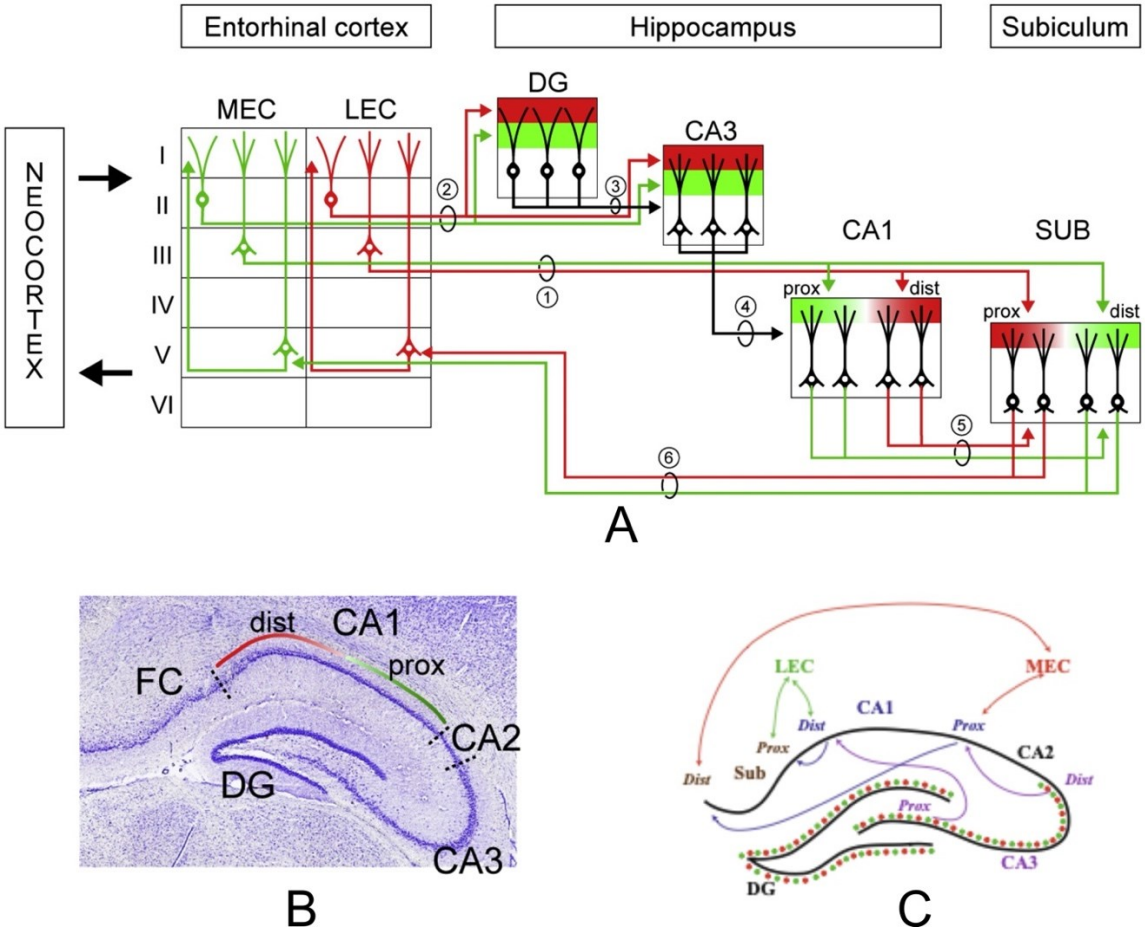

Figure 1.1. Schematic of major connections between the rat hippocampus, entorhinal cortex and subiculum, and Nissl stained section showing hippocampal subfields. (A) Schematic of input and output connection to and from the hippocampal subfields The entorhinal cortex (EC) serves a gateway via which information is received and sent to the neocortex. Direct (1) and indirect (2) pathways between the hippocampus and EC carry information between these areas. The perforant pathways consists of unidirectional projections from superficial layer II of the EC to the dentate gyrus (DG) and CA3 and layer III to CA1 and subiculum. In the indirect pathways medial and lateral entorhinal cortex (MEC and LEC) layer II cells project onto cells with in the DG and CA3. The information from DG is carried by mossy fibres (3) to CA3 and CA3 in turn carries the information to CA1 via Schaffer collaterals (4). Efferents from CA1 carry information to entorhinal cortex via subiculum (SUB). The proximal CA1 sends information to MEC via distal subiculum (5) and distal CA1 sends information to LEC via proximal subiculum (6; adapted from Igarashi et al., 2014). (B) A Nissl stained section from rat hippocampus showing subfields of the hippocampus: CA1, CA2, CA3 and DG. The distal CA1 region is outlined by red line and the proximal region by green line. FC, Fasciola cinereum. (adapted from Igarashi et al., 2014). (C) Schematic highlighting the connections of LEC and MEC with distal and proximal parts of CA1 and subiculum. Note that distal CA1 receives direct inputs from LEC and proximal CA1 receives direct inputs from MEC. Sub, subiculum. (adapted from Deshmukh & Knierim, 2012).

Historically, it has been suggested that there are few differences among the principal cells. However, using next-generation RNA-sequencing (Cembrowski et al., 2016) showed marked differences at transcriptional, proteomic and functional levels in CA1 pyramidal cells.

There is much more diversity among interneurons types than in the principal cells relatively in the hippocampus (Klausberger & Somogyi, 2008). There are at least 21

different types of interneurons that project onto different subdomains of pyramidal cells in the CA1 region. The firing of these interneurons also differ temporally and several of them have been suggested to contribute differentially to different brain oscillations (Klausberger et al., 2003).

1.2 Place cells

The fundamental discovery in the field of spatial navigation was the discovery of neurons tuned to the spatial position in an environment in the rat hippocampus (J. O'Keefe & Dostrovsky, 1971). These neurons were named place cells because they fire when the animal is in a specific part of the environment (figure 1.2). The location where a place cell fires is called its place field. Place cells are complex spike cells, one of the two broad classes of cells found in the hippocampus. John O'Keefe (John O'Keefe, 1976) and Jim Ranck (Ranck, 1973) reported cells whose firing was dependent on factors in addition to location. These cells fire when the animal was in a specific location, previously occupied by an object/reward or recently occupied by an object. They called these cells as misplace cells (John O'Keefe, 1976) or approach consummate mismatch cells (Ranck, 1973). O'Keefe (John O'Keefe, 1976) also reported that some of the place cells recorded did not change the response properties even when the light was turned off. Some other place cells stopped responding when the light was turned off for the first time. Upon further experience with lights on these cells responded when the lights were turned off. It has been reported that visual input is not necessary for the firing of at least some place cells (Save et al., 1998). This study was done in rats that were blinded one week after their birth and the place cells recorded were similar to those in sighted rats except that they had markedly low firing rates. Importantly this study also provided empirical evidence that place cell system uses objects as landmarks. As was shown by the absence of place cell firing when blind rats did not make contact with an previously encountered object.

In the last four decades, the properties of place cells have been extensively studied. The structure and location of the field are influenced by both external and internal cues. The field size increases as one moves from the septal to the temporal pole. The number of firing fields also varies along the proximodistal axis of CA1 (Henriksen et al., 2010) (for distal and proximal CA1 projections see figure 1.1C). Place cells in the distal part are reported to have more dispersed firing and more fields than proximal cells. Other measures of spatial tuning: spatial information, correlation decrease from proximal to the distal end. The authors also reported that proximal cells are relatively strongly phase-

locked to MEC theta than distal cells. Similar to CA1, place fields in proximal CA3 are smaller and sharper than distal CA3 and CA2 (Lu et al., 2015).

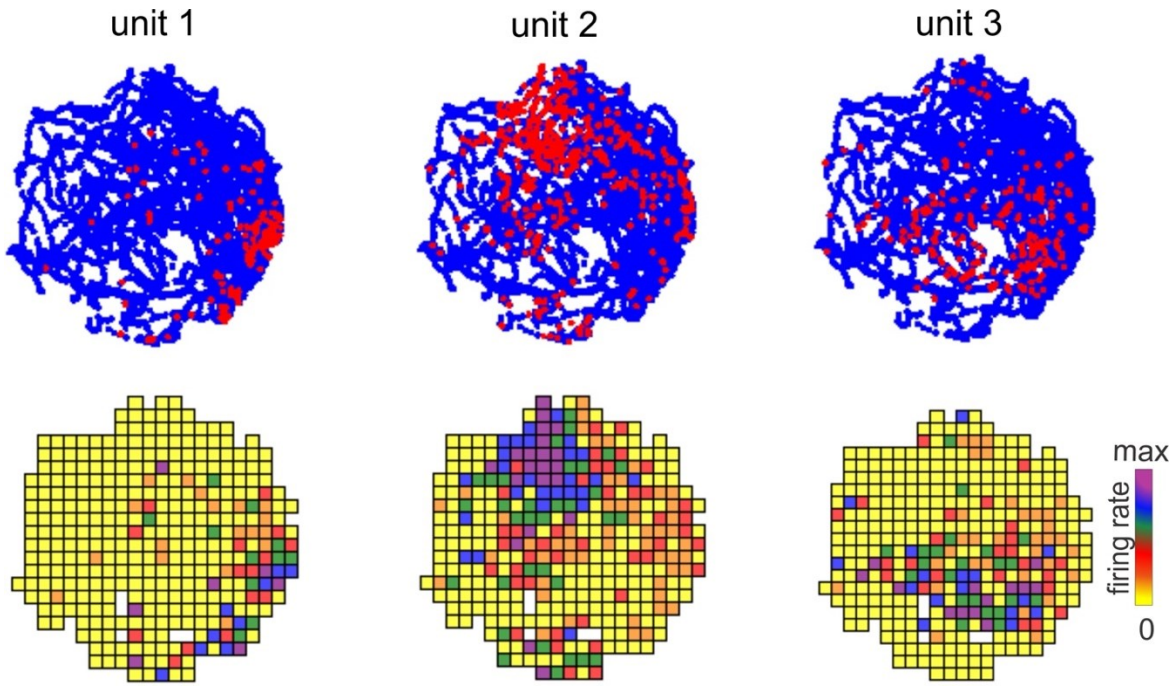

Figure 1.2. Three place cells recorded in a session. The upper part shows spike plots, rat's trajectory is in blue and each spike is shown as a red dot. In the lower part corresponding firing rate maps are shown. Note that the cells mostly fire in a particular place, hence called place cells. Firing rate (Hz) is coded on a color scale from yellow (silent) to magenta (maximum rate; recordings from our lab).

The directionality of place cells

It is interesting to note that place cells are non-directional in open field environments and directional on linear/circular tracks. A study by Bruce McNaughton's group (Battaglia, 2004) found that placing proximal cues on circular tracks led to a significant increase in the number of bidirectional place fields. Another study by the same group (Markus et al., 1995) reported that when rats searched for a food reward on an open circular platform in a stereotypic and directed manner the fields tended to be more directional compared with random foraging in the same environment. The study concluded that the directionality of place fields was more related to the animal's behavior than the difference in visual environments. Spatially selective cells have been found across species, including mice (McHugh et al., 1996), birds (J. J. Siegel et al., 2006) and bats (Ulanovsky & Moss, 2007). They have been reported in non-human primates (Ono et al., 1993) and humans (Ekstrom et al., 2003) as well.

Following the discovery of place cells, decades of research led to the discovery of several other cell types which are believed to form a part of the brain's spatial navigation system. These include head direction cells in postsubiculum, anterior dorsal thalamus, retrosplenial cortex, entorhinal cortex (J. Taube et al., 1990; J. S. Taube, 2007), grid cells in the medial entorhinal cortex and pre and para subiculum (Boccara et al., 2010; Hafting et al., 2005), boundary vector and border cells in the subiculum (Lever et al., 2009). Based on the discovery of place cells and the suggestion that rats create a cognitive map of the environment (Tolman, 1948), J. O'Keefe and L. Nadel put forward their cognitive map theory (O'Keefe, J., Nadel, 1978). In this theory, they argued that the hippocampus provides an objective spatial framework within which items and episodes are bound together and located.

The size of the place field varies as the recording location is changed from dorsal to ventral hippocampus. It usually increases from the dorsal to the ventral region (Jung et al., 1994; Maurer et al., 2005). Based on data from anatomical studies (Dolorfo & Amaral, 1998) it is accepted that the dorsal part of the hippocampus is primarily involved in spatial tasks, and the ventral part is involved in emotional processing and contextual tasks (also see Canto et al., 2008). The afferent and efferent connectivity correspondingly also changes as one moves from the septal to the temporal pole. For example, the septal half of the DG receives input from the caudolateral zone of EC, the intermediate zone projects to the next quarter and the rostromedial zone projects to the temporal quarter (Dolorfo & Amaral, 1998). The lateral and intermediate zones channel information mainly from the sensory cortices and the rostromedial part receives inputs from the amygdala, hypothalamic endocrine nuclei **(**indirect connections through lateral septum, (Risold & Swanson, 1996)) and autonomic nuclei **(**indirect connections through lateral septum, (Risold & Swanson, 1996)).

1.3 Remapping

One of the most important discoveries regarding the representation of place cells was the observation that these cells could change their activity pattern in response to changes in the environment (Muller & Kubie, 1987), a phenomenon known as remapping. In this study, it was found that rotation of a cue card leads to rotation of place fields, also change in the arena shape from cylinder to rectangular lead to a drastic change in the firing field. Changes in the size of the environment only lead the to rescaling of place fields (Muller & Kubie, 1987). Based on these observations it was suggested that the place cell activity represents abstract features of the environment. Remapping could be also partial as was

observed when rats moved between two nearly identical boxes, connected by a corridor, which had a partial overlap of place fields (William E. Skaggs & McNaughton, 1998).

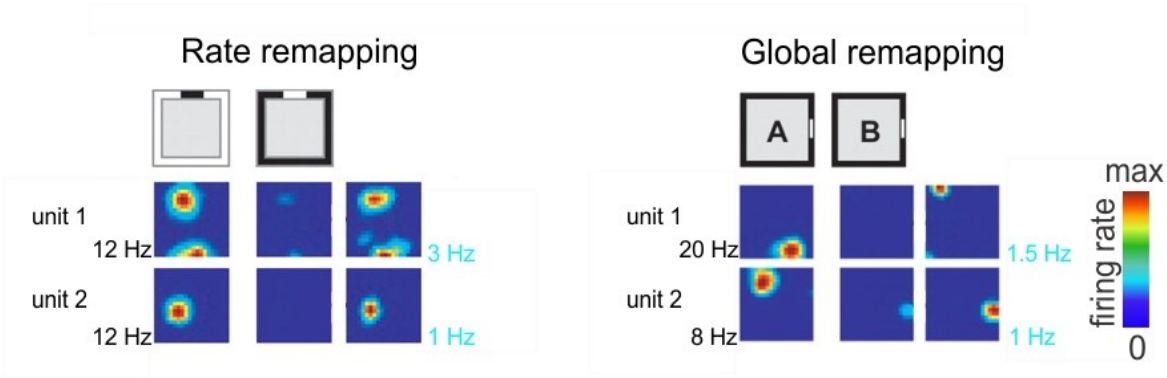

Figure 1.3. Rate and global remapping in hippocampal place cells. Rate remapping: the square boxes with black and white outline denotes constant place and variable cue condition i.e. same room was used but the color of recording chamber' wall was changed (white or black). In white chamber a black cue card was used and vice versa for black chamber. Rate maps for two CA3 neurons are shown. In rate maps on the left, the rate scale corresponds to maximum firing rate (Hz) in that condition (shown on left in black), in the middle are rate maps plotted using the same scale as on the left but for black chamber. Note that different experiences in the same place resulted in fields similar in shape and location but different firing rates. To the right are same rate maps as left but scaled according to their own maximum values (in sky blue). Global remapping: identical square boxes of same color were kept in different rooms, constant cue and variable place condition. The organization of rate maps is similar as for rate mapping. Note that in global remapping the place of firing is also changed. Firing rate (Hz) is coded on a color scale from blue (silent) to red (maximum rate ; Leutgeb et al., 2005).

Remapping can be of two types, rate remapping and global remapping (figure 1.3). Using two different conditions, variable cue same location and same cue but variable location, Leutgeb et al., 2005 showed that place cell remapping can be of two types, rate and global remapping (figure 1.3). When animals were placed in variable cue-same location environment the place cells exhibited rate remapping, where the place of firing remains same but rate changes. The extent of rate remapping has been reported to be more in CA3 than in CA1. In contrast, when animals were exposed to the same cue but variable location the place cells exhibited global remapping, in which both place of firing and rate change. Global remapping could also occur due to noticeable changes in cue configuration without changing the location of the recording apparatus (Bostock et al., 1991). Global remapping also differs from rate mapping in the sense that the former is an all or none phenomenon (Colgin et al., 2008). The existence of different and independent encoding for cue and location configurations shows that place cell ensembles could simultaneously encode spatial as well as non-spatial information.

1.4 Local field potential in the hippocampus

Local field potential (LFP) is the summed activity of the excitatory and inhibitory potentials from a small population of neurons close to the recording electrode.

Several rhythmical and non-rhythmical patterns can be observed if a recording electrode is inserted in the rat hippocampus. Case Vanderwolf (Vanderwolf, 1969) recorded electrical activity from the hippocampus of a rat and classified the patterns observed into rhythmical theta state, large irregular amplitude (LIA) activity, small irregular amplitude (SIA) activity. The electroencephalographic (EEG) activity was also correlated with the animal's behavior. The hippocampal theta rhythm (6-12Hz) is correlated with voluntary movements including walking, exploratory head movements, jumping, etc. It also occurs during rapid eye movement REM sleep. When animals are sitting quietly, drinking, eating, grooming the hippocampal EEG activity prominently exhibits LIA. It is also present during slow-wave sleep. High frequency (200Hz) ripples together with LIA sharp waves are called sharp-wave ripples (SWR). Sharp wave ripples occur during consummatory behavior when an animal intermittently stops during exploratory behavior. It has been suggested that SWRs in CA1 originate due to a barrage of inputs from recurrently connected pyramidal cells of CA3 onto CA1 pyramidal cells dendrites (Buzsáki, 1986; Csicsvari et al., 1999). Sharp waves themselves have been suggested to originate in CA3 due to the temporary disinhibition of afferents. SIA is observed when the animal abruptly stops after a continuous theta train, during a sudden transition from sleep/immobility to alertness. Beta activity (12-20Hz) has been associated with sniffing of predator odors. Gamma activity (20-100Hz) has been associated with the sniffing of a wide range of odors (O'Keefe, J., Nadel, 1978; O'Keefe, 2007). Gamma coupling in various frequencies has been proposed to be a mechanism for routing information among different areas of hippocampal formation (Colgin et al., 2009). This has been further suggested to be a mechanism for preventing the mixing of potentially interfering information.

Phase precession

The systematic and progressive forward shifting of a neuron's firing relative to the theta phase such that the next spike occurs during earlier phases of the theta cycle when an animal traverses through the neuron's place field is defined as phase precession (O'Keefe & Recce, 1993). In the above study, it was also reported that field firing always begins at a specific theta phase and the phase shift was restricted to <=360 degrees.

1.5 What do the place cells respond to?

The firing of place cells is influenced by several factors, including external sensory cues (O'Keefe & Conway, 1978), self-motion cues (McNaughton et al., 1996) boundaries of an environment (John O'Keefe & Burgess, 1996), local cues (J. J. Knierim, 2002), experience (Bostock et al., 1991). By limiting the proximal cues, John O'Keefe and Conway (J. O'Keefe & Conway, 1978) reported that the firing of place cells was related to distal visual landmarks when they were moved around as a unit. Rotating a distal cue card leads to equal rotation of firing fields (Muller & Kubie, 1987). Interestingly, it has been reported that turning off the light does not influence the firing of a place cell (John O'Keefe, 1976) suggesting that place fields are not related to a single proximal or distal cue but rather a more abstract spatial information. John Kubie and Bob Muller (Muller & Kubie, 1987) also found that placing a barrier such that it bisects a place field leads to abolishment of the field and increasing the size of the recording apparatus leads to the rescaling of place fields. Rotations of head direction tuning curves have also been coupled to equal rotations of place fields (J. Knierim et al., 1995; J. J. Knierim et al., 1998) suggesting that these two types of cells are tightly coupled. Bruce McNaughton and colleagues (McNaughton et al., 1996) have argued that the dominant driver of place cell activity is the input from the body movement cues. This allows place cells to perform dead reckoning i.e. how far and in what direction an animal has moved. Accordingly, they have proposed that place cells receive two different types of input one from the body's navigational system (self-motion cues and head direction) and the other from external environmental stimuli. The navigational system, which could rely on information about changes in direction and position in a location, gates the environmental inputs relevant at that specific location. Additionally, it has been found that boundaries of an environment exert a strong influence over the place field. O'Keefe and Burgess (John O'Keefe & Burgess, 1996) observed that changing the size of the walls of an enclosure such that the geometry alternated between rectangles and squares leads to elongation or compression of place fields. Based on these results the investigators proposed the existence of boundary-related cells. Further studies have led to the discovery of these cell types in various brain areas, including MEC (Savelli et al., 2008) and subiculum (Lever et al., 2009). The response of hippocampal place cells also changes with experience (Bostock et al., 1991). Local cues have also been found to influence the place fields, this has been reported mostly when the salience of local cues is enhanced to dominate or match that of distal cues (J. J. Knierim, 2002; Zinyuk et al., 2000). Cressant et al. 1997 (Cressant et al., 1997) also observed place cells that responded to objects placed near the center of the recording apparatus. Further studies have shown that the presence of a moving animal or

object influences the place field (Ho et al., 2008; Kim et al., 2015). It has been further shown that hippocampal place cells encode the position of other animals and objects (Danjo et al., 2018; Omer et al., 2018).

1.6 Role of the hippocampal formation in spatial navigation

Navigation requires the ability to locate oneself in an environment, to use landmarks for guiding along with improvising paths and shortcuts between locations. There is ample evidence available which implicates the hippocampus and its associated areas in this process (Widloski, J. and Fiete, I., 2014). The discovery of place cells and the finding that rats with lesions of the fornix, a major afferent pathway to the hippocampus, were impaired in spatial but not cued learning (John O'Keefe et al., 1975) were crucial for asserting the role of the hippocampus and for the development of the cognitive map theory. In the original treatise, O'Keefe and Nadel argued that the spatial navigation system itself consists of external and internal systems. The external system represents information about sensory cues and the internal system provided information about what to expect at a specific location. The internal system was suggested to follow the self-motion of the animal through space and generate an abstract internal representation of two-dimensional space. Since then various cell types have been discovered which were predicted by the theory.

The discovery of other cells tuned to navigation-specific (such as head direction) and specific-spatial (such as boundary) variables, including head direction, grid, boundary cells laid a solid foundation for our understanding of the cognitive map in the brain. Head direction cells preferentially discharge when the head points in a specific azimuthal direction and are suggested to function as an internal compass. They are influenced by idiothetic cues (Knierim et al., 1995) and vestibular inputs (Stackman & Taube, 1997). Grid cells (Fyhn, 2004) represent allocentric view-independent spatial information and are suggested to be primarily modulated by self-motion (Hafting et al., 2005). Boundary cells fire at the border of the environment and are found in MEC (Solstad et al., 2008). Boundary vector cells, found in the subiculum fire at a finite perpendicular distance from the border (Lever et al., 2009). Unlike boundary vector cells, boundary cells do not fire at a finite perpendicular distance away from the boundary.

The presence of these cells and their connections with the hippocampus indicates that the hippocampus receives both idiothetic and allothetic information and therefore could link the two to generate a map-like representation (figure 1.4). The incoming information

from the entorhinal cortex enters the hippocampus through DG via the perforant path. The DG is suggested to perform pattern separation function, separation of similar environments based on subtle differences (Leutgeb & Leutgeb, 2007) (figure 1.4). This further helps the downstream CA3 to differentiate one place from another and help in forming a map or episodic memories that happened at specific places. Besides the anatomical differences between the CA3 and CA1 they also respond to changes in environmental cues differently (Leutgeb et al., 2004). CA3 neurons respond rapidly to change in the environment compared with CA1 which are comparatively more stable. Further, the representations across environments are more orthogonalized in CA3 than in CA1. There are also differences in anatomical inputs from MEC and LEC into these subfields. In CA1, LEC and MEC axons primarily project onto different populations of cells in distal and proximal parts, respectively. However, in CA3 inputs from MEC and LEC project onto the same population of cells, suggesting that it binds together or associates information coming from these areas. Given the associative function of the CA3 it is inherent to speculate that the CA3 constructs some kind of map. It has been suggested that this map could be topological given the fact that co-firing of place cells implies spatial overlap of fields (figure 1.4).

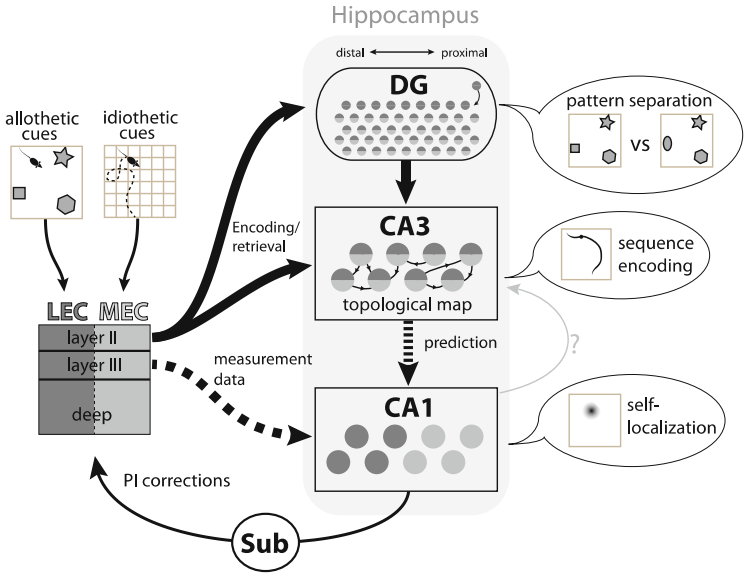

Figure 1.4. Spatial navigation and the hippocampal circuit. Spatial encoding and computations in the hippocampal formation: information about allothetic and idiothetic cues arrive in the hippocampus via projections from the LEC and MEC, respectively. LEC primarily provides information about external sensory stimulus, like objects and MEC primarily provides spatial information. Axons from layer II of the EC, projects to both DG and CA3 (perforant path), where information about allothetic and idiothetic cues is combined (indicated by the shading of the cells). This information is used together with the internal recurrent excitatory collaterals of CA3, which encodes a topological map of the animal's environment, to form a prediction of the current location of the animal. In CA1, the prediction from CA3 is compared with direct sensory information arriving from EC for self-localization. Output from CA1 could be used to correct the path integration (PI) in the MEC through subiculum (Sub) or to change the map in CA3 (gray arrow with question-mark, the question mark highlights the lack of a direct connection from CA1 back to CA3), possibly through EC (adapted from Widloski & Fiete, 2014).

The map formed due to co-firing will be based on connectivity, adjacency and containment i.e. it will be topological (Dabaghian et al., 2012). The hypothesis is that the map is geometric and there is good evidence against the existence of a topographical map (A. D. Redish et al., 2001) (also see Eichenbaum et al., 1989). However, Franca et al. 2019 (França & Monserrat, 2019) have argued that there could be a topographical organization in place cells but it may be organized around an abstract, multidimensional environment containing place fields. Also, location reconstruction from ensemble activity recorded in CA3 shows that the ensemble preplay (Johnson & Redish, 2007) or replay (Karlsson & Frank, 2009) place field sequences suggesting that this subfield is involved in associative learning of location sequences between place cells. CA1 has been argued (Widloski, J. and Fiete, I., 2014) to compare learned inputs from CA3 with sensory inputs from EC to decide whether to fire.

Thus input about a known environment via perforant path could retrieve a learned map in the CA3. This map could potentially make predictions about the spatial position based on the memory of past routes and relative locations. This could be likely used by the CA1 to compare it with sensory information coming from the EC to perform self-localization and probably influence the CA3 map via feedback (Widloski, J. and Fiete, I., 2014).

Path integration

Path integration is the continuous updating of one's position by tracking rotational and translational information (Navratilova, Z. and McNaughton, 2014). It has been suggested that self-motion cues, including optic flow, vestibular senses and proprioception give information about velocity that is integrated over time to calculate the current location of an animal. Terrazas et al. 2005 highlighted that rats use all three self-motion cues, optic flow, vestibular information and proprioception for path integration and place field formation. It has also been hypothesized to be the fundamental mechanism for updating the internal map (representation) and is the basis for the formation of hippocampal place code. As evidence, it has been observed that rats restrained had their place cells silent when placed in the cell's field (Foster et al., 1989), underlining the importance of self-motion in place cell firing. It is now generally accepted that MEC is the site where path integration occurs in the brain. This is based on the data that MEC comprises head-direction cells, grid cells, and cells with conjunctive properties of integrating directional and positional information (Sargolini, 2006).

1.7 Hippocampal place cells in stationary environments

Since the discovery of place cells by O'Keefe and Dostrovsky in 1971 (O'Keefe & Dostrovsky, 1971), most of the studies on understanding the function of the hippocampus in navigation and memory have been done in stationary environments. The pioneering study was done on a raised rectangular platform while the rat did random foraging or responded to a sensory stimulus. Later on, the same group tested how the place cells respond to changes in sensory stimulus, including platform rotation, lights on/off in various types of mazes, including T maze (O'Keefe & Conway, 1978) and circular platform
(O'Keefe et al., 1975). Their data from unit recordings corroborated the earlier hypothesis by O'Keefe and Dostrovsky about the role of the hippocampus in building a cognitive map. Around the same time, James Ranck (Ranck, 1973) independently described the presence of theta and complex spike cells in the hippocampus. It is generally accepted that putative place cells are complex spike cells and interneurons are theta cells, respectively.

In the early 80s place cell studies primarily focused on how the firing of place cells are influenced by various manipulations during random foraging (Muller & Kubie, 1987) or forced behaviors (B. L. McNaughton et al., 1983) (Kubie et al., 1990). Bruce McNaughton and colleagues reported directionality of place cell firing on a radial arm maze and suggested that cells fire in response to complex cue in the extra maze space rather than the absolute location in a non-egocentric framework. This is in contrast to the multidirectionality of place cell firing reported in the open field (John O'Keefe, 1976). Robert Muller along with John Kubie (Muller & Kubie, 1987) observed that rotating a cue card on the wall of the cylinder leads to corresponding rotation of place fields. It was also observed that placing a barrier, opaque or transparent, in a cell's place field led to field attenuation. Howard Eichenbaum and colleagues reported that place cell firing is not only influenced by the location of the animal but also behavioral parameters like speed, direction and turning angle (S. Wiener et al., 1989). In this experiment a spatial navigation task and simultaneous cue-odor discrimination were used. It was further reported that many of the place cells recorded in the first task had behavioral correlates in the odor discrimination task, including during odor sampling, or when the rat moved to perform a discrimination trial. To explain these observations the group argued that the same hippocampal circuits could subserve different representations as was observed in the two different tasks used in the study. Based on these data it was suggested that the hippocampal code is not modality-specific and it appears that what is encoded are

relationships and configurations among relevant events and cues. Importantly, it was also highlighted that both environmental configuration and animal's action are encoded in the hippocampal activity if we consider that the place-related activity in a navigation task is time-locked to appetitive behavior. Using a cylindrical arena with a white cue card attached to the wall (Muller & Kubie, 1987; Quirk et al., 1990) studied the effects of darkness on place cell firing. It was reported that place cells have access to recent memory. This finding was based on the observation that switching off the lights within a session did not alter the firing field of most of the recorded place cells. Further switching on the light during a dark-first session led to partial remapping, 11 of the 22 recorded cells either changed their firing pattern or stopped firing. Remapping was suggested as a way to measure the change in environment by the rat's spatial system and the existence of persistent and non-persistent cells suggest the simultaneous representation of similarities and dissimilarities between environments. Interestingly, when the lights were turned on the firing pattern did not turn to light-first pattern showing that place cell representation is resistant to cue removals or additions during the session.

In an experiment where water was delivered in cups kept at various places on the platform, Breese and colleagues (Breese et al., 1989) argued about the plastic nature of the place cell firing as they observed shifting of fields with selective delivery of water to a specific cup. Similarly, plasticity was observed in an earlier study (Muller & Kubie, 1987) when an increase in the size of the recording apparatus lead to the expansion of place fields. Importantly, in the first study (Breese et al., 1989) the authors dwelled on the point of the salience of a cue to be important for the firing of a place cell as was observed during selective baiting. In contrast, in another study (Speakman & O'Keefe, 1990) goal shifting had no effect on place fields. Place cells also showed properties of spatial working memory as was seen by the maintenance of place fields when cues were removed in between a session. Further place fields in non-start arms were also preserved after cue removal. Interestingly, when the cues were removed before the start of a session, the performance of the animal fell, however, the cells continued to fire. In this experiment, rats were trained on a plus-shaped maze to locate a goal based on the configuration of cues in a curtained enclosure. Based on the results from the earlier study (Breese et al., 1989), the authors argued that place cell firing pattern could undergo modification in an experience-dependent manner, highlighting the plastic nature of the place cell firing. The important point highlighted in this study is that the change in place cell firing is gradual as was observed from rotational to complex remapping when a white cue card was replaced by a black card (Bostock et al., 1991). Place fields can be altered by removing visual cues in a distance-dependent quantitative manner (Hetherington &

Shapiro, 1997). The alteration in place fields was such that if a cue nearby a place field was removed, the firing rate, spatial information content and area decreased and vice versa for a distant cue. Moreover, the spatial information content returned to baseline when the cue was put back.

James Knierim and colleagues (Knierim et al., 1998) found supporting evidence for the hypothesis that prewired connections allow the idiothetic cues to have major control on place cell and head direction firing, while the modifiable connections were influenced by visual cues. Using a series of experiments involving rotation of the recording cylinder and floor of the arena it was reported that place fields rotated with the rotation of visual cues when they are mismatched with idiothetic cues by a small extent, <=45 degrees. When this mismatch was greater, the place cells formed entirely new representations. In contrast, head direction cells followed idiothetic cues when there was a greater mismatch. In the case of a new representation with a greater mismatch, the signal from head direction cells in the CA1 could be combined with a place cell signal to allow for rapid association of directional heading with a reorganized place cell representation when the environment is rotated (Knierim et al., 1998). Based on the results of light on/off experiments in which the apparatus was rotated it was argued that rats did not follow the visual cue if they perceive the environment as unstable. This effect was later found to be experience-dependent i.e. if the rats have had sufficient experience in an environment with a stable visual cue then the place cell firing continued to orient relative to the cue even when it was moved later (Jeffery, 1998).

Several studies by Howard Eichenbaum and colleagues (Wiener et al., 1989; Wiener et al., 1995; Young et al., 1994) suggested that spatial processing is not the only function served by the hippocampus. Extracellular recordings from water-deprived rats in an open-field arena showed that some (14 out of 97) of the recorded hippocampal neurons coded task-related behavior (Wiener et al., 1995). When the hippocampal neuronal activity was recorded in a non-spatial radial-arm maze guided by local visual-tactile cues, with minimized distal cues, place cell firing represented a combination of spatial and non-spatial information (B. Young et al., 1994). Some cells were also reported to have activity correlated with cues but not spatial location.

In an attempt to answer how place cell firing is determined or what does the cells encode Shapiro et al., 1997 used double rotation experiments and found that place cells followed a representational hierarchy. In this hierarchy, most cells encode the relationship between distal and local cues, followed by a lesser proportion of cells that encode configuration of

distal cues and further fewer encode individual distal cues or configuration of local cues. Some of the cells recorded in the double rotations experiments were not altered. To explain this observation the authors argue that memory can override the perceptual influences on place cell representations as one of the ensembles of cells followed the transient position of the experimenter between the trials. The observance of neurons tuned to local cues was linked to the salience of these cues as has been suggested in multiple studies (Breese et al., 1989; Cressant et al., 1997; Gothard et al., 1996; J. J. Knierim, 2002; Zinyuk et al., 2000). It was later found that this response hierarchy is modulated by the environment (Renaudineau et al., 2007). Using double rotation trials the authors (Renaudineau et al., 2007) reported that the fields were mostly controlled by the configuration of proximal and distal cues and when the fields were controlled by specific cues, they were proximal. An important difference between this study and the one by Mathew Shapiro and colleagues (Shapiro et al., 1997) was that the prior one used objects on the arena as proximal cues instead of floor visual inserts. The objects could have acted as potential obstacles for the rat's movement in space. Interestingly, cells controlled by local cues were unlikely to follow single local cues upon scrambling unlike distal cues-controlled cells, which followed a single cue following scrambling. Thus the cells following different cue sets responded differently during scrambling trials. The study also highlighted that both CA3 and CA1 neurons respond to double rotation manipulations similarly.

To find out if the split control of place cells, discussed above, was due to chance because of remapping or a real phenomenon, place cells were recorded from CA1, CA3 and DG (Knierim, 2002). The data made it clear that when two sets of cues were in conflict, some cells followed local cues and some followed distal landmarks. When the cues were put in conflict, some cells remapped, others rotated their field to locations not tied to either set of cues, some changed their rates, etc. The study also reported that some cells were controlled by both sets of cues independently but simultaneously. The split place fields phenomenon was often dynamic in the mismatch session as the firing properties changed their relation between with either set of cues within the course of a session. For example, it could be tied to distal cues early on, then split the field into two and then at the end tied to local cues.

1.8 Object representation in the hippocampus and entorhinal cortex

Rats and other animals encounter objects in real world environments and representation of these objects is an essential component of episodic memory. Based on experimental evidence it has been hypothesized that the perirhinal cortex is the anatomical site for

integrating object information from various sensory areas, as object representation is a polymodal process (Suzuki, 1996). This information is sent to the hippocampus via perirhinal inputs to LEC (Naber et al., 1997; Burwell & Amaral, 1998; Deshmukh & Knierim, 2011). This section is focused on studies where neurons were recorded from the hippocampus and EC. At the end of this section, I also mention two important studies that have had a crucial impact on our understanding of object representation in the anterior cingulate cortex (ACC).

The predominant activity correlate of hippocampal neurons is an animal's position in the environment. However, a number of studies have shown that place fields are modulated by the presence of objects. In a study aimed at determining whether 3-dimensional (3D) objects placed in the recording arena influence place cell firing (Cressant et al., 1997) it was reported that centrally placed stationary objects did not control the firing fields of place cells recorded across CA1 and CA3. No difference was observed when either one or two objects were used. However, the inability of centrally placed objects to control place cells was not absolute as two place cells out of 52 had their firing locked to the object position in the cylinder. One of these cells was consistently controlled by the objects across sessions (for object representation in hippocampus see figure 1.5). As this cell was the last cell recorded from the rat, the authors argued that this effect could be experience-dependent.

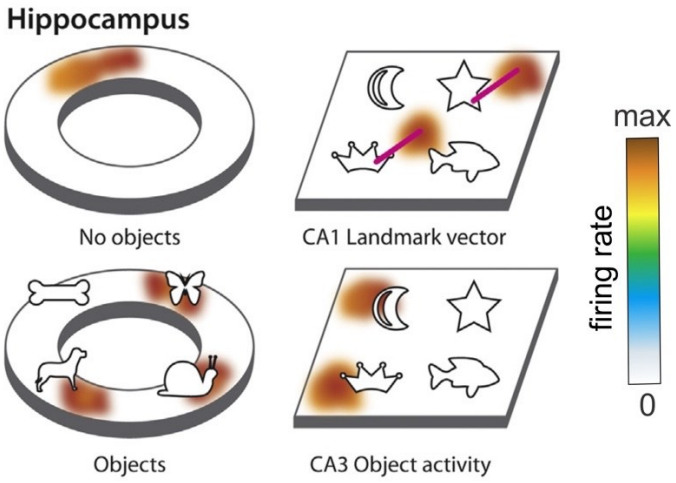

Figure 1.5. 3D object representation in the hippocampus. Schematic examples of 3D objects-related representations in hippocampal CA1 neurons. In the top left panel, activity of a place cell is shown. When objects are present on the recording apparatus distal CA1 neurons are more likely to have multiple place fields near objects (bottom left panel). In an open arena containing 3D objects, CA1 neurons have place fields at a fixed orientation and distance from objects (represented by the colored line, landmark vector (LV) activity, top right panel; also see below). Object related activity is also observed in CA3 though it is more likely to be close to the object (bottom right panel). Firing rate (Hz) is coded on a color scale from white (silent) to brown (maximum rate; adapted from Sara N. Burke & Barnes, 2015).

The weak stimulus control could also be due to the lack of behavioral salience of these objects. Alternatively, it was suggested that this could also be because of the very complex computations, which could be difficult for the rat brain. The relationship between object pairs changes in fundamental ways as the rat moves around in the cylinder. For example, because the rat can see each pair of objects from any angle, one object of the pair may be either to the left or right of the other, depending on the rat's current position. This seems likely because when the objects were moved at the periphery such that rats cannot move around the object the place fields rotated ideally with the objects. However, based on data from our current experiments we could argue that this is not the case, as we were able to train the rats to avoid a particular region around a moving robot. We agree that this could be experience-dependent as it took 6-7 weeks for our rats to perform the behavior successfully.

In a landmark-based navigation task, Bruce McNaughton and colleagues (Gothard et al., 1996) observed cells tuned to reference frames associated with various objects, including goal/landmarks and boxes from which rats were released and removed from the arena. They also observed disjunctive (tuned to two reference frames, independently) and conjunctive cells. Cells with different behavioral correlates were active during a recording session but no clear examples in which cells bound to different reference frames fired simultaneously (also see Kelemen & Fenton, 2010). For example, in those trials in which the goal location fell within the firing field of a place cell, the place cell appeared to be silent while the rat was at the goal; however, many goal-related cells fired strongly at this time (Gothard et al., 1996). These data appear to suggest that subsets of hippocampal neurons could be bound to a fixed environment as well as the movable objects depending on the task and salience of the objects. Further landmarks appeared to be used as a beacon from a large distance and spatial cues from a shorter distance. They further suggested that several changes of reference frames between local and global occurred on the way from the box to the goal. As none of the landmark or box-related cells fired at >=70cm beyond the area in which the corresponding appropriate behavior was required suggesting that behavioral context or salience has an important role to play in switching reference frames.

Hippocampal pyramidal neurons also respond to object identity however information about object identity is represented secondarily to spatial information (Manns & Eichenbaum, 2009). In the above study, repetition of an object in the same location corresponded to increased information about object identity. The overall results suggested that objects were mapped as points of interest on the hippocampal cognitive

map. Similar conjunctive coding was also reported in an item-place conjunction task (Komorowski et al., 2009). In this study, a robust representation of item-place conjunction by hippocampal pyramidal neurons developed independent of the reward contingency and was reflected by stronger activity. This representation developed over a period of sessions from pre-existing spatial coding. This confluence of spatial and non-spatial information is also observed in LEC (Deshmukh & Knierim, 2013). Another example of this item-place conjunction within the hippocampus is the finding from the above study (from Deshmukh & Knierim, 2013) that a subset of hippocampal place cells binds spatial relationships to multiple, independent landmarks (figure 1.6).

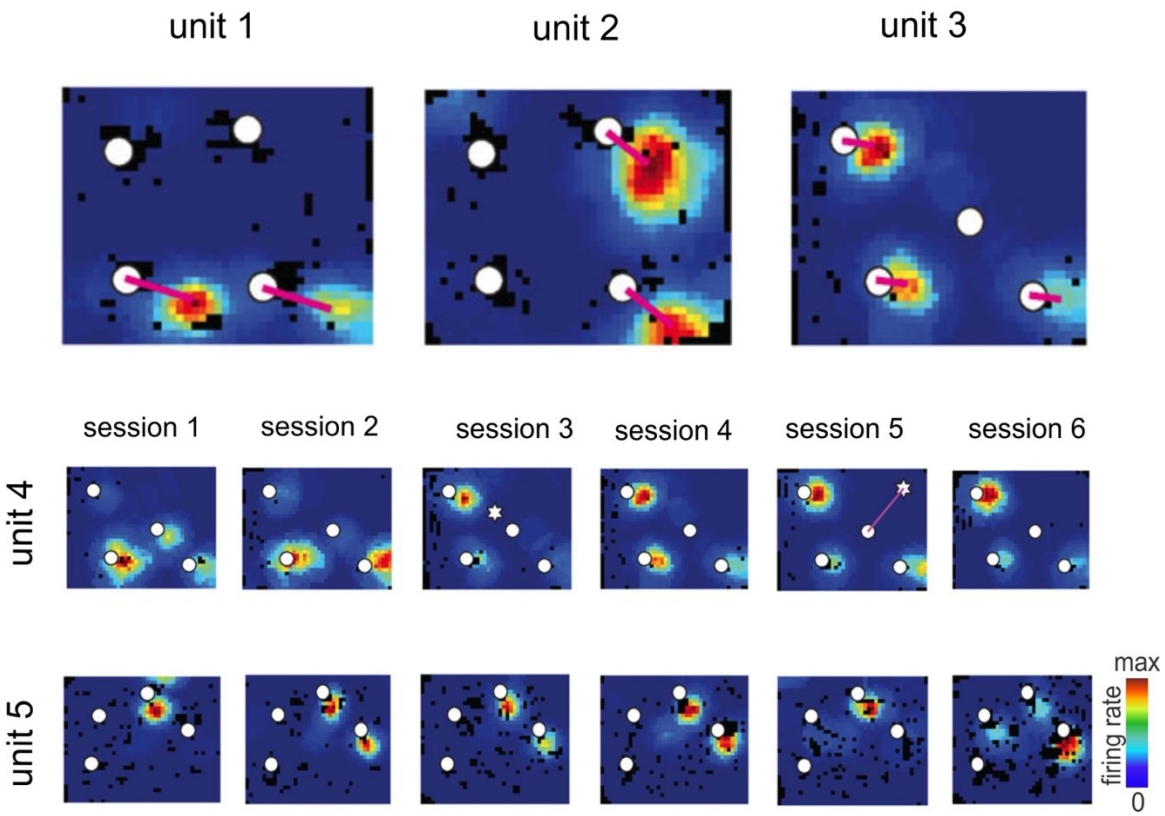

Figure 1.6. Landmark vector (LV) activity in the hippocampus. Units 1, 2 and 3 represent examples of LV cells from CA1. In the lower part, firing pattern of units 4 and 5 (also from CA1) is shown across sessions. Notice that in session 5, unit 4 did not change its spatial firing pattern upon the introduction of a misplaced object at a previously unoccupied position. The magenta line connects the position of the new object (star) with the position of the previous object. Some of the units did show change upon object manipulation however this was not a norm. Blue corresponds to no firing and red represents the peak firing rate. Unvisited pixels are shown in black. Notice the place fields are at a similar vectorial relationship with respect to the objects for a particular unit. Firing rate (Hz) is coded on a color scale from blue (silent) to red (maximum rate; adapted from Deshmukh & Knierim, 2013).

These cells have been called landmark vector (LV) cells because their multiple fields have common vector relationships with several objects such that distance and direction from one of the objects are similar to at least one other field from another object. It has been proposed that LV cells could arise from object-related representation from LEC combined with path integration-related inputs from MEC. These vector relationships are

dynamic as some of these neurons also developed new fields during the course of recordings whose LV matched the ones for existing fields. The existence of LV cells has been proposed in the vector-encoding model (McNaughton et al., 1995) to explain the behavioral data from an experiment with gerbils (Collett et al., 1986). A similar type of vector encoding relative to objects/landmarks has been recently reported to be the predominant form of spatial encoding in MEC (Høydal et al., 2019).

The presence of 3D objects could modulate place field size and changing the location of the objects can result in remapping as was observed when rats encountered several objects on a circular arena (Burke et al., 2011). When the objects were present there was an increased probability of place field expression. This was neither due to the bidirectional nature of the fields nor due to the increase in global excitability (firing rate). Novelty also did not influence the overall firing rate in CA1. Analysis based on population data revealed that field size generally decreased in the presence of objects. Based on data from proportion normalized frequency distribution of place field size it was suggested that the number of large-sized fields decreased while the small ones increased in the presence of objects. These data suggest that 3D objects could cause CA1 place fields to globally remap. Consistent with the above observation the rate of theta precession was more when objects were present. However, the dispersion of phase precession did not change. The mean phase shift was also not different indicating that this difference in field size is not due to the rat running through the field's edge when objects were present. It is important to note that in this experiment, the recordings were made from neurons in the intermediate distal CA1 region. The distal CA1 region preferentially receives input from LEC and the perirhinal cortex as mentioned above.

In between CA3 and CA1, lies CA2, it forms a powerful disynaptic cortico-hippocampal loop that links EC with CA1 (Chevaleyre & Siegelbaum, 2010), independent of much-studied trisynaptic pathway. This region receives inputs from LEC (Hargreaves et al., 2005) and subcortical areas, median raphe nucleus (Hensler, 2006) and hypothalamic supramammillary nucleus (Pan & McNaughton, 2004). Many of the neurons in the CA2 region express vasopressin 1b receptor (AVpr1b), which is believed to mediate social recognition and motivation (Young et al., 2006). The vasopressin 1b receptor (AVpr1b) is highly expressed in CA2 pyramidal neurons and the receptor is believed to mediate social recognition and motivation (Young et al., 2006). A lot less is known about this area comparatively and it has been implicated in sociocognitive memory processing (Hitti & Siegelbaum, 2014). Using a novel transgenic mouse line (Amigo 2 Cre mice injected with adeno-associated virus expressing enhanced green fluorescent protein-tetanus

neurotoxin light chain), the authors genetically inactivated CA2 pyramidal neurons and observed that these mice had severe deficits in social memory as determined by several tests for social memory sociability. This same region, dorsal CA2 sends excitatory inputs to a subregion of ventral CA1 (vCA1) which is implicated in social memory (Meira et al., 2018). Interestingly these mice did not display altered sociability. The CA2 (dorsal) has been also implicated in promoting aggression by acting through the lateral septum (LS) onto the ventrolateral subnucleus of the ventromedial hypothalamus (VMHvl; (Leroy et al., 2018)). This circuit is modulated by arginine vasopressin at the level of presynaptic input from CA2 in dorsal LS (dLS). Dorsal LS sends inhibitory projections to ventral lateral septum (vLS) which in turn inhibits VMHvl. Thus excitation of dLS by CA2 neurons inhibits vLS which in turn leads to disinhibition of VMHvl hypothalamic nucleus. Okuyama et al. 2016 (Okuyama et al., 2016) have also reported that optogenetic silencing of vCA1 neurons impairs performance in social discrimination test and they also implicated vCA1's projection to nucleus accumbens shell in social memory. Similarly, results from another study (Chiang et al., 2018) have implicated ventral CA3 in encoding social stimuli using conditional genetics and pharmacogenetic manipulation. It is generally accepted in the field that non-spatial information for e.g. information about objects, odor, etc. primarily enters the hippocampus from LEC and spatial information enters from MEC, where grid cells are found.

The initial evidence for object responsive activity in LEC came from studies involving object-recognition memory tasks. These studies reported that LEC neurons are responsive to views of objects (Zhu et al., 1995), odors (Young et al., 1997) and pictures of objects
(Wan et al., 1999)**.** Besides object-responsive neurons in LEC, there are neurons with place fields similar to those observed for hippocampal neurons (Deshmukh et al., 2012). Other neurons in LEC encode conjunctively both object and place information. The location of object-related firing in this area does not always coincide with the object's position (figure 1.7). However, it is abolished when the objects are removed (Deshmukh & Knierim, 2011). Some neurons in LEC also encode an object's trace, such that they fire at a place where an object was present earlier (Tsao et al., 2013). These cells are different from mismatch cells (O'Keefe., 1976; Ranck., 1973) in that the latter fired for only a few seconds after mismatch detection and trace activity was present for over many days after the object removal. Finally, object-trace cells and object cells (Deshmukh & Knierim, 2011) most likely represent functionally different cell populations. A similar type of object trace representation has been reported in ACC (Weible et al., 2009 and 2012). In superficial layers of MEC, a different type of vectorial representation has been reported

(Høydal et al., 2019). This allocentric vector encoding was present in relation to objects of different sizes and types. The firing fields were mostly away from the object by tens of centimeters and the field also moved with the object to maintain the same distance and direction. Importantly**,** these cells differ from LV cells in the hippocampus in that they do not differentiate between subsets of objects and also are present from the first trial with the object (Deshmukh & Knierim, 2013). They also differ from border cells in the sense that the fields are stable independently of whether the objects obstruct the animal's trajectory.

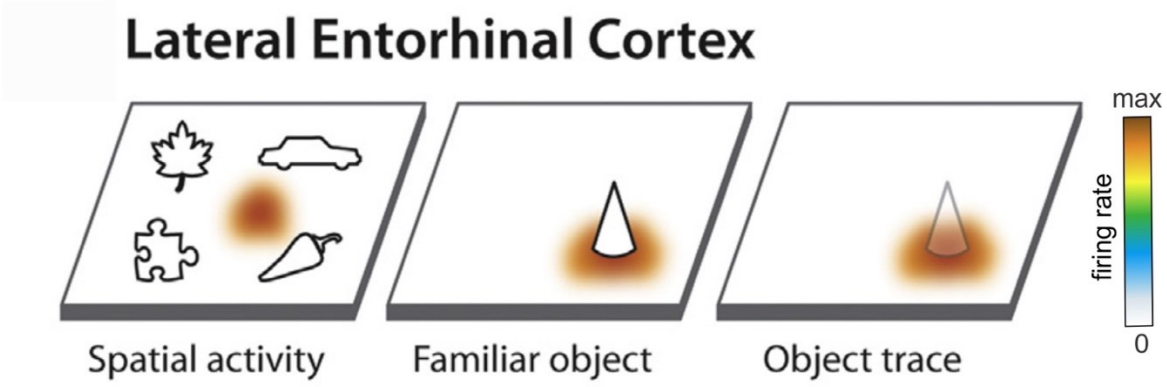

Figure 1.7. Schematic examples of 3D-object related activity in LEC. A portion of LEC neurons show punctate firing fields when rats explore an arena with 3D objects. This activity is not observed close to the locations of objects (left panel) and is absent when objects are not present in the environment. Prinicipal cells in LEC also fire at object locations (middle panel; and a portion of these cells show "object trace" activity by continuing to fire even after the object has been removed (right panel). Firing rate (Hz) is coded on a color scale from white (silent) to brown (maximum rate; adapted from Sara N. Burke & Barnes, 2015))

The hippocampus and MEC provides an objective spatial framework of an episode. This framework allows for the organization of components of an experience that can be stored and retrieved. The information about components of an experience is suggested to be provided by LEC (Hargreaves et al., 2005). Further cells in the LEC had been observed to have sharper egocentric bearing to 3D objects and goal locations (Wang et al., 2018)**.**

1.9 Role of the hippocampus in dynamic tasks

A series of experiments by Jan Bures and their colleagues (Bures et al., 1997) suggested that darkness and visual cues on the cylinder wall increase the significance of idiothetic cues. Using a rotating arena to create a conflict between idiothetic and external cues they reported that the conflict led to disorganization of place fields. Interestingly, when the lights were turned off while the arena was rotating, firing fields in the arena frame were preserved suggesting that rotation induced conflict between the discordant room and arena frames as the cause of field disorganization. These data further suggested that exteroceptive and idiothetic spatial memories were functionally autonomous. In a series

of further experiments, it was found that exteroceptive memories were dominant (Fenton et al., 1998). Further, this conflict was reduced if a cue card was put on the rotating arena wall suggesting that darkness and visual cues enhance the significance of idiothetic inputs but by different mechanisms (Bures et al., 1997). In the field clamp experiment, the idiothetic cues were more persuasive than the exteroceptive cues and led to the disruption of the field established on a stationary arena (Bures et al., 1997). Using a rotating arena, Zinyuk et al., 2000 argued that the effect of change of environment on place cell firing depends on the behavioral task. Importantly they also concluded that the physical attributes of an environment, including walls, surfaces and prominent landmarks establish a reference rather than a goal or abstract environmental features (but see Gothard et al., 1996).

The place field properties and their representations change in a dynamic environment. In a study aimed at determining the contributions of optic self-motion, vestibular and ambulatory signals on CA1 activity (Terrazas, 2005) it was argued that self-motion signals are the primary determinants of place field size and distribution. This was based on data from conditions where rats walked on a circular track versus it drove a car or experienced pseudomotion. The last two conditions had no ambulatory signal and ambulatory plus vestibular input and had decreased spatial information score compared with the walking condition. The representation of the place cell firing is dependent on the behavioral task as discussed above (Zinyuk et al., 2000). In a two-frame, active place-avoidance task, where the animal was trained to avoid two shock zones one defined relative to the room and the other in the arena frame (Kelemen & Fenton, 2010, 2013), it was reported that coactive place cells represented either information related to the room frame or arena frame. The representation switched between frames and the neuronal discharge preferentially represented the spatial frame of the shock zone the animal's approaching.

1.10 Hippocampal activity in the presence of another moving object

In one of the early studies which provided evidence for the encoding of information about another moving object, Ho et al., 2008 recorded rats along with a toy car on an arena. In this study, place cells encoded movement variables of the car when being in the vicinity of the car was reinforced by intracranial stimulation during car-dependent navigation (CDN) or positive reinforcement condition. These variables included turning angle, direction, the distance between rat and toy car. The tuning was sharper again during positive reinforcement task for distance between the rat and robot. It was argued that in the CDN task, rats were paying attention to movement variables of the car to receive the

intracranial stimulation that's why this information needs to be represented in the brain and tuning to movement variables of the car provides one such evidence in that direction. This argument about salience is similar to that, which has been made in previous studies with stationary objects (Cressant et al., 1997) and studies comparing the importance of distal versus proximal cues (Knierim, 2002). In contrast, Larysa Zynyuk and colleagues (Zynyuk et al., 2012) observed weaker or no tuning when a conspecific was placed in an arena along with the subject animal. It is important to note that the proximity between the conspecifics was not reinforced in this experiment. This could be the reason for lack of tuning relative to the conspecific. Coherence decreased non-significantly when the rats were closer compared to when they were far away. The firing rate also decreased for most of the cells. This distance dependency was suggested to be due to the dominance of the second rat on the cue constellation experienced by the recorded rat.
Based on data from the above studies it appears that there is conflicting evidence on the representation of another moving object or its properties. However, later studies suggest that movement of another object and/or its position are encoded in the hippocampus of the subject animal.

In a study aimed at finding how the presence of a moving predatory threat limits foraging boundaries (Kim et al., 2015), the scientists found that the firing of place cells nearest to the threat changed. The studied place cells were divided into different groups based on distance from the threat, a looming robot, into distal, proximal and nest. In the presence of the threat, distal cells showed remapping compared to when the threat was absent. Moreover, there was a significant difference in spatial correlation in the distal zone versus the nest zone. The peak firing position was maximally shifted in cells in the distal zone and this shift was away from the threat. The theta power also increased in distal cells in the presence of the robot. Interestingly, in amygdala-lesioned rats, the distal cells were found to be stable. Also, there were sessions when normal rats went closer to the robot and distal cells recorded during these sessions also had a stable firing. It was suggested that a possible scaling relationship between the magnitude of fear, which varies with distance from the nest, influenced the stability of hippocampal place fields. This type of distance-dependent influence on place cell firing was also observed in another study (Zynyuk et al., 2012).

In one of the two recent studies which reported the representation of a conspecific in the hippocampus of the observer, Danjo et al. 2018 (Danjo et al., 2018) found the representation of the spatial location of a conspecific (another rat) in the recordings from dorsal CA1 of the observer rat (top part of figure1.8 in black box). The observers were

trained to make a left/right choice in an observational T-maze task, where they had to make a choice depending on the task rule and the choice made by the conspecific to get a reward. In this study, about 75% of the observer's units showed theta phase precession relative to the other's location when the observer was at the starting position and was not running. They obtained self and other's rate maps (by replacing self's positional data with other's) and constructed joint place fields, by combining place fields constructed from the same spikes. The spikes of joint place cell ensembles were found to be useful in reconstructing the position of the other at various time points.

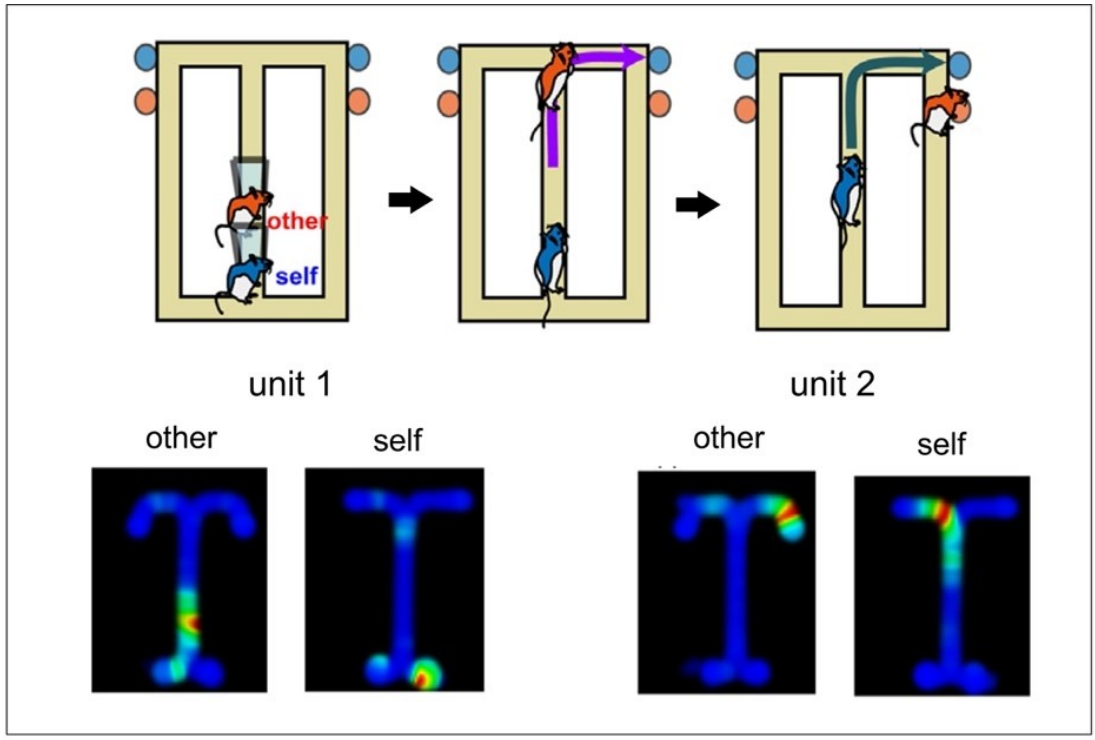

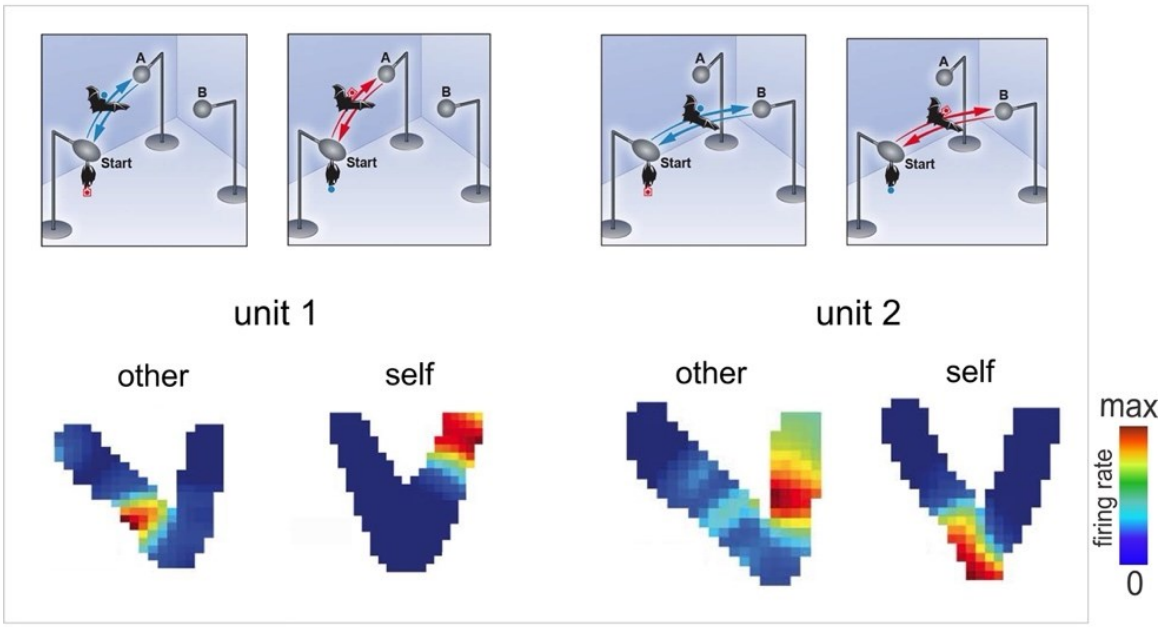

Figure 1.8: Representation of a conspecific in the rat and bat hippocampus. Top: In black box. The schematic depicts an observational T maze task where the recorded (self) rat had to either follow the same or opposite side rule to receive the reward (water) based on the behavior of the other rat (orange). The example shown is of the same side rule, where the recorded rat (self, blue) had to visit the same arm as the other rat. Shown below are examples of two units that encoded both the position of the recorded and other rat. Adapted from Danjo et al., 2018 and Danjo, T., 2020. Lower part: In the gray box, the schematic depicts the experiment where the recorded bat (self, red marker) had to visit the same pole (A or B) as traversed by the other bat (blue). Shown below are two units encoding the position of both the self and other bats. Adapted from Omer et al. 2018.

Nachum Ulanovsky and colleagues have (Omer et al., 2018) reported the representation of conspecific as well as inanimate objects in neurons from the dorsal CA1 of a bat (lower part of figure 1.8 in gray box). They used an observational task in which an observer bat mimicked the behavior of a demonstrator bat. It was reported that out of 378 recorded neurons 68 were social place cells and out of these 68 cells, 39 were also place cells. These cells had low firing rates compared with classic place cells. They also observed a continuum of correlation between self and others' representation. For higher firing neurons there was a tendency towards being more congruent i.e. the social place field and classic place fields overlapped. The social place-cells were allocentric. They also found representation of inanimate objects independent of whether they were associated with a reward. A conspecific was better encoded compared with an informative object followed by a noninformative object. The representation of the objects was nondirectional, representation among objects was better correlated than with a demonstrator. Social place-cells exhibited a gradient along the proximodistal axis of CA1, they were more prevalent in distal CA1. Object cells did not exhibit such a gradient. These points suggest that encoding of the spatial position of a conspecific is not a general sensory response instead these responses are context-dependent. It was suggested that spatial representation of objects could be due to the summation of grid cell inputs from MEC and object-related inputs from LEC and social place cells might also involve inputs from CA2. The authors suggested that the observance of these cells in their task could have been due to the salience as has been suggested in other studies (Cressant et al., 1997; Gothard et al., 1996; Duvelle & Jeffery, 2018). They also noted that at the start the two bats were together on a ball and they often approached, touched and emitted social vocalization which could have contributed to representation of the conspecific. In many studies, the role of CA2 in the representation of non-spatial stimuli has been studied. CA2 spatial representation has been reported to show global remapping upon presentation of known or novel conspecific. However, changes in activity were not detected during stimulation (Alexander et al., 2016).

Another related study by Mou and Ji (Mou & Ji, 2016) found that CA1 place cell sequences observed when an animal ran on a track could also be observed when the subject animal observes a conspecific running on the same track. These sequences were observable even before the subject rat had no prior running experience on the track but were not present when the conspecific was removed.

1.11 Object representation in various regions of the brain

Perirhinal cortex

The representation of 3D objects is a multimodal process and the perirhinal cortex (PRC) has been suggested to be important for integrating sensory information to support object recognition. It receives inputs from several sensory modalities, including visual, olfactory, somatosensory, etc. Perirhinal lesions severely impair object recognition memory in spontaneous object recognition tasks (Winters et al., 2004). It should be noted that PRC-dependent recognition memory is not limited to 3D objects, as PRC is important for odor recognition memory (Feinberg et al., 2012) and is also for integrating information across other modalities, including visual and tactile stimuli (Winters & Reid, 2010). PRC does not encode spatial information in the presence of objects. The landmark-derived spatial information arises *de novo* in LEC (Deshmukh, 2014). Firing in LEC neurons is also tuned to 3D objects and it is believed that LEC inherits non-spatial information from afferents arriving from PRC. However, firing in LEC and PRC differs in two ways. First, the firing field of few LEC neurons does not always overlap with the object position and their field is reminiscent of place fields of hippocampal neurons. Second, LEC neurons also fire at a location previously occupied by an object, this type of activity has not been observed in PRC (Burke & Barnes, 2015; Tsao et al., 2013; figure 1.9A).

Using a battery of behavioral tests, along with selective lesions in various brain regions, Barker et al., 2007 reported that PRC is crucial for discriminating between the novel and familiar objects, object-in-place and temporal order tasks. They also reported that the medial prefrontal cortex and PRC are important for associative recognition memory.

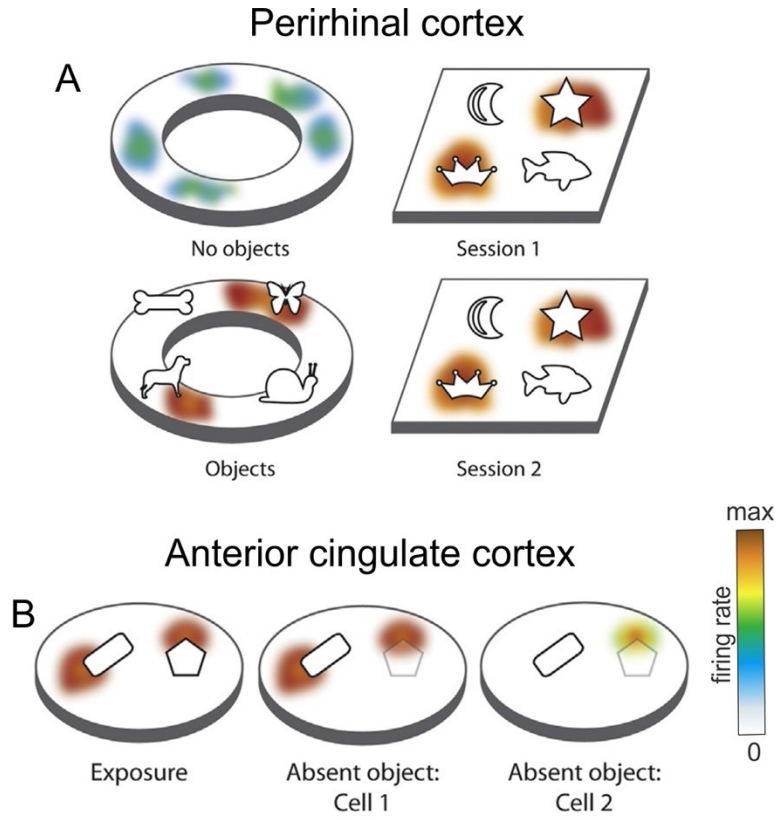

Figure 1.9. 3D object-related activity in PRC and ACC. (A) A schematic of principal cell spiking activity in PRC on a track without objects (top left panel) and with 3D objects (bottom left panel). On an empty track, few PRC neurons show dispersed spiking activity with low firing rate (top left panel). Upon addition of 3D objects (bottom left panel) many of the cells that had non-selective firing on the empty track began to fire close to the objects. Similarly, prinicipal cells fire near object locations (top and bottom right panels) when the animal randomly forage in an open arena. (B) Schematic example of principal cell activity in ACC during object exploration in a circular apparatus. During object familiarization phase, ACC neurons fire close to the objects. Following a delay, few ACC neurons fire at both the location of the present object and where an object was present (lighter object outline; middle panel), or by only firing at the location of removed object (right panel). Firing rate (Hz) is coded on a color scale from white (silent) to brown (maximum rate; adapted from Sara N. Burke & Barnes, 2015).

Anterior Cingulate Cortex

The neurons in the caudal ACC have been found to encode correlates of memory for the location where an object was present (Weible et al., 2009). Another study by the same group (Weible et al., 2012) found that ACC neurons could retain object location memory for over a month (figure 1.9B).

Posterior parietal cortex

The posterior parietal cortex (PPC) is another association area that has shown some form of object-related activity. This area is considered one of the hubs for multimodal integration given it receives inputs from secondary visual, auditory and somatosensory cortices. The activity of neurons in the 7a region of the PPC has been reported to encode

locations in an object-centered framework during a visual object construction task (Chafee et al., 2005). Crowe et al., 2008 reported that PPC activity initially reflects the position of the stimulus and object in egocentric and within 100ms the position is represented such that it was anchored to allocentric space defined by the object. They reported a neural correlate of a viewer to object-centered transformation in area 7a. Using a series of experiments involving unilateral and bilateral lesions of PRC or PPC, Winters and Reid 2010 reported that animals with bilateral PPC lesions were impaired in a crossmodal object recognition (CMOR) task and tactile task but not the visual-only task. In the case of PRC bilateral lesions, animals were impaired on CMOR and visual-only tasks but not a tactile-only task. Unilateral lesions made in opposite hemispheres to PPC and PRC caused impairment in CMOR tasks suggesting that objects can be represented in a distributed manner in the cortex in cognitive tasks involving crossmodal information processing.

Prefrontal cortex

The prefrontal cortex (PFC) is associated with executive functions, including planning and extensive lesions of the area result in damage in the ability to engage effective goal-directed behavior. Rainer et al 1999 (Rainer et al., 1999) reported that PFC neurons in monkeys prospectively encoded expected (visual) objects. This is in line with the fact that planning in complex behavior requires prospective memory processing. It was also reported that PFC neurons encode attributes of the objects as was observed by similar activity in PFC neurons elicited by physically similar visual objects (Rainer & Ranganath, 2002). The encoding of visual objects in PFC has also been shown to be phase-dependent (Leroy et al., 2018; M. Siegel et al., 2009). Using a short-term memory task, it was shown that information about two objects is increased at specific phases of LFP. Medial PFC has also been suggested to integrate spatial and object information (Barker et al., 2007). Based on their lesion data from the object-in-place task it was argued that medial PFC (mPFC) and PRC must function closely to process spatial and object information. In animals with bilateral lesions in mPFC, PRC and contralateral lesions in these areas the performance was impaired in temporal order memory tasks. It was also suggested that these two areas are important for recency discrimination and are interdependent for this function. It is worth noting that there are direct reciprocal connections between the PRC and mPFC.

Inferior temporal cortex

The inferior temporal cortex (IT) is an important component of the ventral visual pathway. This pathway has been hypothesized to determine the content of vision such as objects in an environment. Beyond its role in object recognition, IT is probably involved in determining the valence of an object in nonverbal social communication and in navigating through environments (Conway, 2018). The responsiveness of TE1 and TE2 areas of IT has been reported to decrease after the first encounter with an object (Fahy et al., 1993). Baylis et al. 1987 reported that neurons in the area TEa and TEm respond selectively to faces. Based on data from experiments involving delayed matching-to-sample tasks, Miller et al. 1993 argued that neurons in IT could represent mnemonic information about objects (images) for use in work memory tasks. Hasselmo et al., 1989 found out that some of the cells in the IT encode information in object-centered coordinates. They also found that some of the neurons in IT and superior temporal sulcus respond to head movements performed by one of the experimenters.

1.12 Rat-Rat and Rat-Robot behavioral experiments

We will briefly discuss behavior studies that involved dynamic environments involving either a programmable robot or another rat. The section includes a brief introduction about the original enemy avoidance task (Telensky et al., 2009) and related studies.

A number of studies have been developed which used either rat-rat and/or rat-robot dyad to study behavior between animals or an object and animal. The primary aim of these studies has been to study the interaction between the rat and the other object or study the role of the hippocampus in the task. The task developed in our work has been inspired by previous work in our laboratory (Telensky et al., 2009). In the original task, the enemy avoidance task subject rats were trained to avoid another rat (enemy). Whenever the distance between the two rats was reduced below 25cm the subject rat received a foot shock. The negative reinforcement reduced the distance traveled by the subject rat and increased thigmotaxis, resulting in decreased entrances into the shock zone. Interestingly, the average path covered between two shock zone entrances gradually increased during training, suggesting behavioral changes other than hypolocomotion and thigmotaxis. The enemy rat traveled more distance than the subject rat 3 seconds before the first shock resulting from the given error suggesting that the errors may have been caused by the locomotion of this rat. In an exploratory experiment, a third rat was added as a confounding object later on and this caused an increase in the number of entrances in the shock zone.

To avoid errors due to the movement of the enemy rat, in another experiment (Telensky et al., 2011), the experimenters replaced the enemy rat with a programmable robot. In this study, they observed that pharmacological inactivation of the hippocampus severely impaired the rat's performance in the task. In a similar vein Ortiz, et al., 2016 designed an experiment to control for the variation in analyzing a dyad of animals, due to lack of control over the animals' movements. A programmable robot along with a subject rat was used to analyze several social and non-social behaviors. A comparison was made between non-social and social behaviors when the subject rat interacted either with another rat or a robot. The rats spent a similar amount of time in social as well as non-social behaviors when either they encountered another rat or a robot. Social behavior included sniffing, crawling and approaching and non-social behaviors included evading, being quiet and self-grooming. Notably, in sessions with the robot as a friendly partner in a dyad, the rats' following behavior had the longest duration. Interestingly, we also observed this following behavior during the moving robot condition in our experiment. In some of the cases this was due to the rats' tendency to sit on the robot to avoid getting the shock.

Shi et al., 2013 looked at the response of a rat to a rat-like robot capable of generating different types of behavior: stressful, friendly and neutral. The primary finding of the study was that the rats' activity decreased during the stressful robot condition and increased during the friendly condition. Rearing and grooming frequency was also significantly higher in the friendly groups than in the other groups. The average rat-robot distance was lowest in the friendly group 24cm, 30 cm in neutral and 32cm in the stressful group. This distance is similar to the trigger distance for a shock in our experiment (39cm). It is worth noting that rats in the friendly group were found to be more active when exposed to a more active robot.

Another study (Svoboda et al., 2012) from our lab compared the performance of male and female rats in the enemy avoidance task. Both sexes performed similarly under reinforcement condition in the task. However, the females used a different strategy to avoid the moving robot, they spent more time near the periphery and displayed hypolocomotion even when the shock was off.

Gianelli et al., 2018 showed that rats could be trained to follow a robot moving at different speeds, here 20cm/s or 55cm/s. In this experiment, a commercially available robot, Sphero (Boulder, CO) was used to control the movement and heading direction of

animals. In a series of trajectory manipulation experiments, it was shown that the rat could follow the robot such that its trajectory made a cloverleaf pattern, or followed several parallel lines simulating a hairpin maze. The rats were also able to follow the robot trajectory simulating the letters C, E, N and L. They further showed that the robot can be used to improve the rat's performance in a memory task, in a complex environment. Electrophysiology recordings from this study showed that the robot did not cause significant remapping of the place field of recorded neurons.

2. Aims

Our broader aim is to understand how CA1 neurons encode information about a moving object. The specific aims of the study are as follows:

The first aim is to design and establish a paradigm where rat behavior is linked to a salient moving object. A number of the studies that involved another moving object (Ho et al., 2008; Zynyuk et al., 2012; von Heimendahl et al., 2012), either a conspecific or a robot had conflicting data about neuronal representation of the object. The main problem with these paradigms is weaker or no salience of the object for the subject (recorded) animal. To overcome this important issue we developed a modified version of the enemy avoidance task (Telensky et al., 2011) where the subject had to orient itself relative to a moving object. Towards this aim we hypothesised that a rat can organize its behavior according to position (not just distance) with respect to a moving object and this behavior would inevitably make the moving object salient for the rat.

The second aim is to decipher the mechanism underlying the animal's ability to assess its position relative to a moving object: To understand the underlying mechanism we looked at several parameters including the time to first entrance, average and minimum rat-robot distance, visit path, visit time and average and maximum rat speed in shock and safe zone in probe trials when the rat was in the vicinity of the robot.

The third aim is to look at what does the cell encode and if they had any response to the moving object: Based on current evidence (Danjo et al., 2018; Omer et al., 2018) we hypothesised that hippocampal responses would encode the moving object and unit activity would reflect position of a rat relative to a moving object. To elucidate if the recorded cells encoded the moving object and if the spatial firing pattern is affected by the presence of the moving object. We constructed rate maps in various reference frames from the moving robot sessions to understand if the information is encoded in the reference frame of rat in room, rat to robot and robot to rat. We also looked at how the spatial firing pattern of the cells changes (if at all) across the recorded sessions.

The fourth aim is to compare measures of the spatial organization across representations and compared them between trained and untrained animals: We hypothesised that hippocampal representation of a moving object depends on its behavioral importance. To test this hypothesis we looked at unit responses from trained and untrained animals across sessions and reference frames. Further, we looked at how

coherence, spatial information and information per spike changed, across reference frames and also compared them across trained and untrained animals.

3. Methods

3.1 Animals and experimental set-up

Male Long-Evans rats aged three months (N=15) from the breeding colony of the Institute of Physiology, Czech Academy of Sciences, Prague were used. The animals were given at least two weeks for acclimatization before starting the experiment. Each animal was housed in a separate plastic cage in a temperature-controlled room (22±2 °C) with a 12h light/12h dark cycle (lights on at 6:00 am). Animal training and recording were performed during the light phase of the day. Water was freely available. Diet was restricted to maintain the rats at ≥ 80**%** of their free-feeding weight. The rats weighed between 250-300g at the start of the experiment. All animal procedures were approved by the committee for the ethical treatment of animals and animal welfare at the Institute of Physiology, Czech Academy of Sciences and by the departmental committee of the Czech Academy of Sciences (Project of Experiments No. 136/2013), and complied with the Animal Protection Act of the Czech Republic and European Union directive 2010/63/EC.

Animals (electrophysiology experiments)

For electrophysiology experiments, rats were trained only to avoid one of the sides of the black and white robot (see below for details). This was done because side avoidance allows us to compare two zones that are more similar. Post completion of behavioral training rats were implanted with 32 channel versadrives (Neuralynx, Bozeman, MT). The data for electrophysiology analysis was used from three untrained rats and one trained rat. These four rats were separate from 15 rats used in the behavioral experiment. Trained rats were retrained to criteria followed by probe sessions, post implantation and recovery. After these probe sessions, the electrophysiology recording started.

Experimental set-up

Prior to the experiment, a miniature connector was attached to the skull of each rat using bone screws and dental cement under isoflurane anesthesia. Animals were given postoperative care (antibiotics and analgesics) and left for at least 7 days for recovery. The connector was used to attach colored marks (blue and red) for tracking the rat's position and head direction during behavioral testing. Similar marks of different colors (orange and yellow) were used to track the position and orientation of the robot.

The behavioral experiments were performed on an elevated circular arena (130 cm in diameter) with a transparent plastic wall (50 cm high; for arena schematic see figures 3.5A and 3.5B). The window of the experimental room was darkened, so the room was without natural light and was lit by two tube lights housed in a louver fixture, used for typical indoor office lighting. The rats were trained to avoid a circular shock zone (39 cm in diameter) defined by its position relative to a moving Arduino-programmed robot (16 cm long, 12 cm wide, and 10.5 cm tall). The rats were randomly divided into three groups according to the position of the shock zone: the shock zone was located either 1) in front of the robot (figure 3.5A), or 2) on the left (figure 3.5B) or 3) right side of the robot. Custom-made software (Kachna tracker, author Tomáš Mládek) tracked the position and orientation of both the rat and the robot. Whenever the rat entered the shock zone, it received a mild foot-shock (0.2-0.5 mA, constant current, 50 Hz) lasting 500 milliseconds and repeated after 400 milliseconds until departure from the shock zone. The current level was adjusted for each rat between 0.2-0.5 mA to the lowest level that elicited avoidance behavior. The shock was delivered between two electrodes. One electrode was made of a cable hanging from above the arena and connected via an alligator clip to a piercing ring made of a syringe needle attached to the rat's skin between shoulders. The metal surface of the arena served as the other electrode. The impact of the electric current was localized to the point of the greatest resistance between the paws and the arena. Two robot designs were used: in the first design, the robot was painted white with a black drawing of a stylized cat face at the front, tail at the back and two legs on each side (black and white robot – B&W – left side of figure 3.5A and B). The second robot design was all-white (right side of figure 3.5A and B). The rats were trained with the B&W robot initially and later, the rats were trained with the all-white robot. The rats were trained gradually over successive sessions, first with the robot stationary, then slow-moving (2 cm/s) and finally, fast-moving (4 cm/s). The robot was programmed to move randomly in close to linear trajectories (resembling an arc with a large diameter) until it hit the wall of the arena; then it waited for 15 seconds, moved backward 10 cm and turned at a random angle between 100º and 200º and continued moving forward (Ahuja et al., 2020).

3.2 Versadrive construction and surgical procedure

Male (Long Evans) rats were implanted with 32 channel versadrive (Neuralynx, Bozeman, MT). One of the tetrode holders was used to hold reference wires (76 microns in diameter; California Fine Wire, Grover Beach, CA) which were implanted over the cerebellum. These wires served as reference for EEG. The tetrodes (figure 3.1A) were made by twisting (John O'Keefe & Recce, 1993) four nichrome wires (25.6 microns;

California Fine Wire) followed by heating with a heat gun so to form a bundle. The proximity of the tips of each wire within a tetrode allowed us to record from the same cells, simultaneously (figure 3.1A and B). This was useful in separating neurons as the action potential of any two neurons might look similar on some of the four electrodes but they were likely to be different in at least one of the electrodes. The wires were plated with a gold solution (5-10%; Neuralynx) before implantation to reduce impedance to 50-200 kohms, at 1 kHz. Each tetrode was inserted into a guide tube (polymicro glass; Neuralynx), carried by shuttle. The shuttle could be moved in the z plane with the help of a screw. The shuttles carrying the guide tube were assembled with the help of pins into the versadrive assembly (figure 3.1C). This configuration allowed for the independent movement of one tetrode from another. This allows the experimenter to implant electrodes above the CA1 cell layer and then Each full turn of the screw moved the tetrode by 250microns. The use of drive allows electrical and mechanical connections between the recording electronics and electrodes and it also allows for chronic recording.

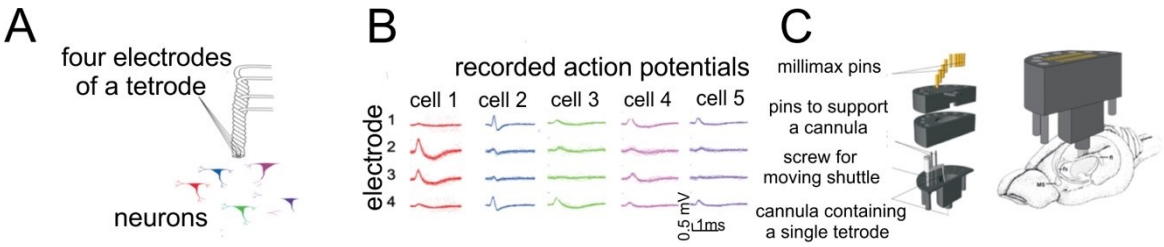

Figure 3.1. Schematics of tetrode and versadrive. (A) Schematic of a tetrode consisting of four electrodes twisted together. Electrodes are positioned in such a way that they record action potentials emitted by the same cells. (B) The schema illustrates a session when five cells were simultaneously recorded. The average shapes of action potentials from all four electrodes are shown. Note that the action potentials from the cell 3 and cell 4 differ on electrodes 3 and 4 and projection on these electrode space can be used to sort these two cells. Similarly, cell 1 and cell 2 differ on electrodes 1 and 2 and can be sorted in the projection space of these electrodes. (C) A schematic drawing of a versa drive. On the very top are Mill-Max pins to which electrode wires (not shown) are connected. Each tetrode is threaded through a cannula. The cannula is attached to a driving screw by a shuttle (white). The cannula can be moved in the z plane by turning the screw. For simplicity the mechanism of attachment is shown only for one tetrode, in practice, the drive carried eight cannulas, eight driving screws, and eight tetrodes. On the right, drawing of an assembled implant showing its position relative to the rat brain, and the dorsal hippocampus is shown. (Drawing courtesy of Bruno Rivard and Jeremy Barry; from Kelemen., E doctoral thesis).

Surgery

Before the surgery, the tips of the electrode coming out through the base of a versadrive were cut with sharp scissors cleaned in saline, and gold-plated so as to reduce the impedance between 50-200 kohms (figure 3.2).

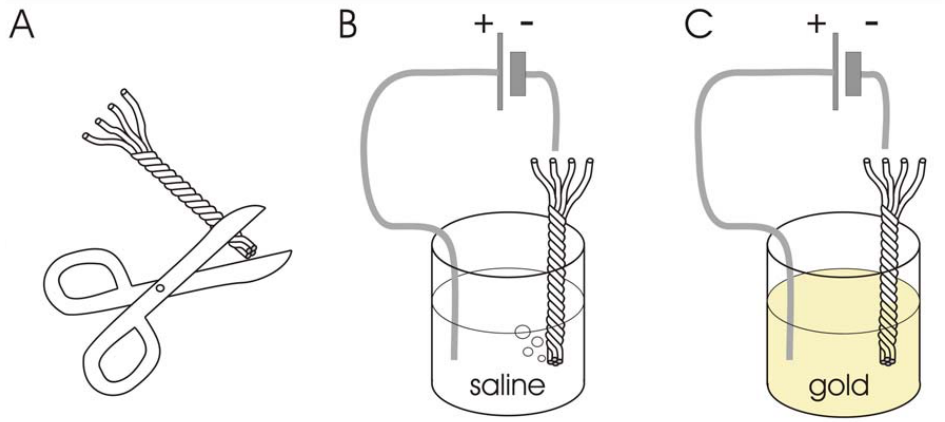

Figure 3.2. Procedure for gold plating tetrodes. (A) Tetrodes were cut at the tip to remove an uneven section, if any. (B) Next, they were cleaned in saline. (C) In the last step, the electrodes were plated with gold. Once the tetrodes were plated their impedance was checked with the impedance meter (from Kelemen, E., doctoral thesis).

The surgery was performed under isoflurane anesthesia. The isoflurane level for induction was 5% while for maintenance it was kept between 2-3%. A thin layer of antibacterial ophthalmic ointment (Vidisic; Bausch and Lomb) was applied to the eyes to keep them moist. The skull was exposed using scissors and scalpel and bregma and lambda were zeroed in the vertical plane. The skull was cleaned to remove any blood marks or muscular tissue debris. The versadrive was implanted above the dorsal hippocampus such that electrodes were centered at a hole made at the following coordinates: 4.2 mm posterior, 2.0 mm lateral to bregma and 1.4-2.0 mm dorso-ventral. The reference for the above coordinates was Paxinos and Watson (1986). Two stainless-steel screws were positioned at the cerebellum and another two screws above the frontal part of the brain. These screws served as ground. Three to four more screws served as an anchor to hold the versadrive to the skull. The versadrive and tetrodes were covered with vaseline to seal the hole. The whole assembly including the screws was daubed with dental cement (Spofa Dental, Czech Republic) as a unit to attach them to the skull surface.

3.3 Unit recording and sorting

After surgery, the animals were given at least one week for recovery. During this time they were given antibiotics and analgesics as part of postoperative care. On recording days, the headstage pre-amplifier was connected to the versadrive implanted on the rat's head. The raw signal was fed into an EEG reference panel, where appropriate references could be selected. This signal was fed to amplifiers (Lynx-8; Neuralynx) from where analog output was fed to an analog to digital converter (Power 3 1401; Cambridge Electronic Design, Cambridge, England). The software for Lynx-8 amplifiers was used to

set filter and gain parameters. The signal was filtered between 1-475 Hz and digitized at 2 kHz for EEG. For unit recordings, the signal was filtered between 300-9000 Hz and digitized at 32 kHz. The electrode with the least background activity was chosen as the reference. The reference changed across days if another electrode fitted the criteria better. The recording software was Spike 2, Version 7.20 (Cambridge Electronic Design). Whenever a trigger level (voltage threshold) was crossed, the software recorded 2 milliseconds (ms) of unit data. Two trigger levels were available, one for negative going and another for positive going signal (figure 3.3). For our recordings, we used the positive trigger. The captured spikes were aligned on the first positive peak. The data capture routines in Spike 2 use a high pass filter to avoid problems due to baseline drifting (Spike 2 version 7 manual). The spike detection algorithm worked as follows:

1) Wait for the signal to lie within half the trigger levels. If it does then move to step 2.
2) Wait for the signal to cross either trigger level. Upon crossing the positive trigger level move to step 3. If it crosses the negative level go to step 4.
3) Track the positive peak signal value. If the signal falls lower than the peak and if sufficient post-peak points are available to define a spike then go to 5. If the signal falls below half the positive trigger level, further peaks were ignored as shown for second spike.
4) Track the negative peak signal value. If the signal rises above the peak, see if we have sufficient post-peak points to define the spike. If available, go to 5. If the signal rises above half the lower trigger level, the further peaks were ignored.
5) Save the waveform and first data point time and go to step 1 for the next spike.

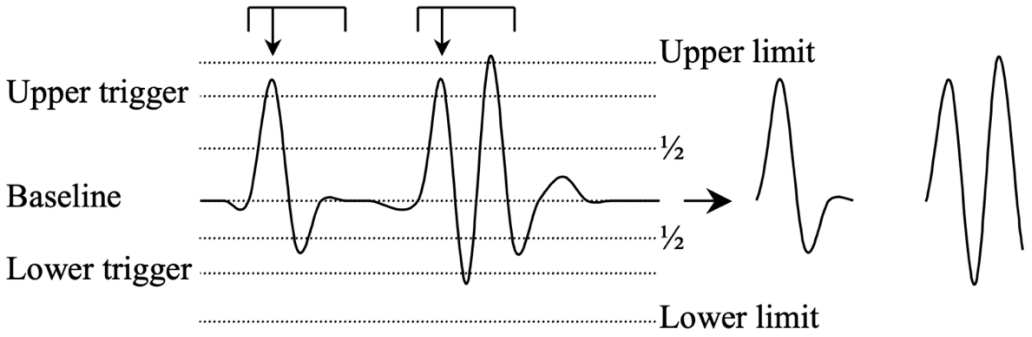

Figure 3.3. Schematic of spike detection in Spike 2 software. Two example spikes are depicted to explain the spike capturing algorithm (Spike 2 manual, CED).

As the tetrodes were implanted above the hippocampus they were moved over a period of two weeks. Each time the screws were moved by 30-60 microns to bring them close to the pyramidal cell layer of CA1. The experimenter waited for at least 4 hours before starting the recording and the signal was checked for the presence of units. The activity in deeper layers of the cortex was characterized by less dense spiking than in the

hippocampal pyramidal layer. When tetrodes reached the upper layers of CA1, ripples (150-250 Hz) were observed riding on sharp waves mostly when the animal was resting. Sharp waves appeared as deflection in the signal and the direction of deflection reversed near the pyramidal cell layer. The tuning was based on unit yield. If the action potentials from putative pyramidal cells were not found or the cells were not separable due to low amplitude, tetrodes were further moved by turning the screws. Fine adjustments were performed if required at the start of the recording day, with a gap of one hour between screw movement and the start of recording. Experiments started once the minimum number of cells were present.

Unit sorting

After the spikes were recorded, they were sorted manually and automatically using the capabilities of Spike 2 inbuilt sorter (figure 3.4). The parameters available for sorting included maximum (positive peak) and minimum (negative peak) amplitudes, the amplitude at various time points of the 2ms signal, slope, etc. The underlying assumption for sorting was that spikes from a single unit will have a similar shape on the four electrodes. For each recorded spike there were four signals from a tetrode, i.e. one signal per electrode of a tetrode. The signal from any of these wires was used to sort the spike by plotting each point, representing a single spike in a scatter plot. The X-axis and Y-axis of the plot chosen were positive peak amplitude (figure 3.4A) or principal component on a wire versus the same parameter on another wire of the same tetrode. During spike sorting, spikes with similar characteristics were organized into clusters. The recorded spikes usually formed several clusters depending on unit yield and each cluster was accepted to be a putative cell.

Principal component analysis – It is a mathematical method that reduces the dimensionality of the data while retaining most of the variation in the data set. The dimensions are reduced by identifying variables or directions, called principal components, along which there is maximal variation in the data. This allows the representation of the sample by few components instead of by values for thousands of variables (Ringnér, 2008).

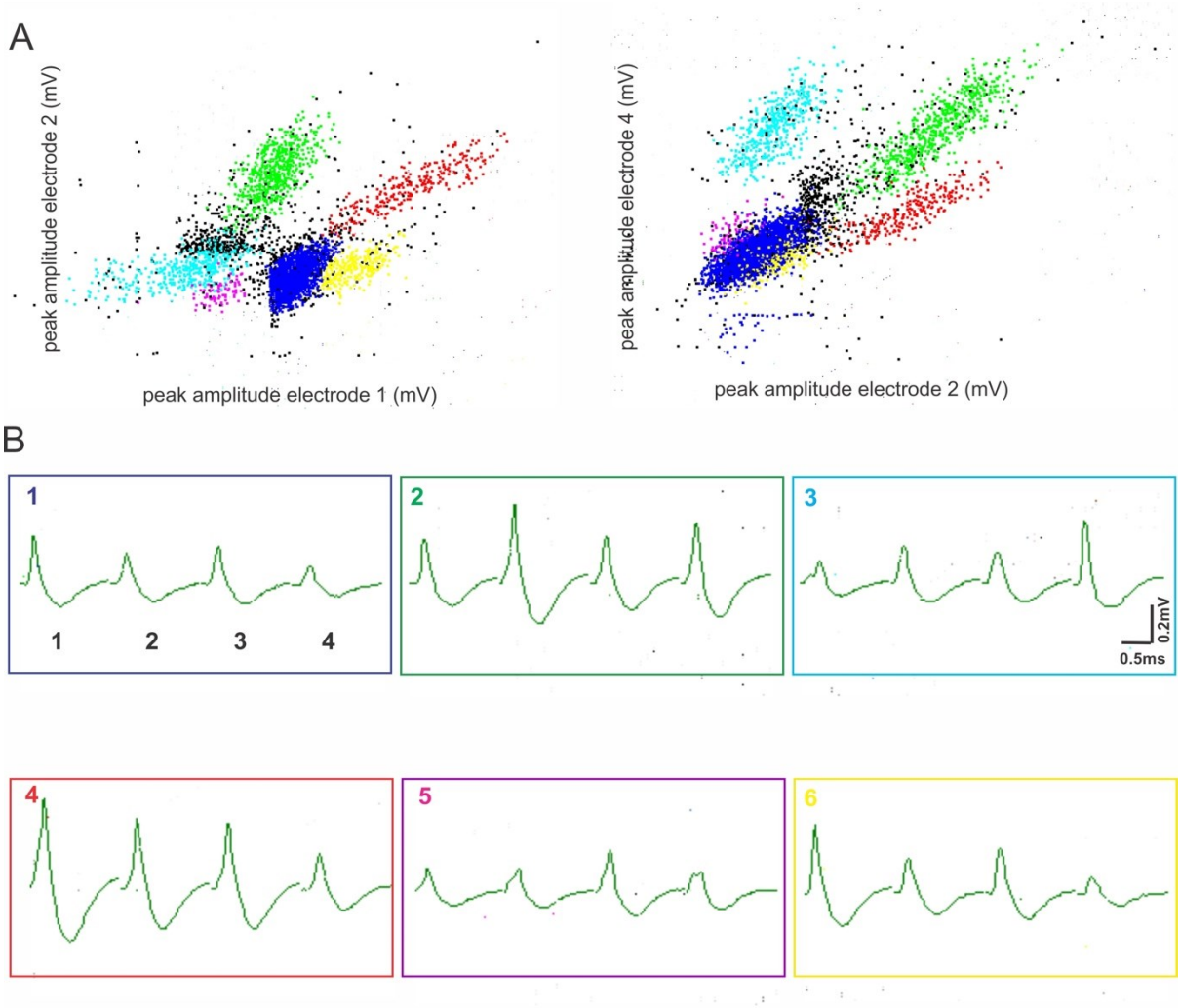

Figure 3.4. Spike sorting in Spike 2 (CED, Cambridge, UK). A) shows clustering strategy, recorded spikes were clustered based on peak amplitude on different wires of a tetrode, on the left spikes are clustered based on a scatterplot of peak amplitude on electrode 1 vs 2 and on the right electrode 2 vs 4. Clusters are color-coded. B) average spikes from four electrodes of a tetrode for each cluster are shown in boxes in a color-coded manner.

Separation between interneurons and pyramidal cells

The recorded units were divided into complex spike cells (CSCs) - putative pyramidal neurons and theta cells - putative interneurons using standard criteria (Ranck, 1973). Complex spike cells have low spontaneous firing rate (about 1 Hz), have broader spikes and display complex spike burst pattern in which later spikes are of low amplitude and longer duration. In contrast, theta cells have high firing rate (10-100Hz) and all spikes of same amplitude and shorter duration (John, 2006).

3.4 Behavioral training procedure and testing protocol

In Experiment 1, one group of rats (N=5) was trained to avoid a shock zone in front of the robot (figure 3.5A), and in Experiment 2 another group of rats (N=10) was trained to avoid the left or right side of the robot (figure 3.5B; Ahuja et al., 2020). The position of the shock zone (left or right) was fixed for each rat for all the experiments. Rats in both experiments were subjected to the same four-stage training and shaping protocol, which only differed in the shock zone location.

Stage 1 - Foraging without the robot: After a week of handling, rats were trained to forage for pasta pellets on the arena without the robot present. The pellets served to reinforce the rats to walk on the arena throughout all subsequent stages of the experiment. Rats had three 10-minute foraging sessions per day with 10 to 15 minutes intervals between the sessions and were trained until they walked ≥40 meters per session in three subsequent sessions. The rats reached this criterion in three to five days.

Stage 2 - Avoiding the stationary robot: The animals were trained to avoid a shock zone in three 10-minute daily sessions with a stationary robot, with 10- to 15-minute intersession intervals. The position of the robot was changed between sessions but did not change within a session. The animals were trained until they reached the criterion of ≤ 8 entrances to the shock zone per session across three consecutive days. The rats reached this criterion in one to two weeks with the B&W robot, and within one week with the all-white robot.

Stage 3 - Avoiding the slow-moving (2 cm/s) robot: The transition from stationary to slow-moving sessions was gradual. Of the three training sessions performed each day, the first two (later in training only the first one) were with the stationary robot and the last one (later, the last two) were with a slow-moving robot. The animals were trained under these conditions until the criterion of ≤ 8 entrances to the shock zone per session across three consecutive days was reached. The rats reached this criterion in one to five weeks with the B&W robot, and within two weeks with the all-white robot. The criterion was reached faster by rats that had to avoid the front of the robot. After the criterion was met, two subsequent sessions with the slow-moving robot were used to characterize and statistically evaluate each animal's performance, as is presented in the Results section.

Stage 4 - Avoiding the fast-moving (4 cm/s) robot: During this stage, the rats were trained in three sessions a day: the first was stationary, the second was with the slow-moving robot, and the third with the fast-moving robot**.** By the end of the training with the fast-

moving robot, the rats were undergoing one stationary, and two fast sessions each day. The rats were trained until they reached the criterion of ≤ 8 entrances to the shock zone per session across three consecutive days. The rats reached this criterion in one to five weeks with the B&W robot, and within two weeks with the all-white robot. The criterion was reached faster in rats that had to avoid the front of the robot. Their performance was analyzed and statistically evaluated in two subsequent fast-moving sessions.

After the rats learned the task, their performance was tested in probe sessions that were performed in the same way as the reinforced sessions except that shocks were not delivered. Probe sessions with the slow-moving (2 cm/s) and fast-moving (4 cm/s) robot were performed on different days, with at least two days of reinforced training in between.

After avoidance behavior was characterized in well-trained rats using the B&W robot (figures 3.5A left, 3.5B left, 4.2A, 4.3A, 4.2B and 4.3B), we proceeded to assess whether avoidance depended on recognition of prominent visual patterns painted on the robot. With the all-white robot we followed the same protocol as with the B&W robot (figures 3.5A right, 3.5B right, 4.2C, 4.3C, 4.2D and 4.3D). We first trained the rats until they reached stable avoidance behavior and then performed probe sessions. Example sessions from front and side avoidance are shown in figure 3.5C, D, E and F.

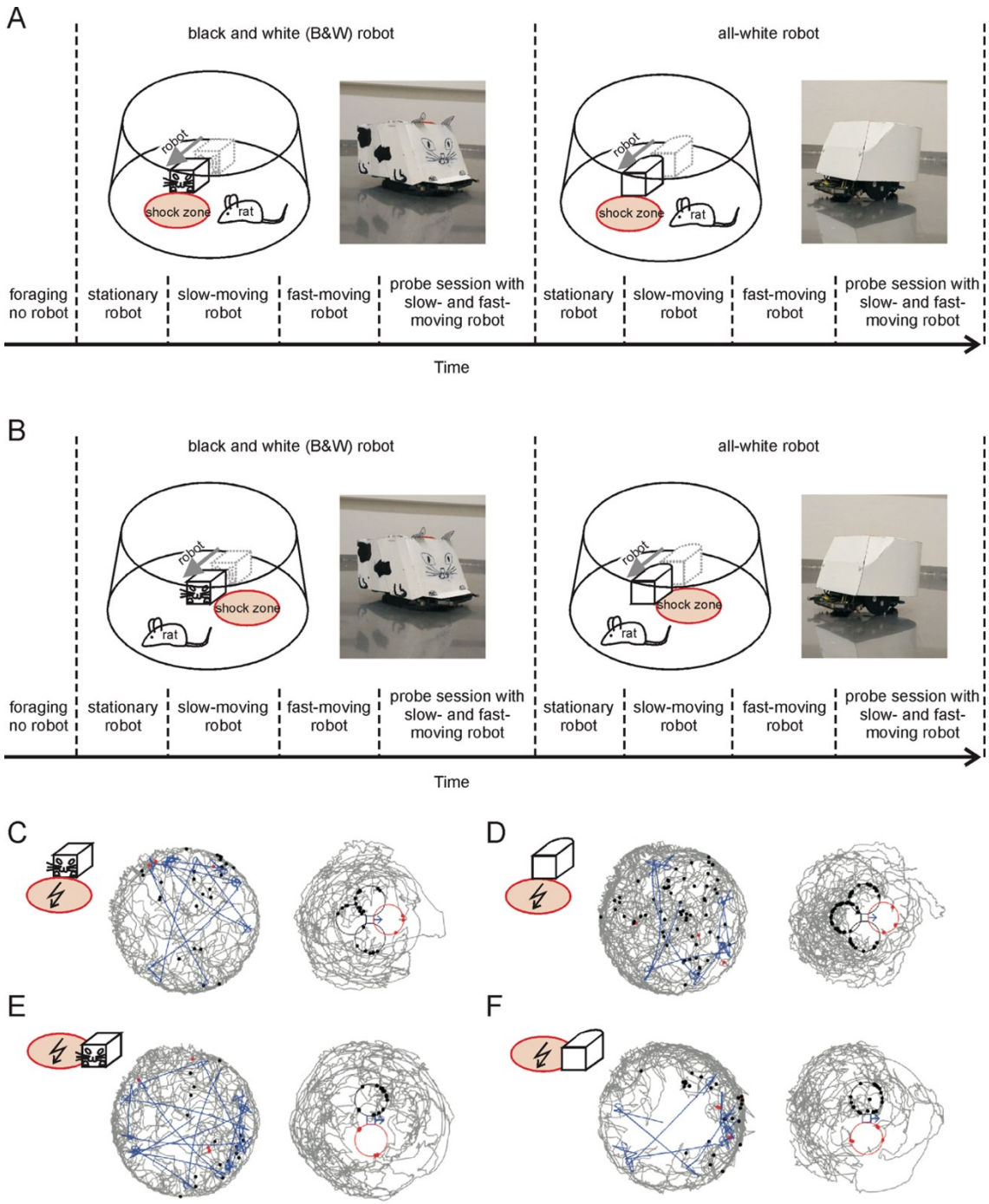

Figure 3.5. Schematic of behavioral paradigm for avoiding a specific zone around the robot and example sessions. (A) Protocol of experiment 1, where the rat avoided a shock zone in front of the robot. The upper left plot shows a schematic of the arena, a rat, and B&W robot with the shock zone at the front. In the adjacent figure, a photograph of the B&W robot is shown; the upper right, shows a schematic of the arena, rat, and all-white robot with the shock zone at the front, and a photograph of the all-white robot. The lower part depicts the timeline of the experiment. (B) Protocol of experiment 2, where a rat avoided the shock zone on one side of the robot. Plots are organized in a way analogous to panel A. (C) Example session of avoidance of the shock zone in front of the B&W robot. The left plot shows the trajectory of a rat (gray) and the robot (blue) on the arena. The right plot shows the trajectory of a rat relative to the robot, which is approximately in the middle of the plot. The shock zone is shown by a red circle, other equidistant safe zones are marked by black circles. Red dots indicate points of rat's entrance to the shock zone and black dots indicate points of entrance to the safe zones. (D) Example session with the shock zone in front of the all-white robot. (E) Example session with the shock zone on the right side of the B&W robot. (F) Example session with the shock zone on the right side of the all-white robot (Ahuja et al., 2020).

Electrophysiology testing protocol

Once the animals were trained, they were implanted with 32 channel versadrive (Neuralynx, Bozeman, MT). They were then retrained to criteria followed by probe sessions, post recovery. After these probe sessions, the electrophysiology recording started. During this period, each recording day was followed by a training day, on which three sessions with the robot were conducted. These three sessions were: one stationary and two fast moving robot sessions in that order. Two important differences between these days were that on each recording day the shock was switched off and four sessions were conducted instead of three. The details are as follows:

Electrophysiology recording days – The four sessions conducted were, no robot (only rat foraged on the arena; session 1), stationary robot (rat with the stationary robot; session 2), fast moving robot (4cm/s; session 3) and no robot (session 4), respectively. Each session lasted 10 minutes and shock was off throughout the sessions, inter-sessions interval was also 10-15 minutes. In no robot sessions, the rats foraged for pellets dropping from the overhead feeder but with no robot on the arena. The first and last no robot sessions allowed us to test the stability of firing fields and cell firing in general.

Analysis within the moving session (session 3) was performed in different reference frames as shown below (figure 3.6):

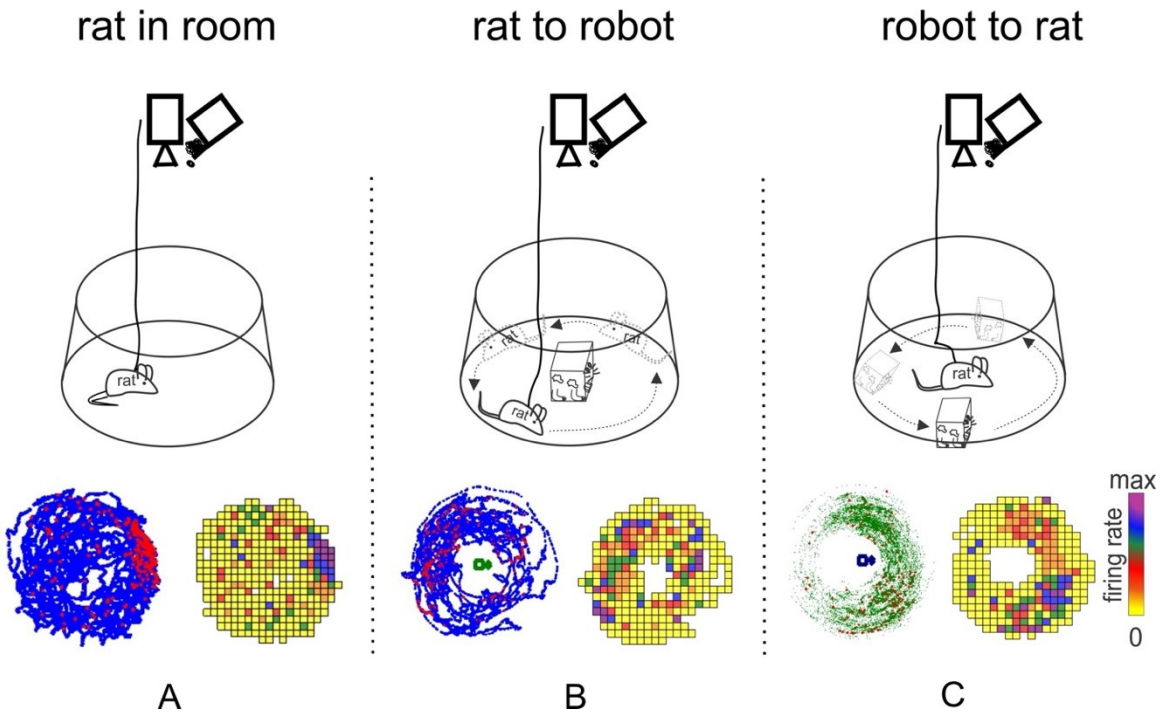

Figure 3.6. Schematic of different reference frames used in the analysis: rat in room. (A) In this frame rat's position on the arena was superimposed on the spiking activity for a cell across the time frame of the session; rat to robot. (B) In this frame the moving robot was brought to the center of the arena (post hoc) and rat's position with respect to the robot was superimposed on the spiking activity; robot to rat (C) In this frame the moving rat was brought to the center of the arena (post hoc) and robot's position with respect to the rat was superimposed on the spiking activity. Shown below are the spike map and firing rate map for a place cell in different reference frames. Firing rate (Hz) is coded on a color scale from yellow (silent) to magenta (maximum rate).

Training days – On these days the animals underwent three sessions, each lasting 10 minutes, intersessions interval 10-15 minutes. These were the same as were done during the behavioral training and were conducted to reinforce the side avoidance behavior. The switching off of the shock during electrophysiology recordings would lead to the extinction of side avoidance behavior making it necessary to have intervening training days.

3.5 Data analysis

To characterize and quantify avoidance behavior in experiment 1 (see figure 3.5A above), the number of the rat's entrances to the shock zone in front of the robot was compared to the mean number of entrances to the three equidistant safe zones on sides of and behind the robot (figures 3.5C and D). The proportion of entrances to the shock zone P(shock) was calculated as:

Equation 1:

$$\mathrm{P(shock)} = \frac{\mathrm{N(shock)}}{\mathrm{N(shock)} + \mathrm{N(safe)}}$$

Where N(shock) is the number of shock zone entrances and N(safe) is the number of entrances to all three safe zones. The mean proportion of entrances to the safe zones P(safe) was calculated as:

Equation 2:

$$\mathrm{P(safe)} = \frac{\mathrm{N(safe)}}{\big(\mathrm{N(shock)} + \mathrm{N(safe)}\big) * 3}$$

Where N(shock) is the number of shock zone entrances and N(safe) is the number of entrances to all three safe zones. Analogous formulas were used to calculate the proportion of time spent in the shock zone and the proportion of time spent in safe zones during probe sessions.

To characterize and quantify avoidance behavior in Experiment 2 (figure 3.5B), the number of the rat's entrances to the shock zone on one side of the robot was compared to the number of entrances to the safe zone on the opposite side of the robot (figures 3.5E and F). The proportion of entrances to the shock zone P(shock) was calculated as:

Equation 3:

$$\mathrm{P(shock)} = \frac{\mathrm{N(shock)}}{\mathrm{N(shock)} + \mathrm{N(opposite)}}$$

Where N(shock) is the number of shock zone entrances and N(opposite) is the number of entrances to the opposite safe zone. The proportion of entrances to the safe zone P(opposite) was calculated as:

Equation 4:

$$\mathrm{P(opposite)} = \frac{\mathrm{N(opposite)}}{\mathrm{N(shock)} + \mathrm{N(opposite)}}$$

Where N(opposite) is the number of safe zone entrances and N(shock) is the number of shock zone entrances. Analogous formulas were used to calculate the proportion of time spent in the shock zone and the proportion of time spent in the opposite safe zone during probe sessions.

The data were analyzed using custom scripts (E. Kelemen) written in MATLAB (MathWorks, MA, USA). For statistical analysis, we used Graphpad PRISM 7 (San Diego,

CA, USA). Statistical significance was tested at $\alpha = 0.05$. For behavioral analysis one-tailed, paired t-tests were used. This analysis include the following parameters: proportion of entrances to shock and safe zones, proportion of time spent in each zone, time to first entrance, average rat-robot distance (cm), minimum rat-robot distance (cm), average rat speed (cm/s), maximum rat speed (cm/s), visit path (cm) and visit duration (sec).

For electrophysiological data the following analysis were used: to compare coherence, spatial information and information per spike across reference frames we used RM, one-way ANOVA. To compare each measure between trained and untrained rats we used two-tailed, unpaired t-test.

Characterization of the spatial firing of place cells

We have used two methods to depict spatially organized firing of hippocampal neurons - a spike plot and firing rate map (lower part of figure 3.6). In the above behavioral task, the rat's position can be defined in the room frame as well as in the robot frame, further, the robot's position can be defined in the rat frame. Thus we constructed spike plots and firing rate maps for all these reference frames (see figure 3.6). Further, we used two parameters, spatial coherence and information content to quantitatively characterize the spatial organization of place cell firing.

Spatial coherence

It is the first-order spatial autocorrelation, an estimate of the orderliness of the spatial firing distribution (Kubie et al., 1990; Muller & Kubie, 1989). It characterizes similarity in the firing rate between adjacent pixels of a firing rate map. It is the z-transform of the Pearson's correlation between firing rates of each pixel and the average firing rate in 8 nearest-neighbors of each pixel. The average firing rate of the eight pixels is calculated by dividing the spike count in the eight pixels by the time spent in the eight pixels. Positive coherence values indicate the presence of a spatial determinant of firing whose spatial frequency is lower than the distance between adjacent pixels.

Information content

A measure that denotes information about the rat's position in an environment encoded by the neuron's activity. It was introduced by Skaggs et al. (Skaggs et al., 1993). The following formula computes the information for a neuron:

Equation 5 (Knierim et al. 1998):

$$I = \sum_j p_j \ \lambda_j \ \log_2 \frac{\lambda_j}{\lambda}$$

Equation (5) denotes the formula for computing information content and its unit is bits per second.

If we divide the equation (5) by λ, mean firing rate, it gives us the information per spike equation (6) and its unit is bits per spike.

Equation 6:

$$I = \sum_j p_j \ \frac{\lambda_j}{\lambda} \log_2 \frac{\lambda_j}{\lambda}$$

Where if a cylinder is divided into square bins, I is the information in bits per spike, pj is the probability of the rat occupying bin j, λ_j is the mean firing rate for bin j, and λ is the mean firing rate for the cylinder.

It is a measure of information about the rat's position conveyed by a single spike from the neuron (Knierim et al., 1995) and thus a measure of spatial tuning. It is a good measure of whether a cell has a statistically significant spatial firing bias.

4. Results

4.1 Behavior in the modified robot avoidance task

In this chapter, I will start by mentioning how much time did rat spent in each phase of training. Then I will move onto the description of the rats' performance and behavior in the modified robot avoidance task. The avoidance behavior in this task is based on recognizing geometrical spatial relationships relative to the moving object. The data shows that rats can navigate according to their position relative to a moving object. In recognizing their position relative to the moving object, rats do not rely only on prominent simple stimuli, such as increased noise levels, the size of the retinal image of an object, or particular visual patterns characterizing the object.

Average training time

The average training time across stages is described below (Table 1). On average rats took more time in each stage in the side avoidance protocol compared with the front avoidance. The average time in a particular stage varied from 3 to 17 days. The animal spent more time in all stage in B&W robot condition compared with the all-white robot. This is likely due to the fact that they were first trained with the B&W robot followed by all-white robot. The cumulative curves for each training condition and phase are shown in figure 4.1.

	Stationary	**Slow**	**Fast**
Front avoidance/B&W robot			
Average time to criterion (days)	8	14.2	8
SEM (days)	0.447214	4.673329	0.447214
Front avoidance/all white robot			
Average time to criterion (days)	3	4.8	5.4
SEM (days)	0	0.734847	1.122497
Side avoidance/B&W robot			
Average time to criterion (days)	8.7	16.9	12.2
SEM (days)	0.334996	2.77608	2.803965
Side avoidance/all white robot			
Average time to criterion (days)	4	7.4	7
SEM (days)	0.421637	0.669992	0.298142

Table 1. Average training time across stages and conditions. The table shows the average time required to reach the criterion for three phases of training, stationary, slow and fast along with the variation among animals (standard error of the mean, SEM) (Ahuja et al., 2020).

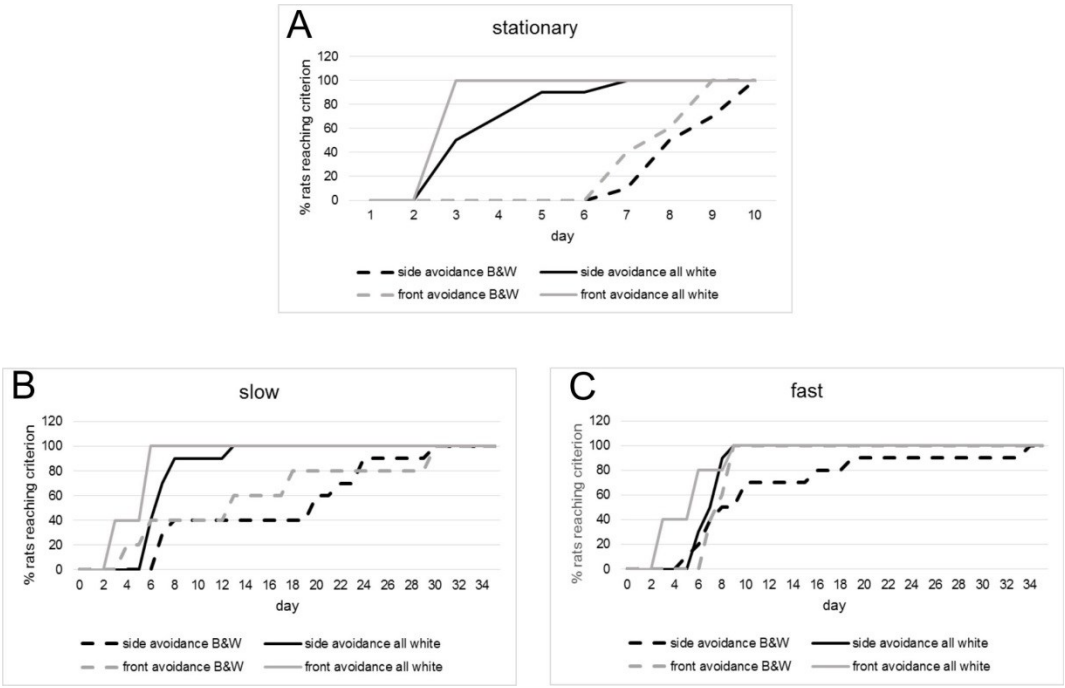

Figure 4.1. Cumulative curves for each training condition and phase. A, B and C show percentage of rats achieving the behavioral criterion (≤ 8 entrances to the shock zone per session across three consecutive days) on different days of training for stationary, slow and fast phases of training (Ahuja et al., 2020).

Experiment 1: Rats can organize their behavior relative to a moving robot

We used five rats to study whether the animals can learn to avoid a shock zone in front of the moving robot (Ahuja et al., 2020). After foraging for up to five days on an empty arena, the rats were trained gradually to avoid a black and white moving robot for approximately four weeks. On each day, the rats underwent training for three sessions each lasting 10 minutes. This experiment showed that the rats avoided the shock zone in front of the moving robot. After completion of the training with the B&W robot, the animals were tested in probe sessions. In probe sessions, the avoidance was not reinforced by the foot shock. Following probe sessions with the B&W robot, training with the all-white robot was carried out. This training lasted approximately two weeks followed by testing in probe sessions. The performance of well-trained rats during example sessions avoiding the B&W robot and the all-white robot is shown in figure 3.5C and 3.5D (methods), respectively.

The rats were trained to the criterion of ≤ 8 entrances to the shock zone per session across three consecutive days, according to the training protocol described in the Methods section (Ahuja et al., 2020). The performance of all five rats during the first two post-criterion sessions is depicted in the left column of figure 4.2 for each of the four experimental conditions: 1) slow-moving (2 cm/sec) B&W robot (figure 4.2A), 2) fast-

moving (4 cm/sec) B&W robot (figure 4.2B), 3) slow-moving all-white robot (figure 4.2C) and 4) fast-moving all-white robot (figure 4.2D). The animals' tendency to enter the shock zone less than safe zones is shown by data points above the diagonal in plots in the left column of figure 3.2. With progressive training, the number of shock zone entrances decreased to 2.5±0.8, while the number of entrances to the safe zones remained at 5.8±0.9 in two post-criterion sessions with the fast-moving all-white robot (figure 4.2D).

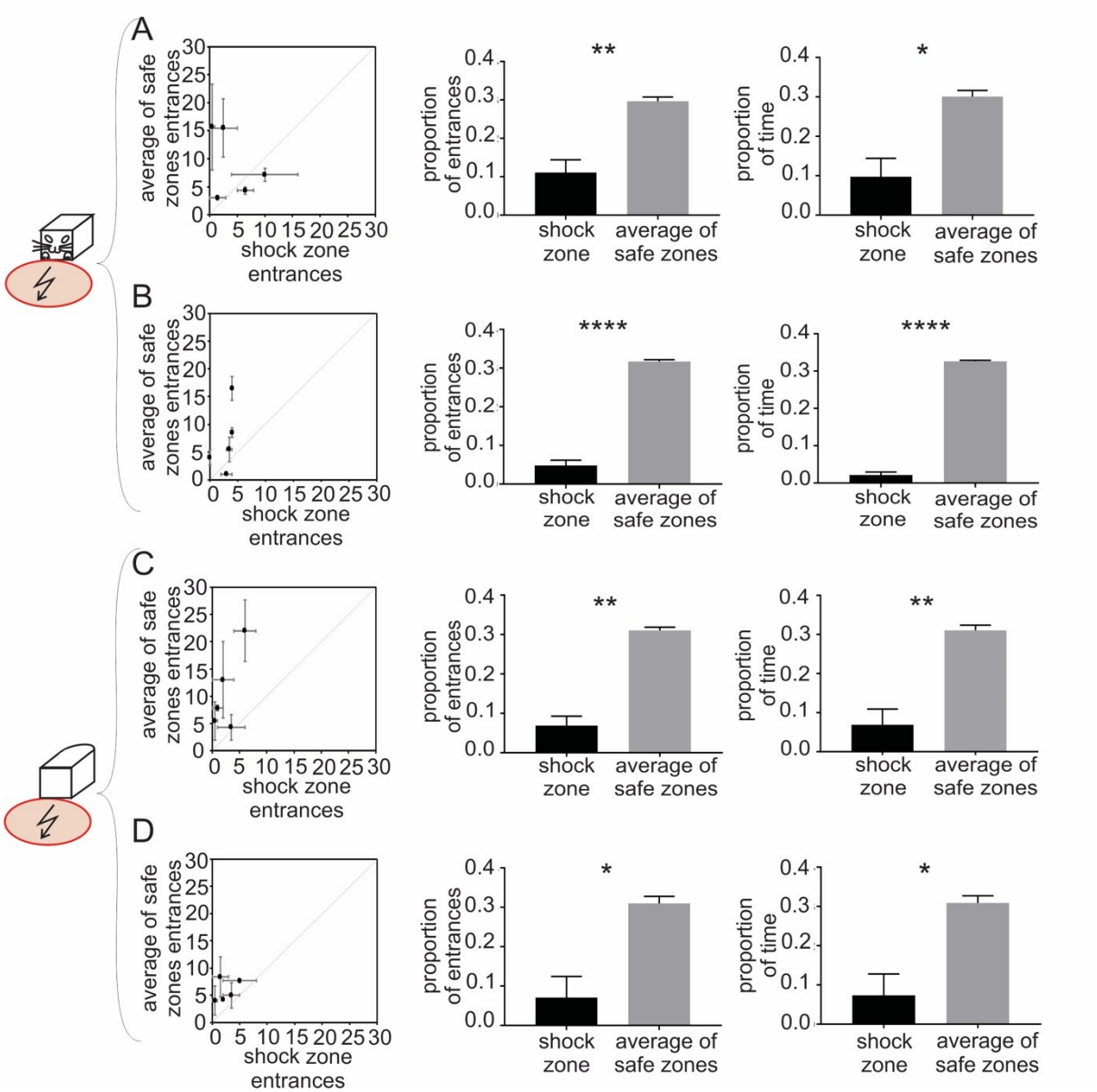

Figure 4.2. Entrances and time spent in front versus average of safe zones. Experiment 1 – Avoidance of a shock zone in front of the robot. Data from slow-moving B&W robot (A), fast-moving B&W robot (B), slow-moving all-white robot (C) and fast-moving all-white robot (D) are shown. Left scatter plots show the number of entrances to the shock zone *versus* the mean number of entrances to the three safe zones, during two reinforced sessions after the training criteria was met for each of five rats (see Methods). Central figures quantify entrances to the shock zone and safe zones in unreinforced probe sessions. Right figures show time spent in the shock zone and safe zones in unreinforced probe sessions. Plots show means ± SEM. *p<0.05, **p<0.01, ****p<0.0001 (Ahuja et al., 2020).

In probe sessions, both the proportion of entrances to the shock zone ($t(4) = 4.167$ $p = 0.007$, one-tailed, paired t-test, figure 4.2A, middle) and time spent in the shock zone

($t(4) = 3.264$, $p = 0.015$, one-tailed, paired t-test, figure 4.2A, right) were significantly smaller than in corresponding safe zones for the B&W slow-moving robot. The median values for proportion of entrances in front and average of safe zones were 0.1220 and 0.2927, respectively and for time spent the values were 0.05791 and 0.3140, respectively. For the B&W fast-moving robot, both the proportion of entrances to the shock zone ($t(4) = 14.79$, $p < 0.0001$, one-tailed, paired t-test, figure 4.2B, middle) and time spent in the shock zone ($t(4) = 28.99$, $p < 0.0001$, one-tailed, paired t-test, figure 4.2B, right) were significantly smaller than in corresponding safe zones. For proportion of entrances, the median values were 0.05882 and 3137 for front and average of safe zones, respectively and for time spent the values were 0.02570 and 0.3248, respectively. In the case of the all-white slow-moving robot, both the proportion of entrances to the shock zone ($t(4) = 6.61$, $p = 0.0014$, one-tailed, paired t-test, figure 4.2C, middle) and time spent in the shock zone ($t(4) = 4.277$, $p = 0.0065$, one-tailed, paired t-test, figure 4.2C, right) were significantly smaller than in corresponding safe zones. The median values for proportion of entrances were 0.07692 and 0.3077, respectively, for front and average of safe zones; and for time spent the values were 0.1137 and 0.2954, respectively. For the all-white fast-moving robot, both the proportion of entrances to the shock zone ($t(4) = 3.332$, $p = 0.0145$, one-tailed, paired t-test, figure 4.2D, middle) and time spent in the shock zone ($t(4) = 3.247$, $p = 0.016$, one-tailed, paired t-test, figure 4.2D, right) were significantly smaller than in corresponding safe zones. The median values for proportion of entrances were 0.000 and 0.333 for front and average of safe zones, respectively, and for time spent, the values were 0.01053 and 0.3298, respectively.

Experiment 2: Rats can avoid a shock zone on one of the sides of the robot

We used ten rats to explore whether rats can be trained to avoid a shock on either side of a moving robot (Ahuja et al., 2020). This is inherently a difficult task compared with front avoidance, as the left side and right side of the robot are mirror images of each other. The results showed that the rats can successfully perform this task albeit it took them more time to get trained. The performance of well-trained rats during example sessions avoiding the B&W robot and the all-white robot is shown in figures 3.5E and 3.5F, respectively.

The performance of all ten rats during two post-criterion sessions (see Methods) is depicted in the left column of figure 4.3 for each of the four experimental conditions: 1)

slow-moving B&W robot (figure 4.3A), 2) fast-moving B&W robot (figure 4.3B), 3) slow-moving all-white robot (figure 4.3C) and 4) fast-moving all-white robot (figure 4.3D). The animals' tendency to enter the shock zone less than the safe zone on the opposite side is shown by data points above the diagonal in figures 4.3A, 4.3B, 4.3C, and 4.3D. With progressive training, the number of shock zone entrances decreased to 1.5±0.4, while the number of entrances to the safe zone remained at 4.1±1.9 in two post-criterion sessions with the fast-moving all-white robot (figure 4.3D).

In probe sessions, both the proportion of entrances to the shock zone ($t(8) = 4.696$, $p = 0.0008$, one-tailed, paired t-test, figure 4.3A, middle) and time spent in the shock zone ($t(8) = 11.860$, $p < 0.0001$, one-tailed, paired t-test, figure 4.3A, right) were significantly smaller than in the corresponding opposite safe zone for the B&W slow-moving robot condition. The median values for proportion of entrances in shock and safe zones were 0.5263 and 0.9474, and for time spent the values were 0.009901 and 0.9901. For the B&W fast-moving robot, the proportion of entrances to the shock zone ($t(7) = 1.262$, $p = 0.124$, one-tailed, paired t-test, figure 4.3B, middle) and time spent in the shock zone ($t(7) = 1.369$, $p = 0.107$, one-tailed, paired t-test, figure 4.3B, right) were smaller than in the corresponding opposite safe zone, however this was non-significant. The median values for proportion of entrances in shock and safe zones were 0.2250 and 0.7750, and for time spent the values were 0.2733 and 0.7269, respectively. For the all-white slow-moving robot, both the proportion of entrances to the shock zone ($t(8) = 3.222$, $p = 0.006$, one-tailed, paired t-test, figure 4.3C, middle) and time spent in the shock zone ($t(8) = 3.044$, $p = 0.008$, one-tailed, paired t-test, figure 4.3C, right) were significantly smaller than in the corresponding opposite safe zone. The median values for proportion of entrances in shock and safe zones were 0.00 and 1.00, and for time spent the values were 0.00 and 1.00, respectively.

For the all-white fast-moving robot, both the proportion of entrances to the shock zone ($t(8)= 3.845$, $p=0.003$, one-tailed, paired t-test, figure 4.3D, middle) and time spent in the shock zone ($t(8) = 2.890$, $p=0.01$, one-tailed, paired t-test, figure 4.3D, right) were significantly smaller than in the corresponding opposite safe zone. The median values for proportion of entrances in shock and safe zones were 0.3333 and 0.6667, and for time spent the values were 0.3211 and 0.6789, respectively.

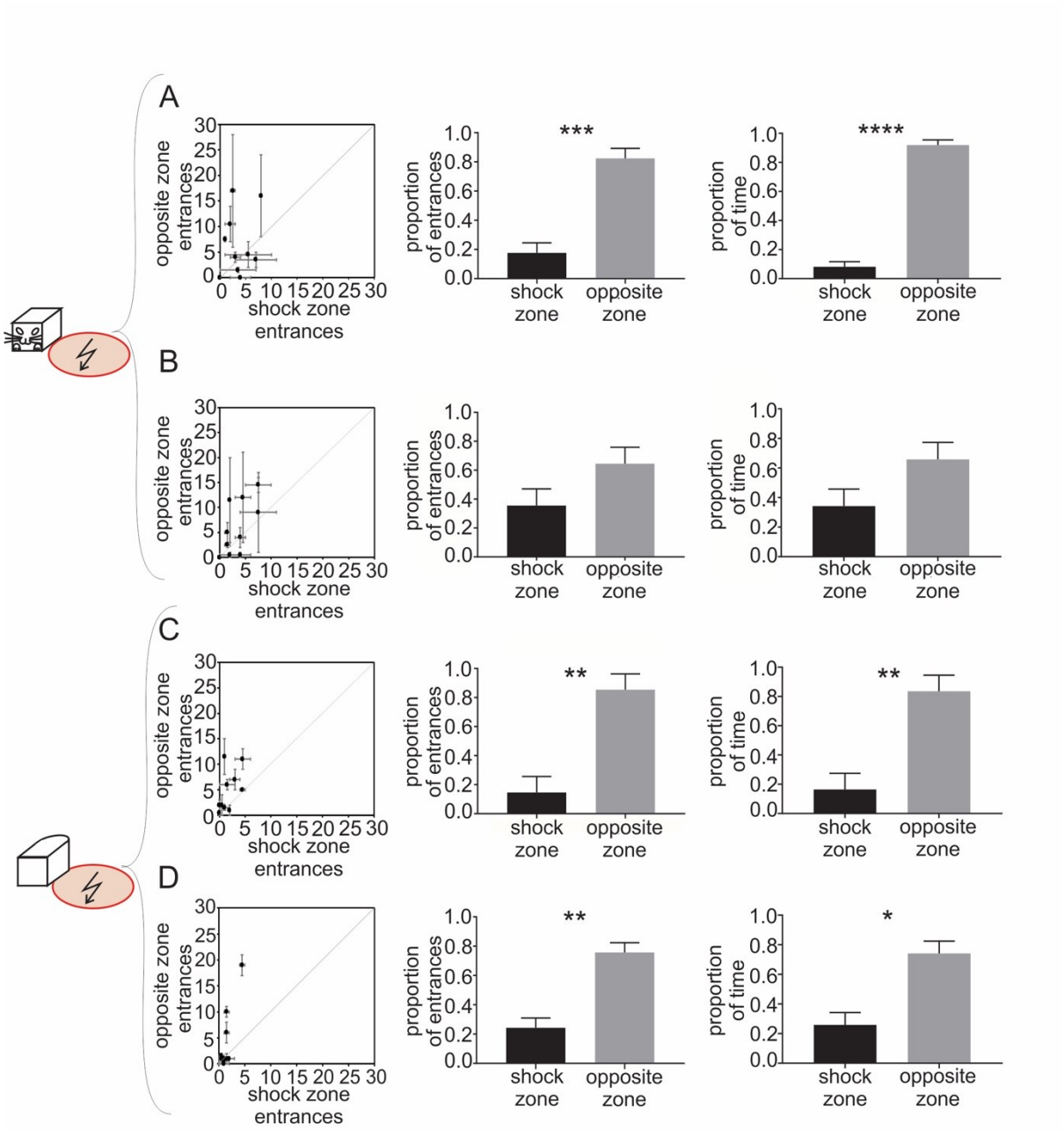

Figure 4.3. Entrances and time spent in shock versus opposite zone. Experiment 2 – Avoidance of a shock zone at the side of the robot. Data from slow-moving B&W robot (A), fast-moving B&W robot (B), slow-moving all-white robot (C) and fast-moving all-white robot (D) are shown. Left scatter plots show the number of entrances to the shock zone *versus* the number of entrances to the safe zone, during two reinforced sessions after the training criterion was met by each of the ten rats. Central figures show the proportion of entrances to the shock zone and safe zone in unreinforced probe sessions. Right figures show the proportion of time spent in the shock zone and safe zone in unreinforced probe sessions. Plots show means ± SEM. *p<0.05, **p<0.01, ***p<0.001, ****p<0.0001(Ahuja et al., 2020).

4.2 Mechanism of avoidance

To further explore the mechanistic details of this avoidance behavior we performed several analyses as mentioned below.

First, we looked at the behavior of untrained rats in moving sessions. These rats were never shocked. We constructed average heatmaps of mean dwell time from eight sessions with a moving robot from these animals (figure 4.4A). Figure in panels B and C are heatmaps from front avoidance and side (right) avoidance, respectively. The average heatmap in figure A shows that untrained rats spent more of their time near the robot, unlike trained rats which avoided the robot in general and specifically the shock zone. This also points to the tendency of rats to be curious about the object rather than being afraid of it if they were not shocked at all. For trained rats, they generally avoided the whole robot during the first few sessions in each training stage and especially with the fast moving robot. On subsequent training, they gradually learn to avoid entering into the shock zone.

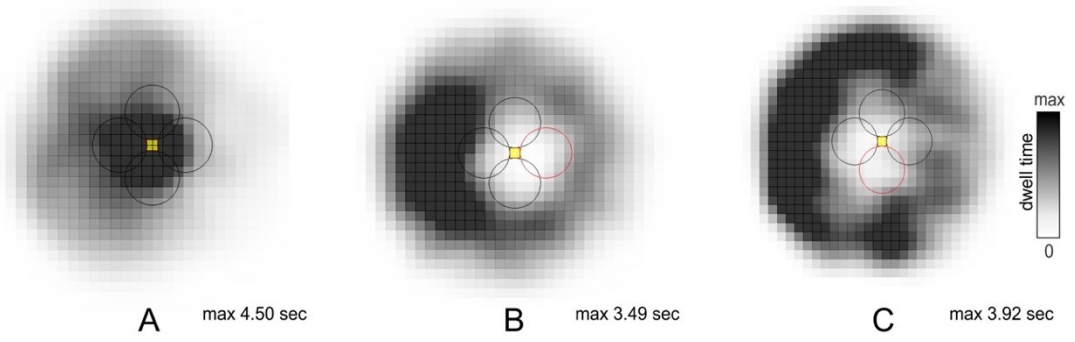

Figure 4.4. Heatmaps of dwell time for untrained and trained rats. Average heatmaps from untrained rats (A) and rats trained to avoid the front (B) and right side (C) of the robot (shock zone shown in red). Maximum dwell time (max) is shown at the bottom. Dwell time (sec) is coded on a color scale from white (0 sec) to black (maximum).

In subfigures 4.5A and B two example no-shock sessions from untrained rats are shown. On the right side, bar graphs depicting the number of entrances and time spent in each zone for example sessions. In subfigure 4.5C the bar graphs with the average number of entrances and time spent are shown. These parameters were similar across zones. These data are from three untrained rats recorded in eight sessions. The average heatmap (left side) in subfigure C shows that untrained rats spent more of their time near the robot, unlike trained rats which avoided the robot in general and specifically the shock zone.

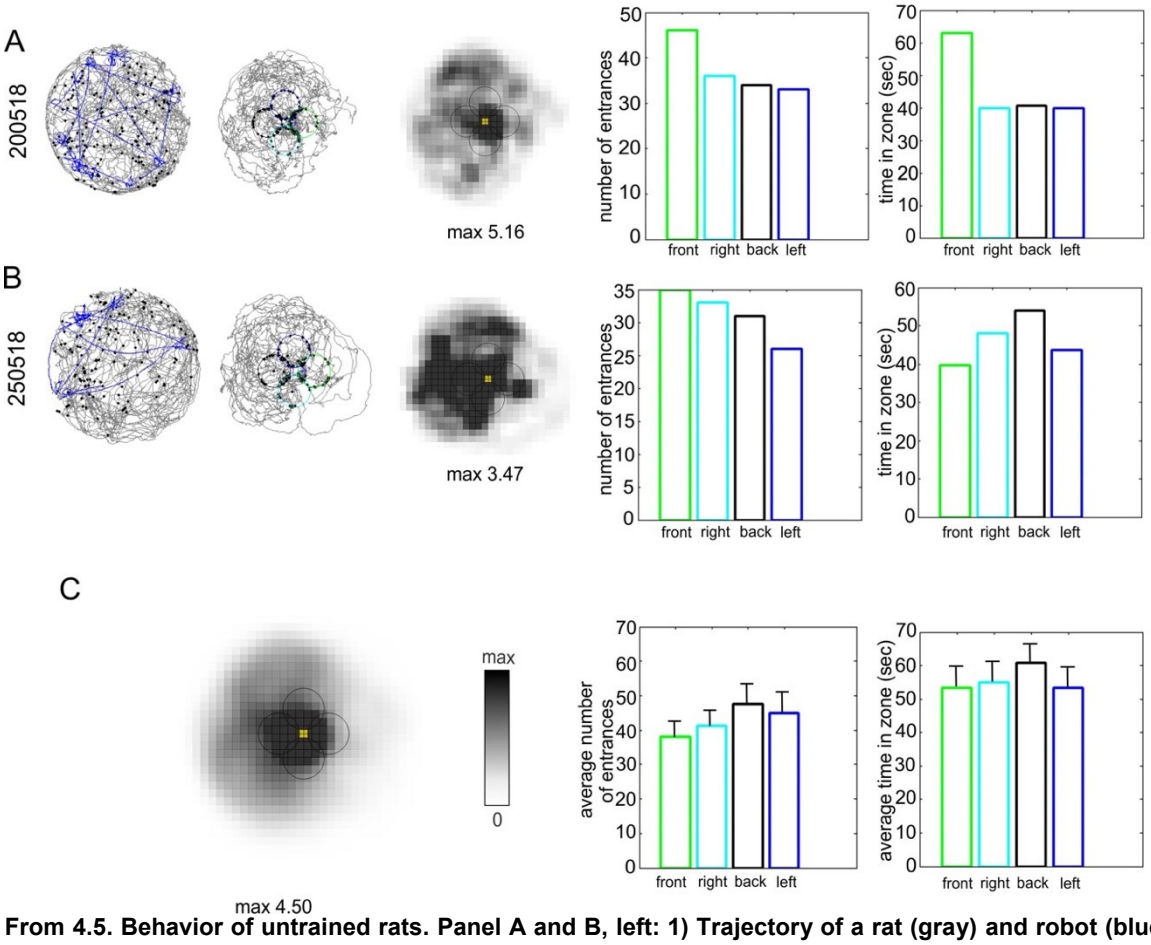

From 4.5. Behavior of untrained rats. Panel A and B, left: 1) Trajectory of a rat (gray) and robot (blue) in the room. 2) Trajectory of a rat relative to the robot. 3) Heat map of the rat's position relative to the robot. Black color indicates pixels with maximal dwelling time, white indicates unvisited pixels. Value in seconds corresponding to black color is given. Dwell time (sec) is coded on a color scale from white (0 sec) to black (maximum). 4) Number of entrances to four zones around the robot (front, back left and right). 5) Time spent in the four zones. Panel C shows the average calculated across all sessions from left: 1) Heat map for mean dwell time around the robot. 2) Mean number of entrances to four zones. 3) Mean time spent in the four zones.

Next, we looked at the time of the first entrance for trained rats in shock versus safe zone in probe sessions. The time of first entrance was explored to see if the trained rats entered first into the shock zone or a safe zone. Trained rats had more entrances in the safe zone and avoided shock zone hence it is reasonable to expect that they are more likely to enter the safe zone first. As rats entered more in the safe zones, this also raises the probability that their first entrance would be in a safe zone (less time on the graph). In general, trained rats entered first into the safe zone before entering into the shock zone. However, the difference in entrance time was not significant in general. If the animal did not enter a particular zone during the whole session, 600 sec – corresponding to the duration of a session was scored.

In rats trained to avoid the front side of the robot, there was no significant difference in the time to the first entrance between front and average of safe zones for slow probe

sessions (t(4)= 2.119; p=0.0507, one-tailed, paired t-test, figure 4.6A). The median values for time to first entrance in front and average of safe zones were 142.037 and 95.906 sec, respectively. Similarly, there was no significant difference in time to the first entrance between front and average of safe zones for fast B&W probe sessions (t(4)=0.7809; p=0.2393, one-tailed, paired t-test, figure 4.6A). The median values were 116.278 and 124.733 sec for front and average of safe zones, respectively. In the all-white slow-moving robot condition there was no significant difference (t(4)=1.245); p=0.1405, one-tailed, paired t-test, figure 4.6A). The median values were 336.195 and 115.893 sec for front and average of safe zones, respectively. However, in the all-white fast-moving robot condition a significant difference was observed for fast (t(4)=2.824; p=0.0238, one-tailed, paired t-test, figure 4.6A) probe sessions. The median values were 340.474 and 155.679 sec for front and average of safe zones, respectively, respectively.

In rats trained to avoid the side of the robot, a significant difference was observed in time to first entrance in the shock versus opposite zone, for slow (t(9)=2.529; p=0.0161, one-tailed, paired t-test, figure 4.6B) B&W probe sessions. The median values for shock and opposite zones were 583.997 and 262.435 sec, respectively. However for fast-moving B&W robot the difference was not significant (t(9)=1.179; p=0.1343, one-tailed, paired t-test, figure 4.6B). The median values for shock and opposite zones were 225.196 and 645.62. sec, respectively. Similarly, in the all-white sessions a significant difference was observed for slow probe sessions (t(9)=3.948; p=0.0017, one-tailed, paired t-test, figure 4.6B). The median values for shock and opposite zones were 600 and 271.017 sec, respectively. In all-white fast-moving sessions there was no significant difference (t(9)=1.151; p=0.1397, one-tailed, paired t-test, figure 4.6B). The median values for shock and opposite zones were 228.177 and 161.078 sec, respectively.

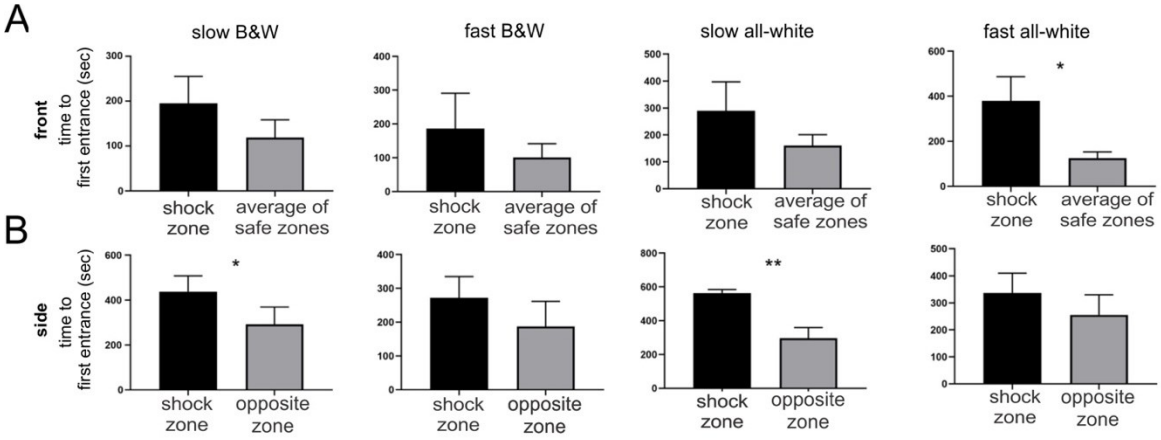

Figure 4.6. Time to first entrance in shock and safe or opposite zones. Data from probe sessions from rats trained to avoid the front (A) and side (B) of the robot. *p<0.05, **p<0.01.

We further looked at rats' behavior during approaches (within 20 cm) of shock zone and safe zones. Examples of such single trajectories are shown below (figure 4.7). In probe trials, where the behavior was not directly affected by foot shocks, we identified each entrance to the shock and safe zones and characterized every single entrance using the following parameters: time spent in a particular zone, average and minimum distance between a rat and the robot, speed of the rat, visit path and duration.

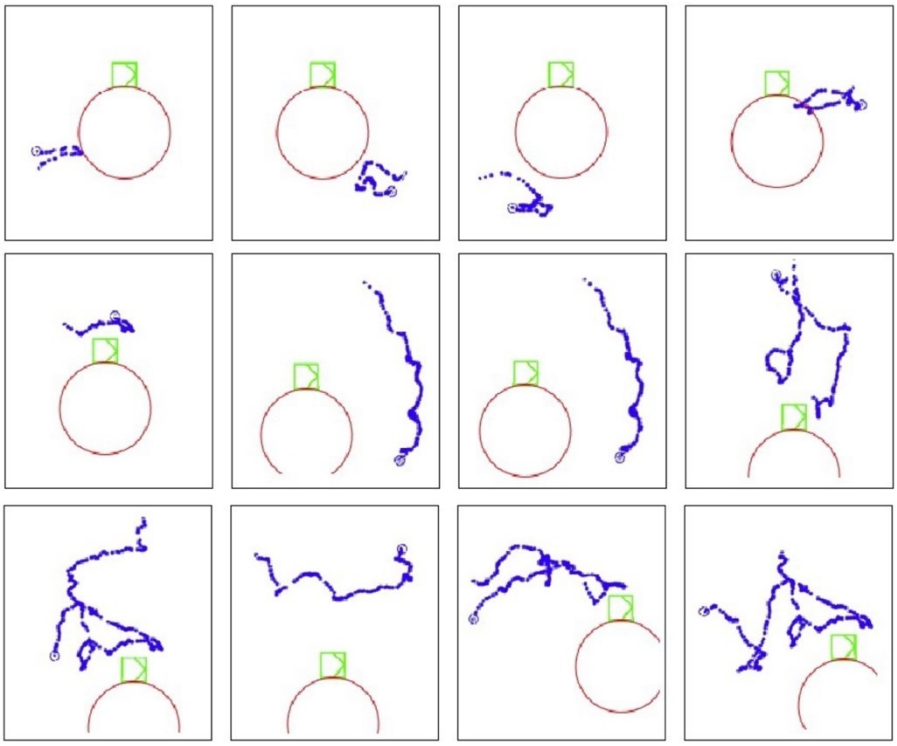

Figure 4.7: Examples of a rat's behavior close to the robot. Twelve examples of approaches within 20 cm of the shock zone (at the right side of the robot) and three equidistant zones "safe" areas around the robot are shown. The robot is in green, the rat's trajectory is blue. Shock zone in red. Note the first three plots that show avoidance behavior, when the rat approaches the robot and before entering the shock zone turns around and retreats. (All examples are from the session shown in 3.5D in methods; (Ahuja et al., 2020)).

We did not detect a systematic difference between shock zone and safe zone entrances in any of these parameters.

Average rat-robot distance – This parameter measures the average distance between the rat and robot when the rat was within 20cm or less from the shock zone or equal size safe zone around the robot. The parameter tell us whether the rats were closer to the robot when within 20cm or less from the safe zones versus the shock zone.

In experiment 1, there was no significant difference in average rat robot distance between front and average of safe zones for slow ($t(4)=0.2662$, $p=0.4016$, one-tailed, paired t-test). The median values were 38.92 and 35.46cm for front and average of safe zones, respectively. However, a significant difference was observed for fast ($t(3)=3.196$,

p=0.0247, one-tailed, paired t-test) B&W probe sessions (figure 4.8A). The median values were 39.51 and 36.47cm for front and average of safe zones, respectively. Similar to slow B&W slow probe session no significant difference was observed in slow (t(3)=0.6904, p=0.2698, one-tailed, paired t-test, figure 4.8A) and fast (t(1)=3. 410, p=0.0908, one-tailed, paired t-test, figure 4.8A) all-white probe sessions. The median values for all-white slow probe sessions were 36.18 and 39.36cm for front and average of safe zones, respectively. For all-white fast probe sessions the median values were 33.46 and 38.74, respectively.

Minimum rat-robot distance - This parameter measures the minimum distance between the rat and robot when the rat was within 20cm or less from the shock zone or equal size safe zone around the robot. Unlike average rat-robot distance, this parameter tells how much closer does the rats went to the robot when they were within 20cm from either in the shock or safe zones. The lesser the distance, the more closer the rat went to the robot. This distance could signify that rats were at ease in going closer to the robot when they were close to or within a particular zone.

The minimum rat-robot distance also did not show any significant difference between front and average of safe zones in slow probe sessions (t(4)=0.1089, p=0.4593, one-tailed, paired t-test, figure 4.8B). The median values for front and average of safe zones were 36.33 and 33.03, respectively. However, in the fast probe sessions with B&W robot there was a significant difference (t(4)=3.590, p=0.0115, one-tailed, paired t-test, figure 4.8B). The median values for front and average of safe zones were 39.00 and 34.23. For the all-white robot condition there was no significant difference in minimum distance between the front and average of safe zones in slow (t(4)=0.7902, p=0.2368, one-tailed, paired t-test, figure 4.8B) and fast (t(4)=0.2105, p=0.4218, one-tailed, paired t-test, figure 4.8B) probe sessions. The median values for all-white slow probe sessions were 34.04 and 37.77 for front and average of safe zones. For all-white fast probe sessions, the median values were 39.00 and 36.74, respectively. The minimum rat-robot distance was taken as 39cm in case of no entrance to any of the compared zones.

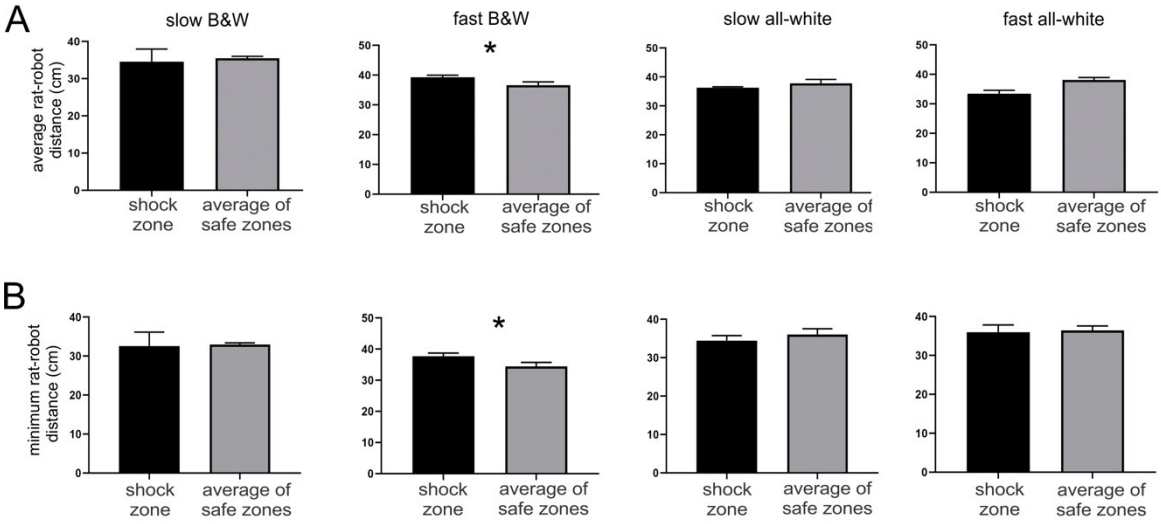

Figure 4.8. Minimum and average rat-robot distance when rats were in the vicinity of the robot in front avoidance condition. Graphs show a comparison between average rat-robot distance (A) and minimum rat-robot distance (B) in shock and the average of safe zones. These data are from probe sessions. *p<0.05.

Average rat speed – It measures the average speed of the rat when it was in close proximity or with in the shock or safe zones. This parameter tells us if the rat was moving a lower or higher speed when he was with in 20cm of the shock or safe zones. It is possible that trained rats would move at higher speed when in the shock zone compared with the safe zones.

For average rat speed between front and average of safe zones no significant difference was observed in B&W slow ($t(4)=0.1829$, $p=0.4319$, one-tailed, paired t-test, figure 4.9A) and fast probe sessions ($t(3)=0.3554$, $p=0.3729$, one-tailed, paired t-test, figure 4.9A). The median values for front and average of safe zones were 12.55 and 15.17 cm/s, respectively, for slow sessions and 17.20 and 15.55 cm/s for fast sessions. Similarly no difference was found in all-white slow probe sessions ($t(3)=1.344$, $p=0.1358$, one-tailed, paired t-test, figure 4.9A). However, a significant difference was observed in all-white fast probe sessions ($t(1)=41.87$, $p=0.0076$, one-tailed, paired t-test, figure 4.9A). The median values for all-white slow probe sessions were 18.34 and 12.91 cm/s, respectively in shock zone and average of safe zones. The median values in all-white fats probe sessions were 12.10 and 21.54 cm/s, respectively.

Maximum rat speed – It measures the maximum speed at which the rats moved when in proximity to the shock or safe zones. It differs from average rat speed in the sense that it tell us about the maximum speed with which the rats moved when they were closer to the robot.

There was no significant difference in max rat speed between front and average of all safe zones in both slow and fast B&W probe sessions (t(4)=1.118, p=0.1631; t(3)=0.7958, p=0.2422, one-tailed, paired t-test, respectively, figure 4.9B). The media values for slow sessions were 42.40 and 47.81 cm/s in front and average of safe zones, respectively. The median values for fast sessions were 48.14 and 45.26 cm/s. Similarly, in slow and fast all-white probe sessions there was no significant difference (t(3)=1.901, p=0.0767; t(1)=0.4356, p=0.3692, one-tailed, paired t-test, respectively, figure 4.9B). The media values for slow all-white sessions were 61.87 and 39.55 cm/s in front and average of safe zones, respectively. The median values for fast all-white sessions were 45.09 and 53.05 cm/s, respectively.

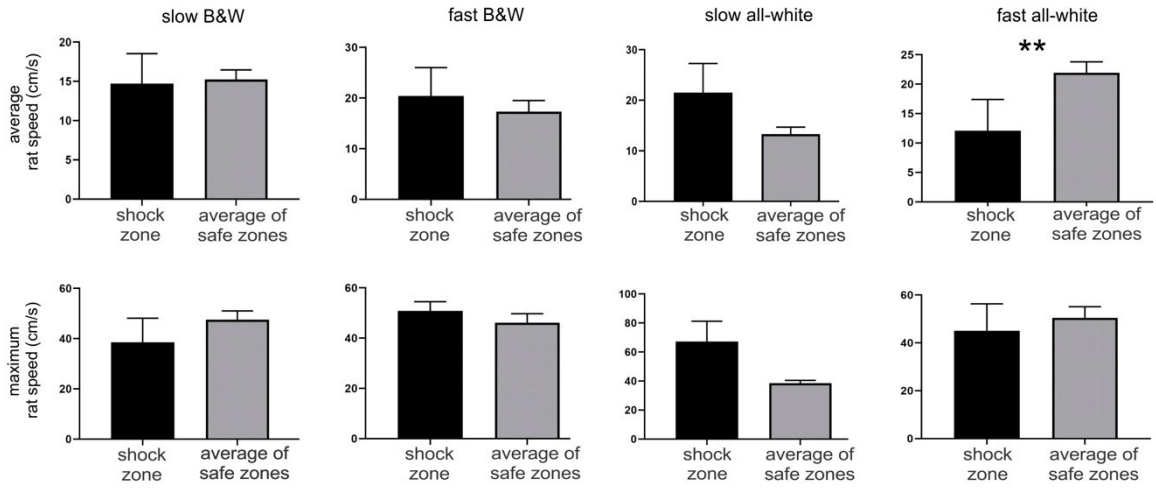

Figure 4.9. Average and maximum rat speed when rats were in the vicinity of the robot in front avoidance condition. Graphs shows a comparison between average rat speed (A) and maximum rat speed (B) in front (shock) and average of safe zones. These data are from probe trials. **p<0.01.

Visit path – This parameter tell us about how much the rat walked when they entered within 20 cm of the safe or shock zones before moving away to a distance of greater than 20 cm from the safe or shock zones.

We next compared the visit path in shock versus the average of safe zones, there was no significant difference in slow (t(4)=1.985, p=0.0591, one-tailed, paired t-test, figure 4.10A) however, a significant difference was observed in fast probe sessions (t(4)= 3.990, p=0.0081, one-tailed, paired t-test, figure 4.10A) with B&W robot. The media values for slow sessions were 9.23 and 23.25 cm in front and average of safe zones, respectively. The median values for fast sessions were 6.98 and 14.38 cm, respectively. Similar to results obtained with B&W slow robot, no significant difference was observed in either slow (t(4)=0.4672, p=0.3323, one-tailed, paired t-test, figure 4.10A) or fast (t(4)=0.8566, p=0.2200, one-tailed, paired t-test figure 4.10A) probe sessions with all-white robot. The

media values for slow sessions were 17.43 and 14.00 cm in front and average of safe zones, respectively. The median values for fast sessions were 0.00 and 16.67 cm/s, respectively.

Visit duration – This parameter measures how much time a rat spent on average once it entered within 20 cm or less of the safe or shock zones before moving away to a distance of greater than 20 cm from the safe or shock zones. It tell us about the amount of time the rats spent in vicinity of the robot. We can expect a trained animal to spend more time in the vicinity of the robot.

Finally, we looked at the difference in visit duration in front and average of all safe zones. There was no significant difference between compared zones in slow (t(4)=1.866, p=0.0677, one-tailed, paired t-test, figure 4.10B) B&W probe sessions. However, a significant difference was observed in fast B&W probe sessions (t(4)=4.244, p=0.0066, one-tailed, paired t-test, figure 4.10B). The median values for slow sessions were 0.8477 and 1.701 sec in front and average of safe zones, respectively. The median values for fast sessions were 0.3600 and 1.038 sec, respectively. For slow (t(4)=0.8341, p=0.2256, one-tailed, paired t-test, figure 4.10B) and fast (t(4)=1.467, p=0.1081, one-tailed, paired t-test, figure 4.10B) all-white probe sessions no significant difference was observed**.** The median values for all-white slow sessions were 1.009 and 1.580 sec in front and average of safe zones, respectively. The median values for all-white fast sessions were 0.00 and 1.132 sec, respectively.

The visit path and visit duration were taken as zero in case of no entrance in any of the compared zones.

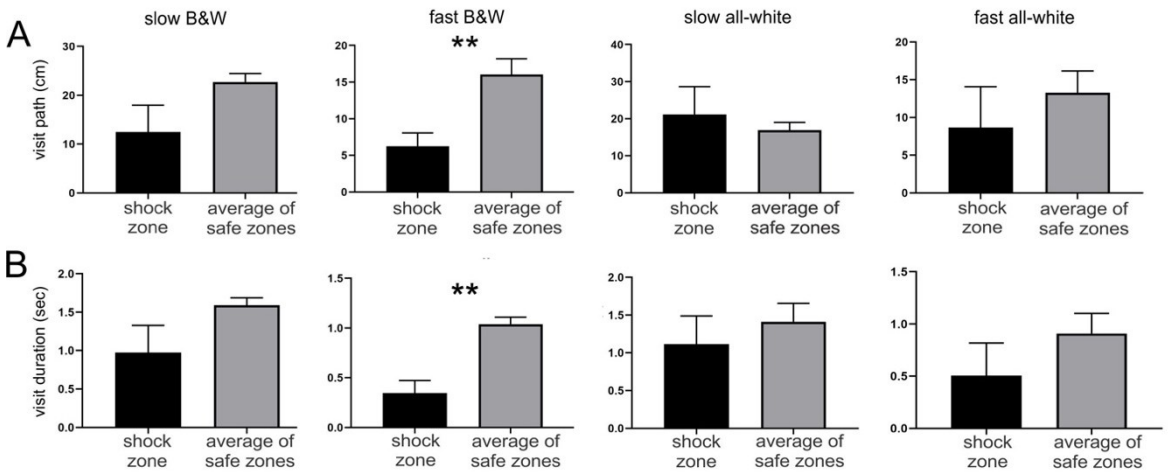

Figure 4.10. Visit path and duration when rats were in the vicinity of the robot in front avoidance condition. Graphs show a comparison between visit path (A) and visit duration (B) in front (shock) and the average of safe zones. These data are from probe trials. **p<0.01.

In experiment 2, there was no significant difference in average rat-robot distance between shock and and opposite safe zones for slow ($t(4)=0.04747$, $p=0.4822$, one-tailed, paired t-test), and fast ($t(5)=1.184$, $p=0.1488$, one-tailed, paired t-test, figure 4.11A) B&W probe sessions. The median values for slow sessions were 36.18 and 35.80 cm in shock and opposite safe zones, respectively. The median values for fast sessions were 34.18 and 32.25 cm, respectively.

Similarly no significant difference was observed in slow ($t(1)=1.933$, $p=0.1520$, one-tailed, paired t-test) and fast ($t(5)=1.333$, $p=0.1201$, one-tailed, paired t-test, figure 4.11A) all-white probe sessions. The median values for all-white slow sessions were 37.33 and 35.61 cm in shock and opposite safe zones, respectively. The median values for all-white fast sessions were 33.03 and 39.11 cm, respectively.

The minimum rat-robot distance also did not show any significant difference between shock and opposite safe zones in slow ($t(9)=0.7866$, $p=0.2259$, one-tailed, paired t-test, figure 4.11B) and fast ($t(9)=1.010$, $p=0.1695$, one-tailed, paired t-test, figure 4.11B) probe sessions in B&W robot condition. The median values for slow sessions were 38.96 and 34.60 cm in shock and safe zones, respectively. The median values for fast sessions were 33.55 and 33.26 cm, respectively. For all-white robot condition, there was a significant difference in minimum distance between the shock and opposite safe zones in slow ($t(9)=2.502$, $p=0.0169$, one-tailed, paired t-test, figure 4.11B) probe sessions but no significant difference was observed in fast ($t(9)=1.181$, $p=0.1338$, one-tailed, paired t-test, figure 4.11B) probe sessions. The median values for all-white slow sessions were 39.00 and 35.43 cm in shock and opposite safe zones, respectively. The median values for all-white fast sessions were 37.20 and 38.19 cm, respectively. The minimum rat-robot distance was taken as 39cm in case of no entrance to any of the compared zones.

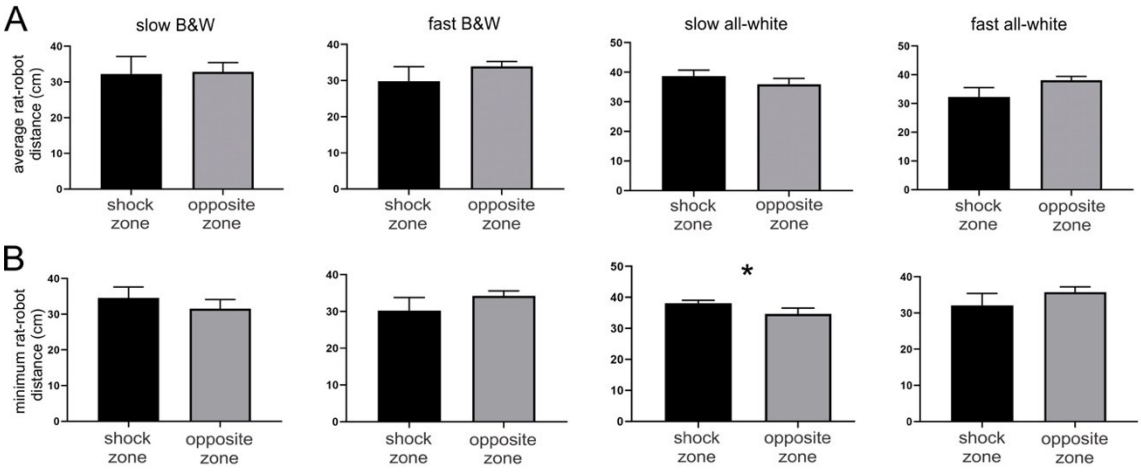

Figure 4.11. Average and minimum rat-robot distance when rat was in the vicinity of the robot in side avoidance condition. Graphs show a comparison between average rat-robot distance (A) and minimum rat-robot distance (B) in shock versus safe zones. These data are from probe trials. *p<0.05.

Next we looked at average rat speed between shock and opposite safe zones, there was no significant between the two zones neither in slow ($t(4)=1.335$, $p=0.1264$, one-tailed, paired t-test, figure 4.12A) nor in fast ($t(5)=0.4735$, $p=0.3279$, one-tailed, paired t-test, figure 4.12A) B&W probe sessions. The median values for slow sessions were 17.92 and 12.24 cm/s in shock and opposite safe zones, respectively. The median values for fast sessions were 9.87 and 11.73 cm/s, respectively. Similarly no significant difference was observed between the compared zones for all-white slow ($t(1)=0.6593$, $p=0.3145$, one-tailed, paired t-test, figure 4.12A) and fast ($t(5)=0.5893$, $p=0.2906$, one-tailed, paired t-test, figure 4.12A) robot conditions. The median values for slow all-white probe sessions were 17.11 and 14.89 cm/s in shock and opposite safe zones, respectively. The median values for fast sessions were 18.98 and 15.18 cm/s, respectively.

There was no significant difference in maximum rat speed between shock and opposite safe zones in both slow and fast B&W ($t(4)=0.3692$, $p=0.3654$; $t(5)=0.8860$, $p=0.2081$, respectively, one-tailed, paired t-test, figure 4.12B). The median values for slow sessions were 46.49 and 43.57 cm/s in shock and opposite safe zones, respectively. In fast sessions, the median values were 56.04 and 40.10 cm/s, respectively. Similarly, in slow and fast all-white probe sessions there was no significant difference in maximum rat speed between shock and opposite safe zones ($t(1)=1.389$, $p=0.1986$; $t(5)=0.6221$, $p=0.2806$, respectively, one-tailed, paired t-test, figure 4.12B) all-white robot probe sessions. The median values for slow all-white probe sessions were 67.46 and 40.72 cm/s in shock and opposite safe zones, respectively. The median values for fast sessions were 60.40 and 53.26 cm/s, respectively.

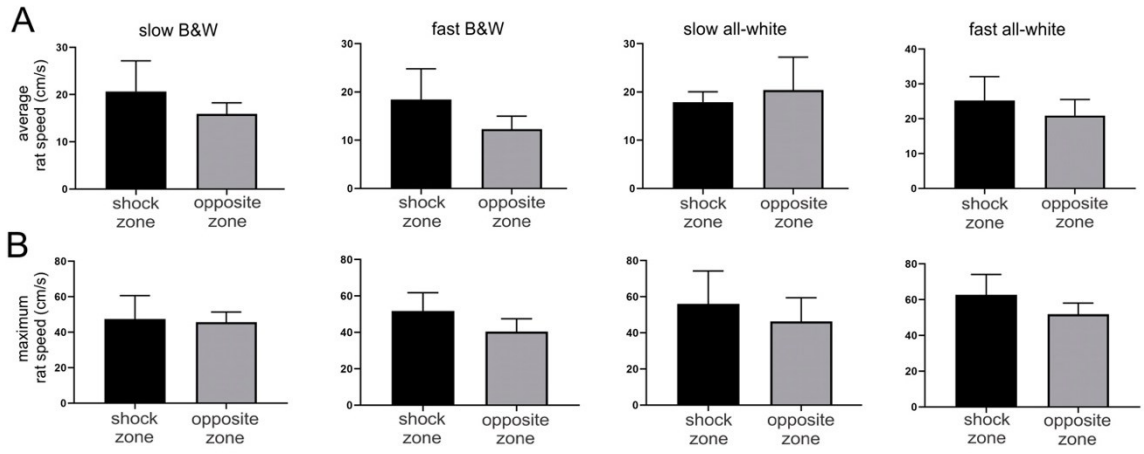

Figure 4.12. Average and maximum rat speed when rat was in the vicinity of the robot in side avoidance condition. Graphs show comparison between average rat speed (A) and maximum rat speed (B) in shock versus safe zones. These data are from probe trials.

We next compared the visit path in shock and opposite safe zones, there was no significant difference in slow ($t(9)=1.035$, $p=0.1638$, one-tailed, paired t-test, figure 4.13A) as well as in fast ($t(9)=1.419$, $p=0.0948$, one-tailed, paired t-test, figure 4.13A) probe sessions with B&W robot. The median values for slow sessions were 0.074 and 14.74 cm in shock and opposite safe zones, respectively. In fast sessions, the median values were 17.74 and 7.96 cm, respectively. Similar to results with the B&W robot, there was no significant difference in slow ($t(9)=1.358$, $p=0.1037$, one-tailed, paired t-test, figure 4.13A) and fast ($t(9)=0.5263$, $p=0.3057$, one-tailed, paired t-test, figure 4.13A) probe sessions with the all-white robot. The median values for slow all-white probe sessions were 0.00 and 7.51 cm in shock and safe zones, respectively. In fast sessions, the median values were 14.04 and 13.33 cm, respectively.

Finally, we looked at the difference in visit duration in shock and opposite safe zones. There was no significant difference between compared zones in slow ($t(9)=1.681$, $p=0.0636$, one-tailed, paired t-test, figure 4.13B) and fast ($t(9)=0.6430$, $p=0.2681$, one-tailed, paired t-test, figure 4.13B) B&W probe sessions. The median values for slow sessions were 0.02 and 0.59 sec in shock and opposite safe zones, respectively. In fast sessions, the median values were 1.14 and 0.93 cm, respectively. Similarly, for slow ($t(9)=1.202$, $p=0.1299$, one-tailed, paired t-test, figure 4.13B) and fast ($t(9)=0.4955$, $p=0.3161$, one-tailed, paired t-test, figure 4.13B) all-white probe sessions no significant difference was observed. The median values for slow all-white probe sessions were 0.00 and 0.57 sec in shock and safe zones, respectively. In fast sessions, the median values were 0.50 and 0.81 sec, respectively. As above, the visit path and visit duration were taken as zero in case of no entrance in any of the compared zones.

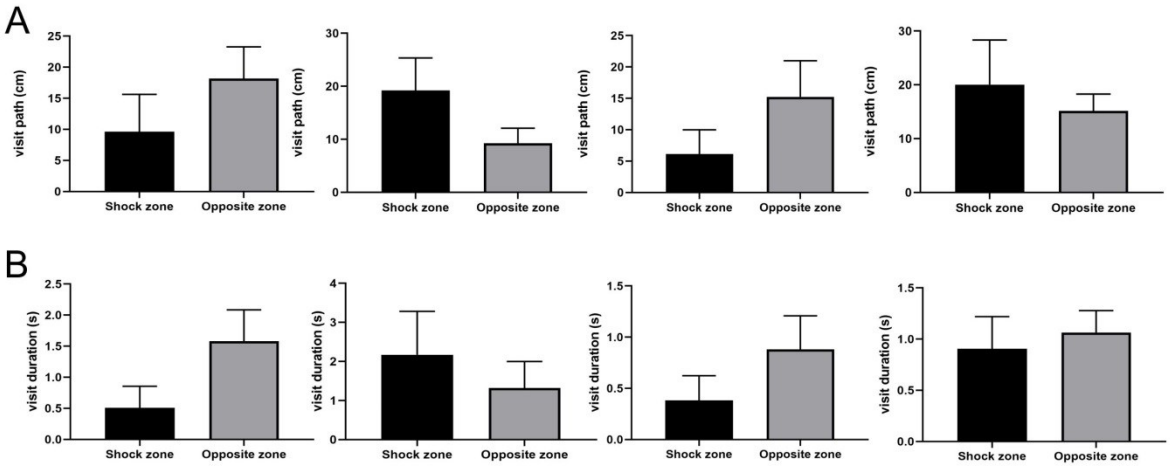

Figure 4.13. Visit path and duration when rat was in the vicinity of the robot in side avoidance condition. shows a comparison between visit path (A) and visit duration (B) in shock versus safe zones. These data are from probe trials. *p<0.05.

The lack of an underlying pattern suggests that despite significantly lower numbers of shock zone entrances, once an animal entered the shock zone, its behavior there was not distinct from behavior in the safe zone.

4.3 Activity of hippocampal units during the task

To understand the neuronal basis of navigation relative to the moving robot and relevant representations we recorded electrophysiology data from trained and untrained rats. These data are from three untrained rats who were never shocked and a trained rat. We looked at responses of cells across sessions and representation in the moving robot session.

Responses of individual cells

We recorded 42 hippocampal CA1 complex spike cells (CSCs, putative pyramidal neurons) and four theta cells (table 2) from three rats in no-shock conditions and 46 CSCs and eight theta cells (table 3) from one rat trained in robot avoidance task. We observed various representations both across sessions and representation in different reference frames within the moving robot session which could assist the rat in navigating around a moving object. More details on the cells are mentioned below in the tabulated form.

	Untrained			
Session number	s1	s2	s3	s4
Number of sessions	08	08	08	08
Total cells	46	46	46	46
Cells without place fields (PFs)	17	11	21	19
Cells with at least one PF	29	35	23	27
Proportion of cells with >=1 PF	09	07	09	07

* two cells did not fire in s3

Table 2. Number of cells with place fields from untrained rats

	Trained			
Session number	s1	s2	s3	s4
Number of sessions	06	06	06	06
Total cells	52	54	54	54
Cells without place fields (PFs)	18	21	19	25
Cells with at least one PF	34	33	33	29
Proportion of cells with >=1 PF	11	10	09	12

* two cells did not fire in s3

Table 3. Number of cells with place fields from trained rat

Firing pattern for cells across sessions

As mentioned above some of the units did not change their firing pattern dramatically after encountering the robot. This type of units was found in both untrained (unit 1, figure 4.14) and trained animals (unit 2, figure 4.14). Importantly, the correlation between the two no robot sessions, first and last sessions, was positive. For these units, it seems that they continued to represent the rat's position in space after removal of robot in the fourth session (s4), such that their spatial firing pattern did not change much. The correlation

values between spike rate maps in sessions 1 and 4 for all the units are shown in the legend as C_{14}.

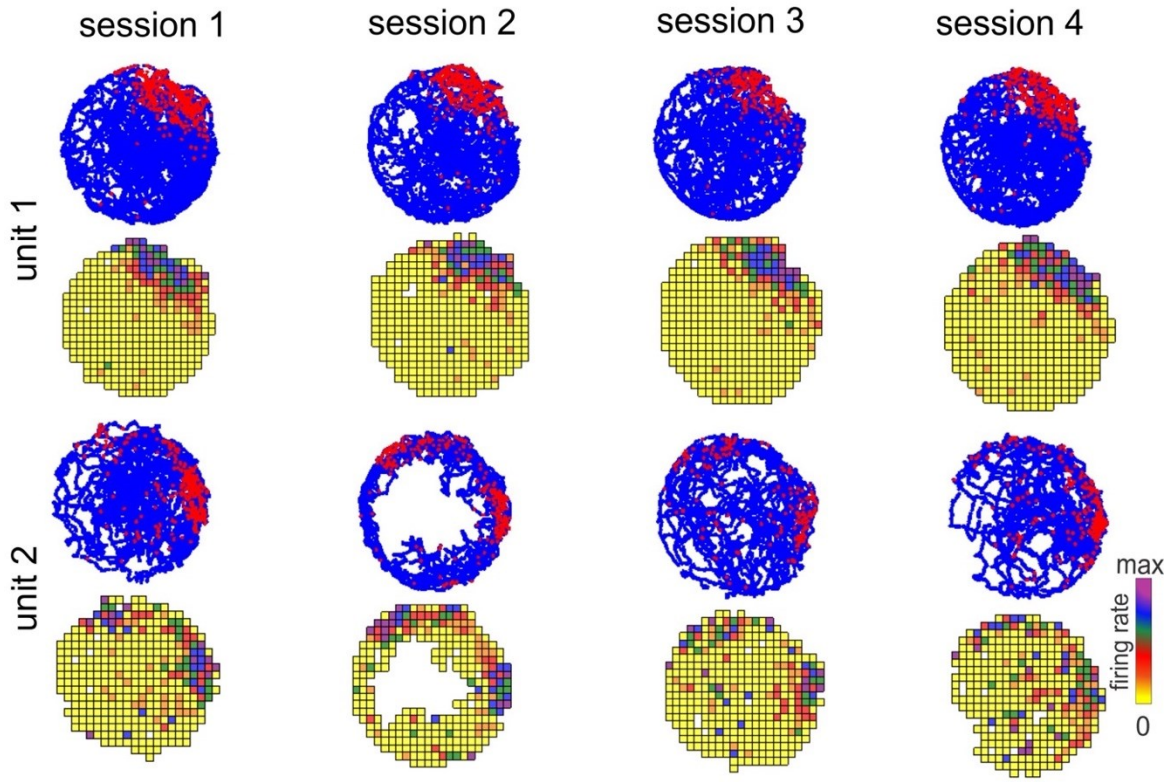

Figure 4.14. Two examples of units whose firing patterns did not change much across four sessions. Spike plots and firing rate maps are shown for each unit. Spike plot shows rats trajectory in blue and a single spike as red dot. The colors on rate maps corresponds to the color bar. Unit 1 is from an untrained rat and unit 2 is from the trained animal. C_{14_1}=0.8982 and C_{14_2}=0.3784 are correlation values (for smoothed map) between first and fourth sessions for unit 1 and 2, respectively. Firing rate (Hz) is coded on a color scale from yellow (silent) to magenta (maximum rate).

While there were units that did not change their firing pattern much, we also observed units that changed their firing pattern dramatically. The spatial correlation between sessions 1 and 4 for these units was negative (unit 1 and 2, figure 4.15). It appears that for units 1 as the sessions progressed from the first no robot session to the moving robot session the firing field moves across the arena and in the last session, the second no robot session, the cell fired less. One of the reasons for this could be that the firing of the cell gets hinged to the object or started representing the object in a specific place and when the object was removed the cell changed its firing pattern again.

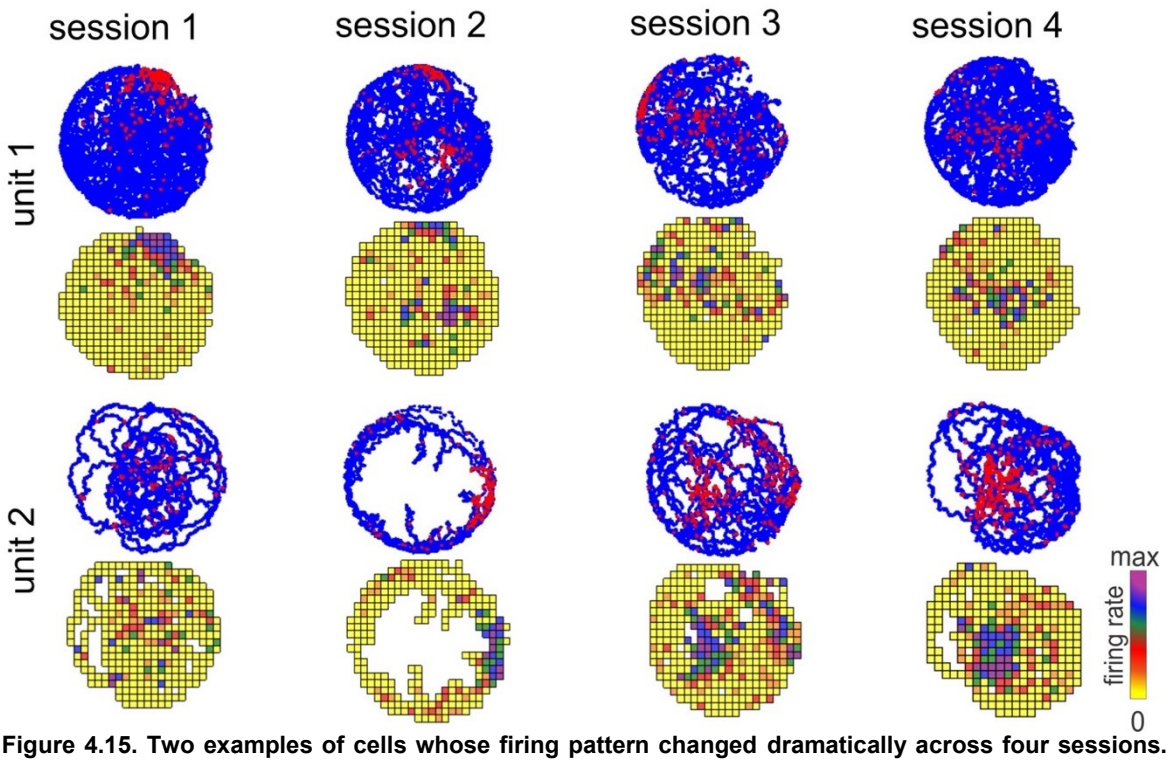

Figure 4.15. Two examples of cells whose firing pattern changed dramatically across four sessions. Spike plots and firing rate maps are shown for each unit. Spike plot shows rats trajectory in blue and a single spike as red dot. The colors on rate maps corresponds to the color bar. Unit 1 is from a untrained rat and units 2 is from the trained animal. C_{14_1}=0.1751 and C_{14_2}= -0.0841 are correlation values (for smoothed map) between first and fourth sessions for unit 1 and 2, respectively. Firing rate (Hz) is coded on a color scale from yellow (silent) to magenta (maximum rate).

Cells across representations

Besides the cell behavior mentioned above, we also observed cells that represented the position of the rat in the room as well as its position relative to the robot or robot relative to the rat. This was observed in moving sessions. The data are from 14 experimental sessions: eight sessions with three untrained rats and 6 sessions with a trained rat. To look for a representation of the rat relative to the robot, we constructed spike rat maps such that in the moving session the robot was made the center point around which the rat moved across the session and mapped spike data onto rat's movement around the robot. Analogously, we constructed a robot to rat spatial rate maps.

In our data, we observed examples of cells with different representation 1) some units only represented the position of rat in the room (unit 1 figure 4.16), 2) some units encoded the position of rat relative to the robot as well as robot relative to the rat but not the position of rat in the room (unit 2, figure 4.16; unit 2, figure 4.17), 3) other cells represented the position of rat in the room as well as in the two other frames, rat relative to robot and robot relative to the rat (unit units 3 and 4, figure 4.16; unit 3, figure 4.17). We also found cells which conjunctively represented the position of rat in the room, rat relative to the robot and robot relative to the rat in the sample of units from untrained rats

(unit 3, figure 4.16). On the other hand, we also found cells which were not organized in any of the reference frames (unit 4, figure 4.17).

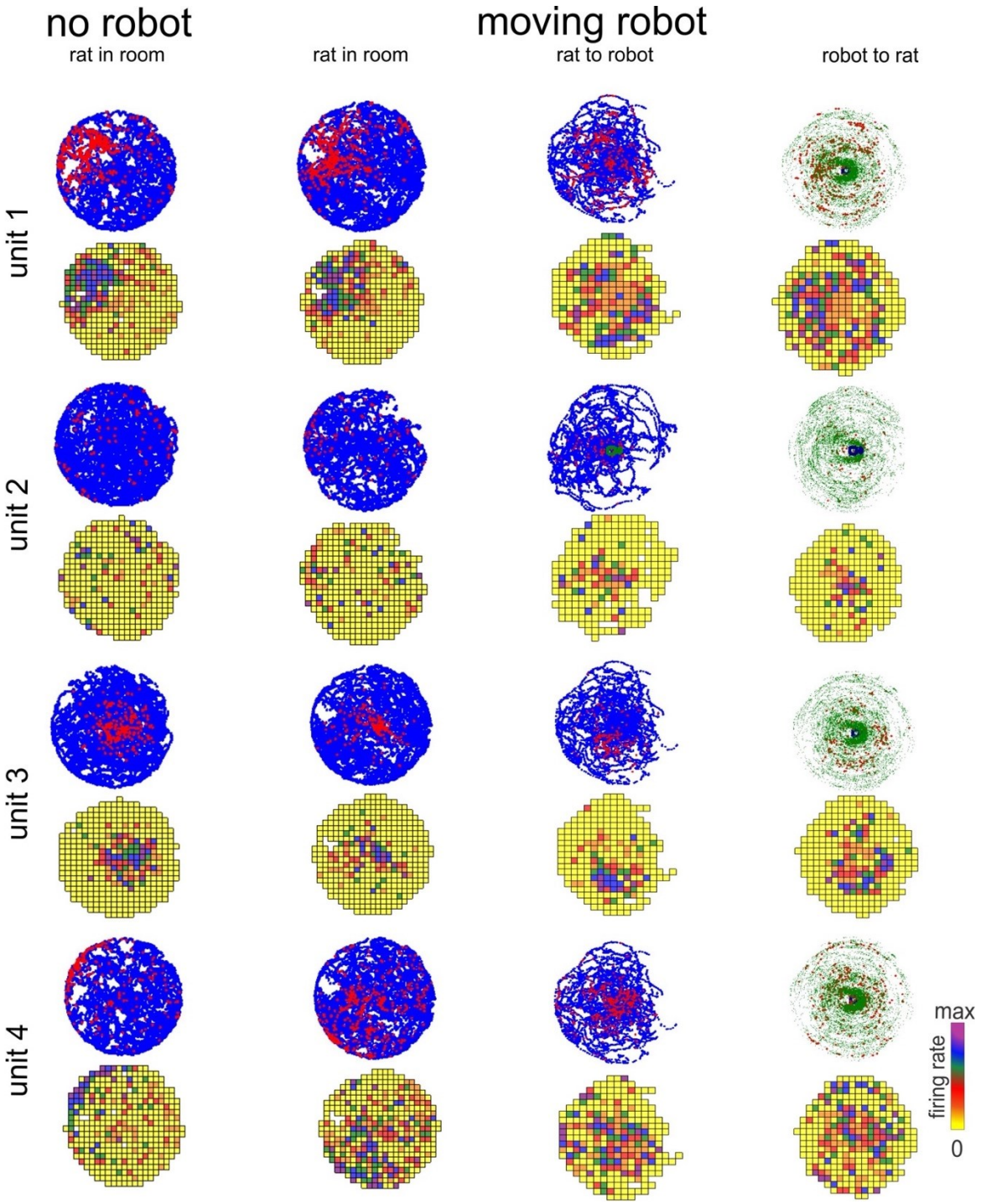

Figure 4.16. Four example units from 'untrained' rats showing representation in various reference frames. Spike plots and firing rate maps are shown for each unit. Spike plot shows rats trajectory in blue and a single spike as red dot. The colors on rate maps corresponds to the color bar. Only the no robot (session 1) and moving robot (session 3) sessions are shown. For moving robot, representation has been constructed for three reference frames: rat in room, rat relative to the robot and robot relative to the rat. For no robot session, only rat in room representation is possible which is shown on the left. Firing rate (Hz) is coded on a color scale from yellow (silent) to magenta (maximum rate).

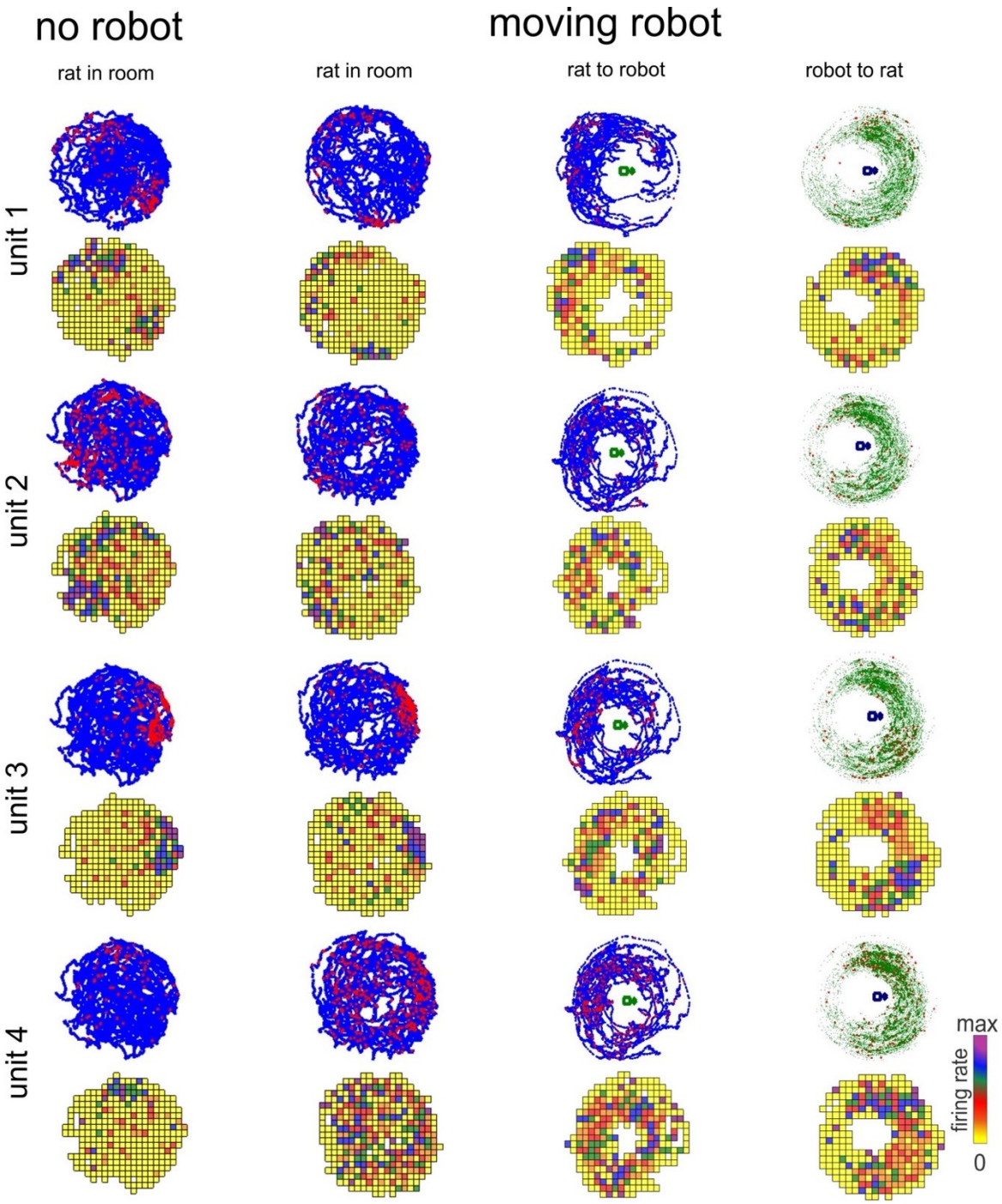

Figure 4.17. Four example units from 'trained' rat showing representation in various reference frames. Spike plots and firing rate maps are shown for each unit. Spike plot shows rats trajectory in blue and a single spike as red dot. The colors on rate maps corresponds to the color bar. Only the no robot (session 1) and moving robot (session 3) sessions are shown. For moving robot, representation has been constructed for three reference frames: rat in room, rat relative to the robot and robot relative to the rat. For no robot session, only rat in room representation is possible which is shown on the left. Firing rate (Hz) is coded on a color scale from yellow (silent) to magenta (maximum rate).

4.4 Absence of distinct cell types in the task

To understand if our data contained cells with different characteristics we looked at the distribution of coherence and spatial information across sessions for both trained and untrained animals. We observed that the distributions were similar and continuous for both groups in all reference frames with a continuum of values from low to high. There were no distinct peaks which point to the absence of different cell types (figure 4.18, 4.19, 4.20 and 4.21).

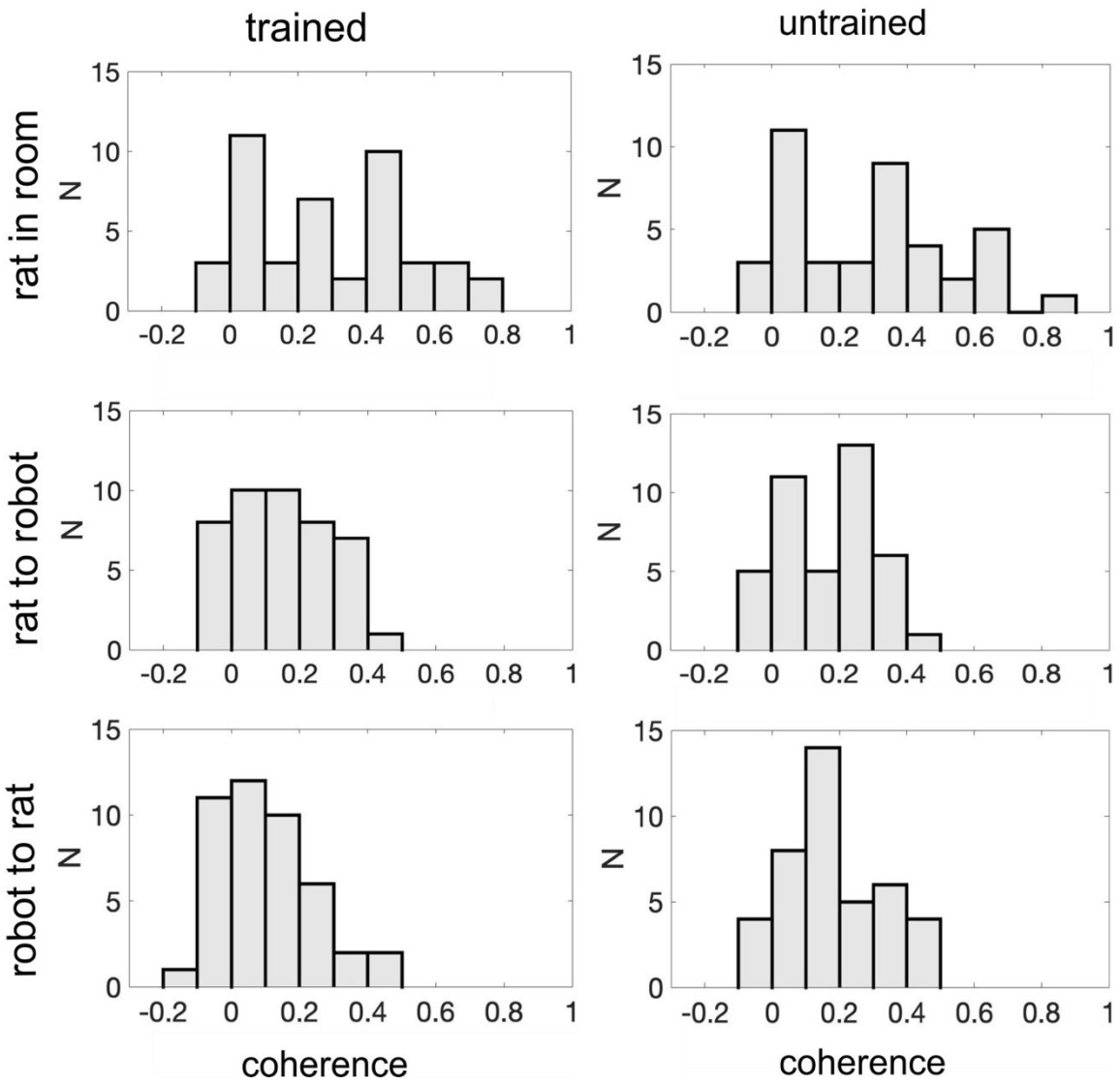

Figure 4.18. Distributions for coherence in different frames for CSCs recorded from trained and untrained rats. Distributions are continuous which shows that there are no different types of unit in the recordings.

We did not observe different cell types within the recorded CSCs (figure 4.18 and 4.20) as well as theta cells (figure 4.19 and 4.21).

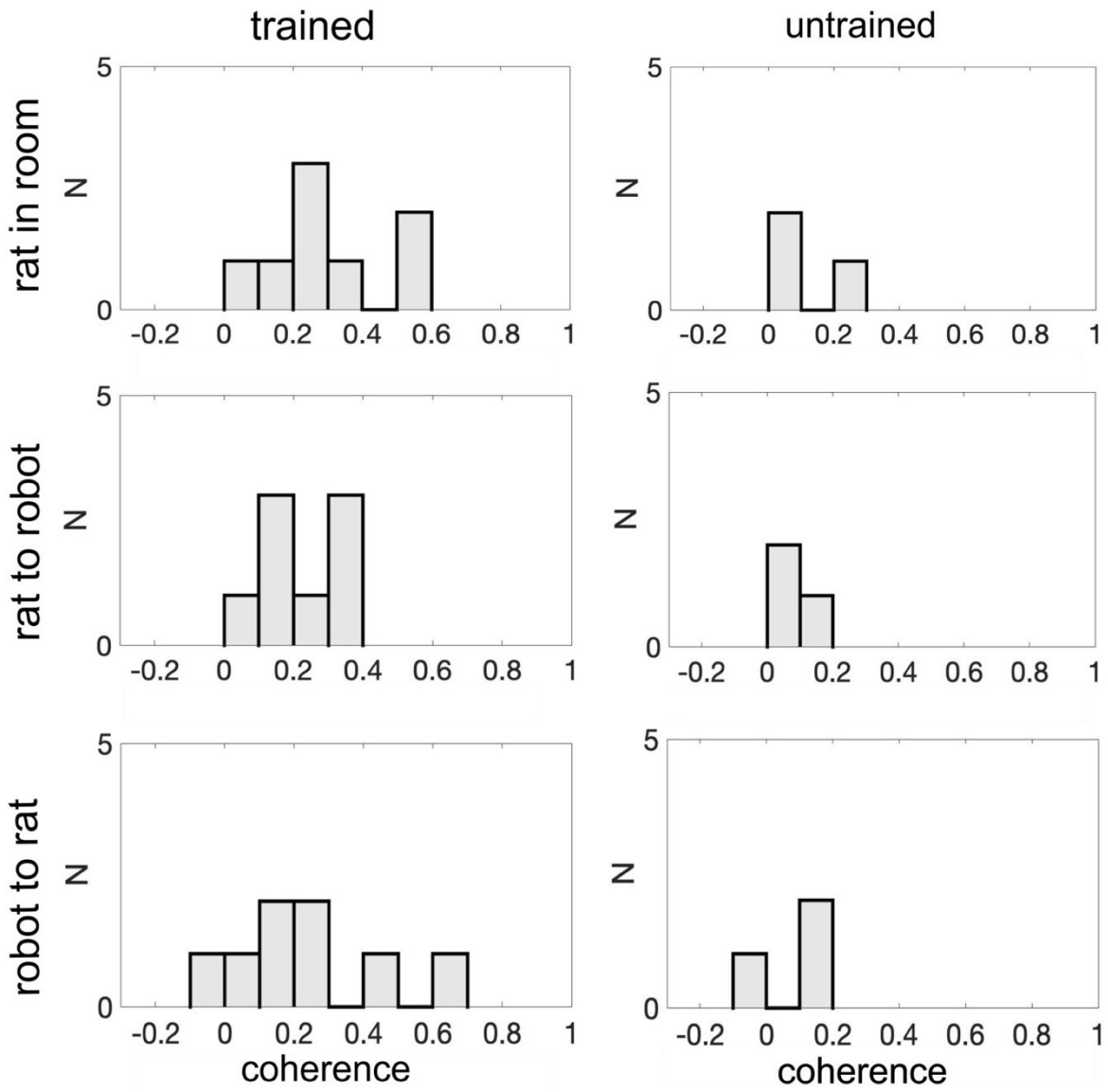

Figure 4.19. Distributions for coherence in different frames for theta cells recorded from trained and untrained rats. Distributions are continuous which shows that there are no different types of unit in the recordings.

Similarly, the distribution of spatial information across reference frames was continuous for CSCs in both trained and untrained animals (figure 4.20).

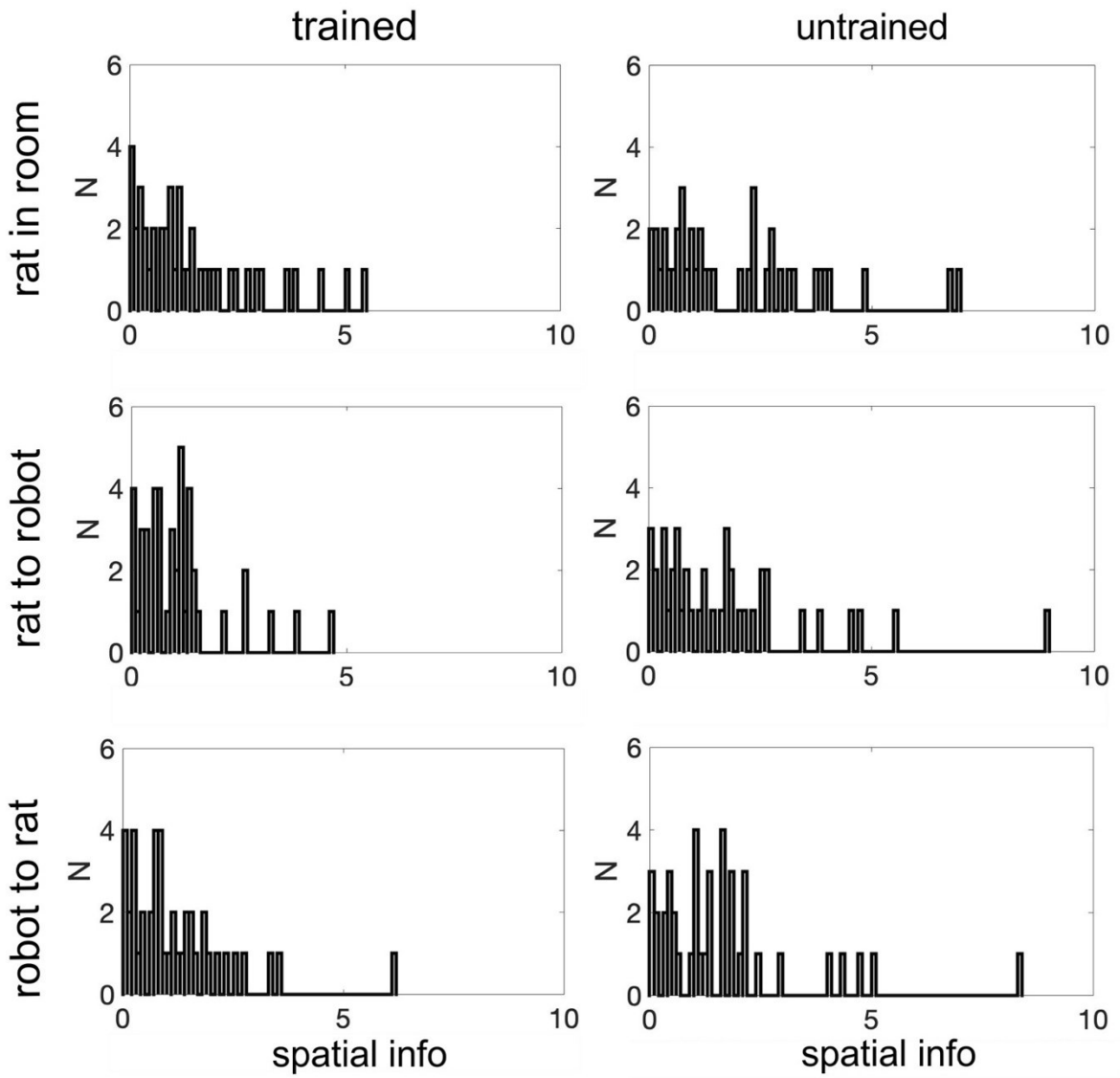

Figure 4.20. Distributions of spatial information (spatial info; bits/sec) across reference frames in both trained and untrained rats for CSCs. The distributions are mostly continuous except for a few outliers.

Similar to the distributions for CSCs, there were no different cell types within the recorded theta cells (figure 4.21).

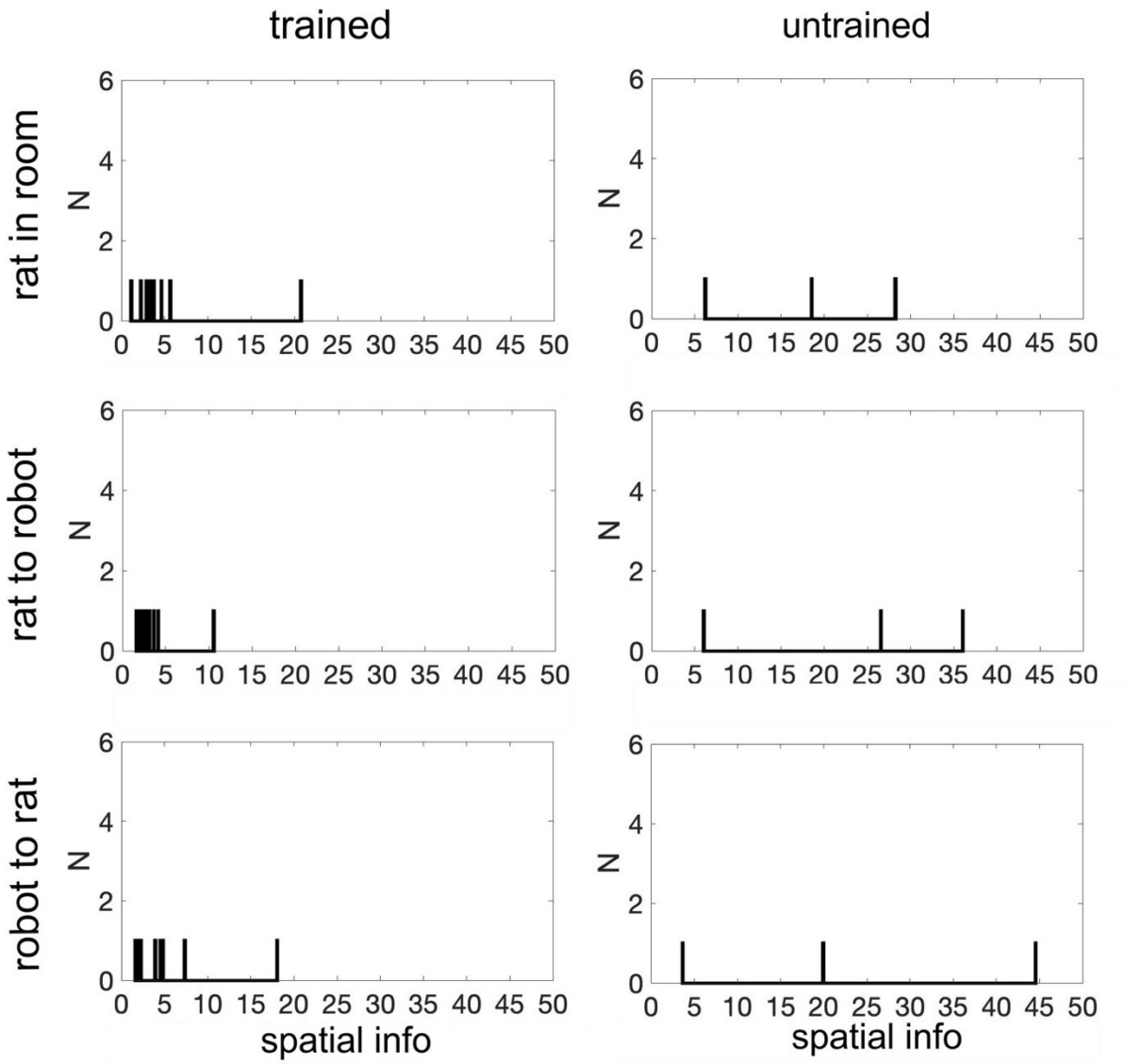

Figure 4.21 Distributions of spatial information (spatial info; bits/sec) across reference frames in both trained and untrained rats for theta cells. The distributions are mostly continuous except for a few outliers.

4.5 Spatial parameters across sessions and between groups

Next, we compared measures of spatial specificity such as coherence and spatial information (bits/sec), information per spike (bits/spike), etc. In sessions with the moving robot, we looked at the representations in various reference frames: rat in room, rat relative to the robot and robot relative to the rat.

Coherence and spatial information

We used parameters of spatial coherence (Muller & Kubie, 1989) and spatial information (Skaggs et al., 1993) to quantify the spatial organization of neuronal activity in all three reference frames (coordinate systems) for all the recorded cells.

Coherence measures similarity in firing rate between adjacent pixels. Average coherence across sessions was generally higher in the first only rat session and stationary robot session for both untrained and trained rats.

Coherence and spatial info across representations for CSCs

In the trained rat, ANOVA revealed a significant effect of spatial reference frame on spatial coherence ($F(2,86)=34.10$, $p<0.0001$, repeated measure (RM), one-way ANOVA, figure 4.22A) for CSCs. Tukey post-hoc test showed higher spatial coherence values for rat-in-room coordinate system than for rat-to-robot and robot-to-rat coordinate systems (p's<0.0001). The median values for rat in room, rat to robot and robot to rat frames were 0.2752, 0.1499, 0.09234, respectively. In untrained rats, a similar effect was observed on coherence ($F(2,80)=9.615$, $p=0.0002$, RM, one-way ANOVA, figure 4.22A) for CSCs. Tukey post-hoc test showed higher spatial coherence values for rat-in-room coordinate system than for rat-to-robot and robot-to-rat coordinate systems ($p=0.0007$ and $p=0.0010$, respectively). The median values for rat in room, rat to robot and robot to rat frames were 0.3093, 0.1690, 0.1512, respectively, in CSCs from untrained rats.

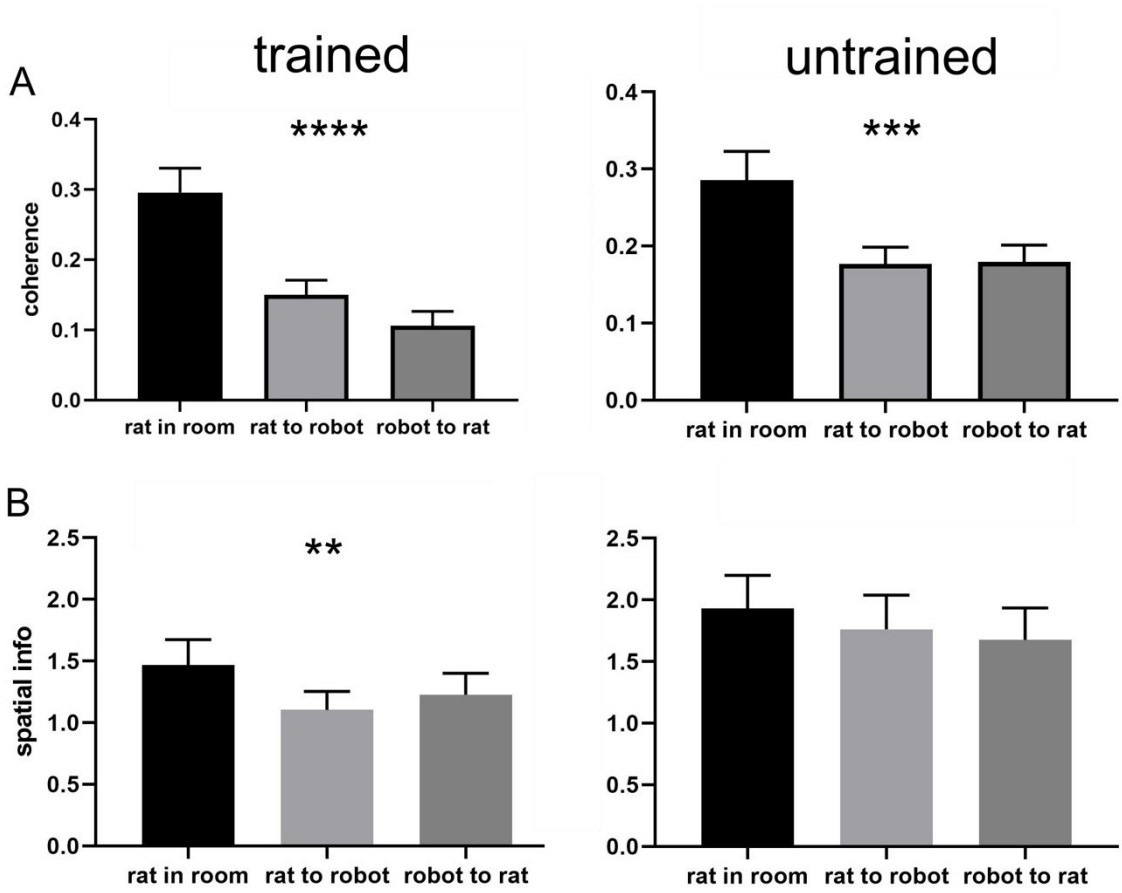

Figure 4.22. Comparison of spatial parameters across reference frames for CSCs. (A) Coherence in trained and untrained rats. (B) Spatial information (spatial info) for trained and untrained animals. Note that there was no difference in spatial information across reference frames for untrained rats. Spatial info was measured in bits/sec. Plots show means ± SEM. **p<0.01, ***p<0.001, ****p<0.0001.

In theta cells recorded from trained and untrained rats there was no. significant difference across reference frames for trained rats ($F(2,14)=0.7717$, $p=0.4809$, trained rats, RM, one-way ANOVA; $F(2, 4)=0.005934$; $p=0.9941$, untrained rats, RM, one-way ANOVA, figure 4.23A). In trained rat, the median values for rat in room, rat to robot and robot to rat frames were 0.2683, 0.2421, 0.2199, respectively. The median values for rat in room, rat to robot and robot to rat frames were 0.2651, 0.07237, 0.1876, respectively, in theta cells from untrained rats.

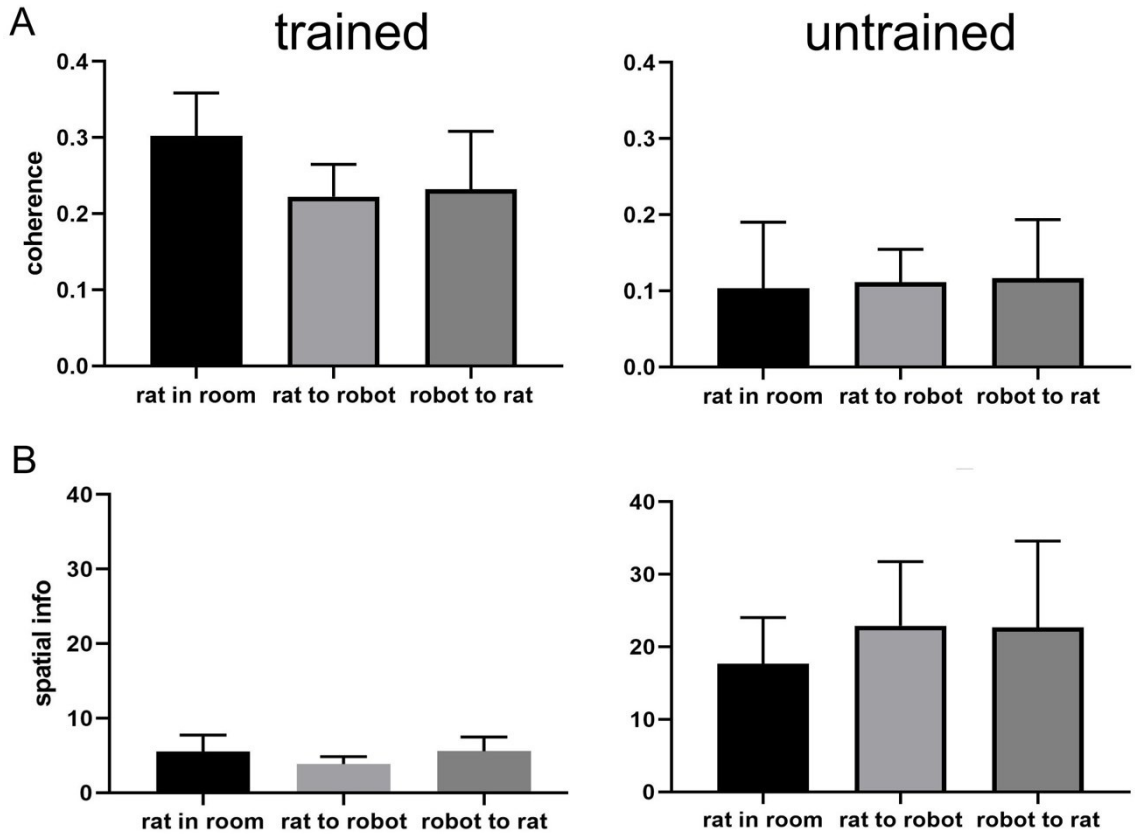

Figure 4.23 Comparison of spatial parameters across reference frames for theta cells. (A) Coherence in trained and untrained rats.. (B) Spatial information (spatial info) for trained and untrained animals. Note that there was no difference in spatial information across reference frames for trained as well as untrained rats. Spatial info was measured in bits/sec. Plots show means ± SEM.

Spatial information (bits/sec)

In trained rats, ANOVA revealed a significant effect of spatial reference frame on spatial information ($F(2,86)=6.827$, $p=0.0018$, RM, one-way ANOVA, figure 4.22B) in CSCs. Tukey post-hoc test showed higher information values for rat-in-room coordinate system than for rat-to-robot ($p=0.0014$) and for robot-to-rat ($p=0.0481$). The median values for rat in room, rat to robot and robot to rat frames were 1.077, 0.9276, 0.8478 bits/sec, respectively. For untrained rats, no significant difference was found in the information content across reference frames ($F(2,80)=1.522$, $p=0.2246$, RM, one-way ANOVA, figure 4.22B). The median values for rat in room, rat to robot and robot to rat frames were 1.278, 1.298, 1.313 bits/sec, respectively, in CSCs from untrained rats.

In theta cells from trained rats, there was no significant difference in spatial info across reference frames ($F(2, 14)=1.977$, $p=0.1753$, RM, one-way ANOVA, figure 4.23B). The median values for rat in room, rat to robot and robot to rat frames were 3.497, 3.027, 4.244 bits/sec, respectively. Similarly, no significant difference was observed across frames in theta cells from untrained rats ($F(2,4)=0.3087$, $p=0.7505$, RM, one-way

ANOVA, figure 4.23B). The median values for rat in room, rat to robot and robot to rat frames were 18.54, 26.60, 19.90 bits/sec, respectively, in theta cells from untrained rats.

Information per spike (bits/spike)

In the trained rat, ANOVA revealed a significant effect of spatial reference frame on information (info) per spike ($F(2,94)=13.00$, $p<0.0001$, RM, one-way ANOVA, figure 4.24). Tukey post-hoc test showed higher spatial coherence values for rat-in-room coordinate system than for rat-to-robot and robot-to-rat coordinate systems (p's<0.0001 and 0.0098, respectively). The median values for rat in room, rat to robot and robot to rat frames were 2.397, 2.132, 2.238 bits/spike, respectively. In untrained rats, no difference was observed across reference frames on info per spike ($F(2, 80)=0.1629$, $p=0.8499$, RM, one-way ANOVA, figure 4.24). The median values for rat in room, rat to robot and robot to rat frames were 2.749, 2.616, 2.537 bits/spike, respectively, in CSCs from untrained rats.

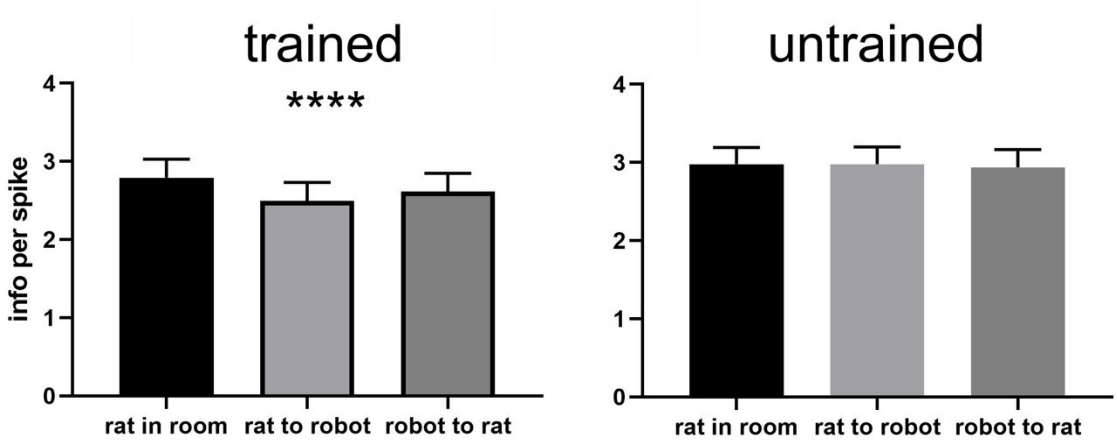

Figure 4.24. Comparison of information per spike (info per spike; bits/spike) across reference frames from trained and untrained rats for CSCs. Plots show means ± SEM. ****p<0.0001.

In the trained rat, there was no significant difference in info per spike across reference frames ($F(2, 14)=0.2485$, $p=0.7834$, RM, one-way ANOVA, figure 4.25) for theta cells. The median values for rat in room, rat to robot and robot to rat frames were 0.5969, 0.6538, 0.6513 bits/spike, respectively. Similarly, no difference was found in untrained rats across reference frames ($F(2, 4)=0.4532$, $p=0.6647$, RM, one-way ANOVA, figure 4.25). The median values for rat in room, rat to robot and robot to rat frames were 0.3317, 0.6219, 0.3858 bits/spike, respectively, in theta cells from untrained rats.

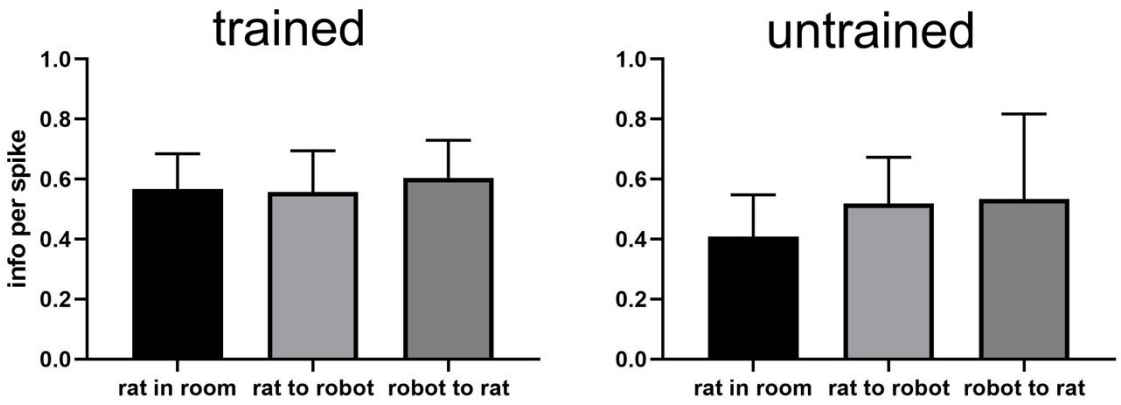

Figure 4.25. Comparison of information per spike (info per spike; bits/spike) across reference frames from trained and untrained rats for theta cells. Plot show means±SEM.

Comparison between trained and untrained animals across representations

Coherence

We further compared all the above parameters in different reference frames among trained and untrained rats. There was no significant difference in coherence between trained and untrained rats in rat in room ($t(83)=0.1990$, $p=0.8427$, two-tailed, unpaired t-test, figure 4.26A, left) reference frame for CSCs. The median values for trained and untrained rats were 0.2752 and 0.3093, respectively. Similarly in rat to robot frame ($t(83)=0.8767$, $p=0.3832$, two-tailed, unpaired t-test, figure 4.26A, middle) there was no significant difference between the two group of animals. The median values for trained and untrained rats were 0.1499 and 0.1690, respectively. Interestingly, in robot to rat reference frame, there was a significant difference between trained and untrained animals; coherence was more for untrained rats ($t(83)=2.463$, $p=0.0158$, two-tailed, unpaired t-test, figure 4.26A, right). The median values for trained and untrained rats were 0.09234 and 0.1512, respectively.

Interestingly there was a tendency for spatial info (bits/sec) to be higher across all reference frames for untrained compared with trained animals (figure 4.26B) for recorded CSCs. However, there was no significant difference across reference frames for the two groups (rat in room: $t(83)=1.377$, $p=0.1721$ and robot to rat: $t(83)=1.459$, $p=0.1484$, two-tailed, unpaired t-test, figure 4.26B, left and right, respectively). The median values for trained and untrained rats were 1.077 and 1.278 bits/sec, respectively, in rat in room frame. For robot to rat frame, the median values for trained and untrained rats were 0.8478 and 1.313 bits/sec, respectively. In the rat to robot reference frame there was a significant difference in spatial info across the two animal groups ($t(83)=2.132$, $p=0.0359$,

two-tailed unpaired t-test, figure 4.26B, middle). The median values for trained and untrained rats were 0.9276 and 1.298 bits/sec, respectively.

Similarly, info per spike (bits/spike) did not show any significant difference between groups in any of the reference frames (rat in room: t(83)=0.5807, p=0.5630; rat to robot: t(83)=1.487, p=0.1407 and robot to rat: t(83)=0.9895, p=0.3253, two-tailed, unpaired t-test, figure 4.26C, left, middle and right, respectively). The median values for trained and untrained rats were 2.397 and 2.749 bits/spike, respectively, for rat in room frame. For rat to robot frame, the median values were 2.132 and 2.616 bits/spike, respectively. In robot to rat frame, the median values were 2.238 and 2.537 bits/spike, respectively.

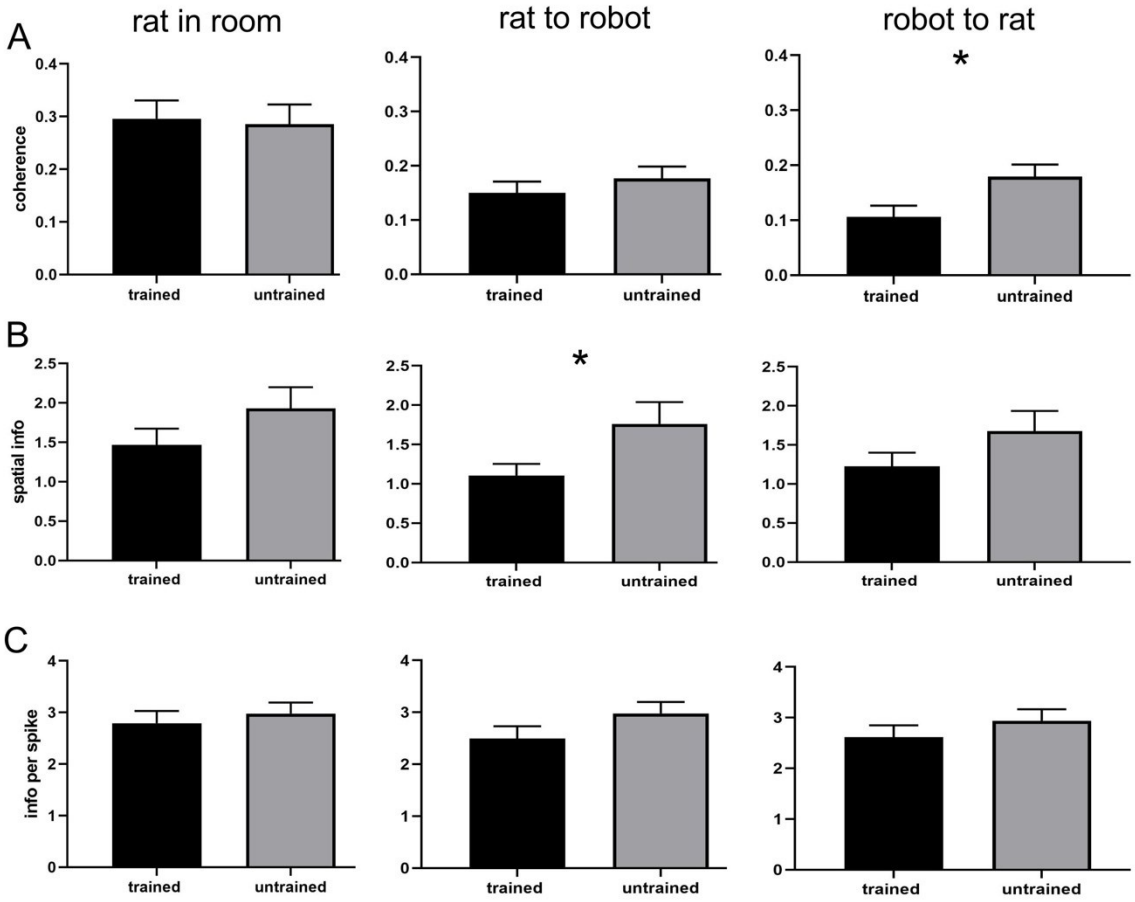

Figure 4.26. Comparison of spatial parameters across reference frames between CSCs from trained and untrained rats. (A) Coherence, (B) spatial information (bits/sec) and (C) information per spike (bits/spike) are compared between trained and untrained rats. Plots show means ± SEM. *p<0.05.

In theta cells there was no difference between the two groups in coherence across reference frames (rat in room: t(9)=1.871, p=0.0942; rat to robot: t(9)=1.463, p=0.1776 and robot to rat: t(9)=0.8517, p=0.4165, two-tailed, unpaired t-test, figure 4.27A, left, middle and right, respectively). The median values for trained and untrained rats were 0.2683 and 0.02651, respectively, for rat in room frame. For rat to robot frame, the

median values were 0.2421 and 0.07237, respectively. In robot to rat frame, the median values were 0.2199 and 0.1876, respectively.

We also did not observe significant difference in info per spike between trained and untrained rats across reference frames (rat in room: t(9)=0.7439, p=0.4759; rat to robot: t(9)=0.1551, p=0.8802 and robot to rat: t(9)=0.2723, p=0.7915, two-tailed, unpaired t-test, figure 4.27C, left, middle and right, respectively). The median values for trained and untrained rats were 0.5969 and 0.3317 bits/spike, respectively, for rat in room frame. For rat to robot frame, the median values were 0.6538 and 0.6219 bits/spike, respectively. In robot to rat frame, the median values were 0.6513 and 0.3858 bits/spike, respectively.

Interestingly, there was a significant difference in spatial info for theta cells across reference frames (rat in room: t(9)=2.364, p=0.0424; rat to robot: t(9)=3.686, p=0.0050; robot to rat: t(9)=2.340, p=0.0440, two-tailed, unpaired t-test, figure 4.27B, left, middle and right, respectively). The median values for trained and untrained rats were 3.497 and 18.54 bits/sec, respectively, for rat in room frame. For rat to robot frame, the median values were 3.027 and 26.60 bits/sec, respectively. In robot to rat frame, the median values were 4.244 and 19.90 bits/sec, respectively.

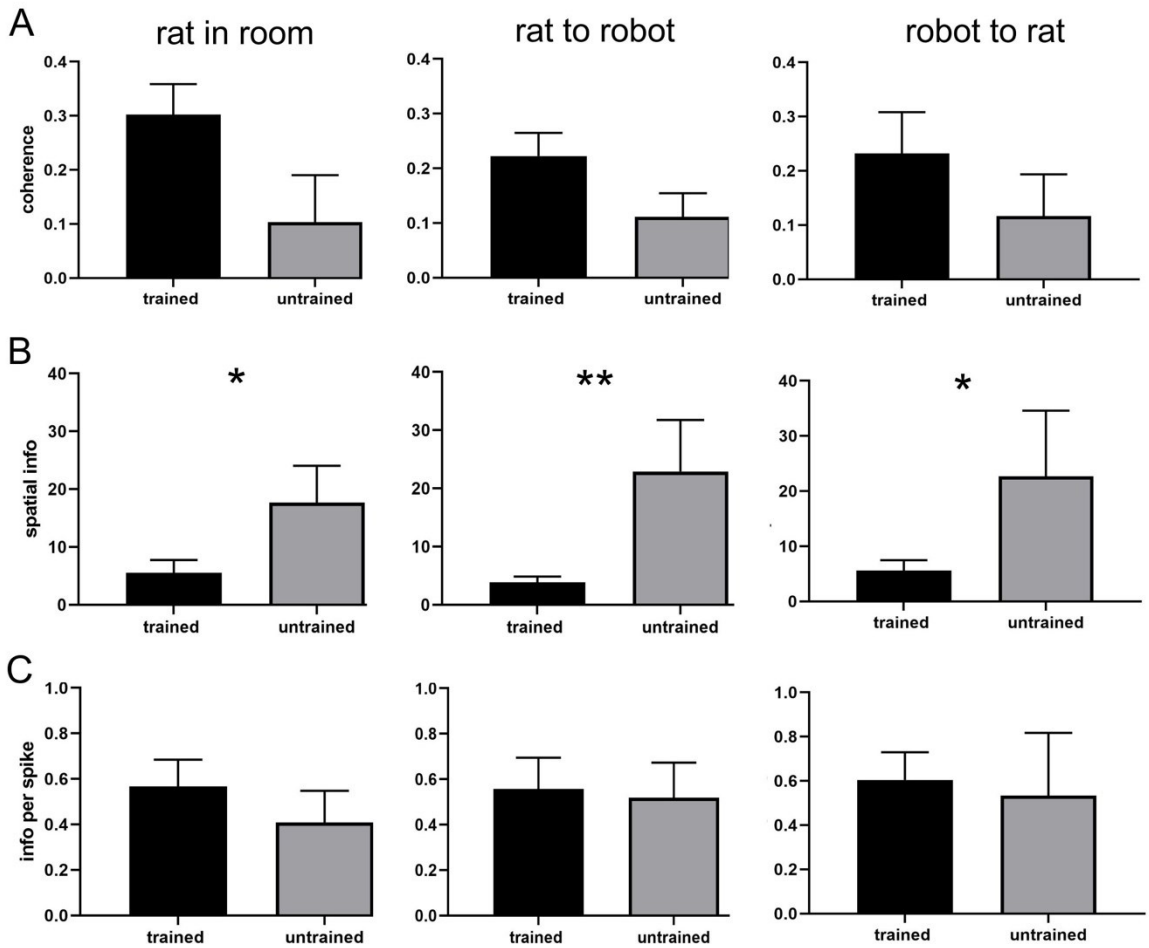

Figure 4.27. Comparison of spatial parameters across reference frames between theta cells from trained and untrained rats. (A) Coherence, (B) spatial information (bits/sec) and (C) information per spike (bits/spike) are compared between units from trained and untrained rats for CSCs. Plots show means ± SEM. *p<0.05 and **p<0.01.

5. Discussion

In my doctoral study, we developed a behavioral paradigm to study the neuronal basis of how an animal assesses its position relative to a moving object. Further, we looked at how neurons in the hippocampus encode the position of the animal and object in different reference frames. In doing so we trained rats to avoid a specific zone around the moving robot and we trained the rats to do so with slow (2 cm/s) as well as fast (4 cm/s) moving robot. The zone to be avoided was either front or left or right side and this zone remained the shock zone for all the sessions for a particular rat. The rat received a mild foot shock upon entering the shock zone. Upon reaching the criterion of ≤ 8 entrances to the shock zone per session across three consecutive days, we tested the rats in probe sessions. In these sessions the shock was turned off in contrast to the training sessions, otherwise, they were similar to the training sessions. Further, we also checked if this ability to assess one's position relative to a moving object depended on the patterns and general shape of the object. Towards this end, we used an all-white robot instead of a black and white (B&W) robot used in the first part of the experiment. The B&W and the all-white robot only differed in the façade that made them look different. On testing the rats in probe sessions after training with the all-white robot, the animals visited the shock zone less than in the compared safe zone/s. Further, they also spent less time in the shock zone versus the safe zone/s as was observed with the B&W robot. Importantly, the rats took less time to reach the criterion than with the B&W robot condition. This could most likely be because the animals had already been trained with the B&W robot. The avoidance behavior in both experiments was such that the rats avoided the robot in general and more specifically the shock zone.

After establishing this task, we moved to the next stage of recording neurons from the hippocampus in a different set of rats. These animals were only trained to avoid a side of the robot as this offered us the ability to compare exactly opposite zones. Following training, we implanted animals with versa drives and retrained the animals to reach the criterion followed by probe sessions. Following retraining we recorded the trained animal every alternate day in four sessions, a session with stationary and another with the fast moving robot flanked by two no robot sessions. In recorded cells, we observed representation of room as well as representation of rat relative to the robot and the robot relative to the rat.

The main findings from our study are as follows:

The first aim of the experiment was to test whether rats can be trained in the laboratory to assess their position relative to a moving object and if this behavior depended on the physical appearance of the moving object, like patterns or its general shape: our data shows that a rat can organize its behavior according to position (not just distance) with respect to a moving object. In support of our hypothesis, we observed that rats can be trained to avoid either front, left or right side of the robot. We also found that they can do so both with a slow as well as a fast moving robot. Using an all-white robot we showed that rats can be trained to avoid an object with a different appearance or bodily pattern. We further found that it took the rats less time to get trained with an all-white robot if the training was followed by training with the B&W robot.

The second aim was to decipher the mechanism underlying the animal's ability to assess its position relative to a moving object: there was no systematic difference in the evaluated parameters related to rat-robot distance, speed of the rat, visited path and duration once they entered either the shock or safe zone. However, we did find that rats had the tendency to enter first in the safe zone.

The third aim was to understand if the hippocampal unit activity is affected by presence of a robot in a familiar environment and look at the representation of recorded cells: we observed that the activity of hippocampal cells is affected by the presence of a robot in an environment in some cases, but not always, in line with our hypothesis and recent evidence. We also observed that within the same session some cells could encode the position of the animal in the room but also the position of the animal relative to the robot and the position of the robot relative to the rat. We also found similar responses in cells recorded from untrained animals. We also observed typical place cells, some of which changed their firing pattern with the introduction of the robot, while others did not change their spatial firing pattern.

The fourth aim was to compare measures of the spatial organization across representations and compared them between trained and untrained animals: Qualitative and quantitative analysis of hippocampal representation of a moving object did not show effect of object's behavioral importance. We found that spatial coherence was higher in rat in room frame compared with rat to robot or robot to rat frame. This pattern was similar for both trained and untrained animals. We also found a similar pattern in spatial information across representations. However, in untrained rats we did not find a significant difference between representations.

Ability to orient relative to a moving object in a dynamic environment

Social interactions make an important part of an animal's life. During these interactions, the ambient environment is filled with significant moving objects, including conspecific, potential predators, or prey. In such environments, an animal often needs to orient itself relative to other members of a pack or a prey/predator to exhibit successful behavior such as while catching a prey or during migration. In a new behavioral paradigm, we showed that animals can recognize specific spatial positions relative to a moving object and use this information for navigation in a dynamic environment. In experiment 1 (figure 4.2), we demonstrated that the rats learned to avoid the circular shock zone in front of the moving robot. In experiment 2 (figure 4.3), we demonstrated the rats' ability to avoid the shock zone on one side (left or right) of the moving robot. Using the all-white robot, we showed that the rats were able to perform the same tasks under the conditions when prominent visual patterns could not be used as cues controlling avoidance behavior. This set of experiments showed that avoidance behavior is based not merely on recognizing prominent simple stimuli, such as increased noise levels, the size of the retinal image of an object, or particular visual patterns characterizing the object, but is based on recognizing spatial relationships in the object's moving reference frame.

In experiment 2, when the rats had to avoid the shock zone on the side of the fast-moving B&W robot, the tendency for avoidance was not statistically significant at $\alpha=0.05$ (figure 4.3B) and was weaker than in experiment 1 with the shock zone in front of the robot (Ahuja et al., 2020). We can speculate that this difference can be attributed to the fact that avoiding the front of a dangerous object (animal or inanimate object) is an ethologically more common situation than avoiding the side of it. It is also possible that it is easier to recognize the front of the robot from the other relatively distinct-looking sides than it is to recognize the left side from the right, which looks more similar. Nevertheless, after additional training the rats were able to avoid the side of the robot as accurately as the front, as was manifested in the subsequent avoidance behavior with the all-white robot (figure 4.3C and D).

Previously, several experiments were aimed at studying rat orientation and navigation with respect to moving objects, some of them originating in our laboratory. Pastalkova et al. (Pastalkova et al., 2003) demonstrated the ability of rats to assess the position of objects on a rotating, but inaccessible scene. Since in this work rats were restrained in a Skinner box, this experiment did not reveal whether the rats recognized the position of the moving object in allocentric space or the position of the moving object relative to the rat itself. These two options can be dissociated when a moving rat is observing another

moving object. In a series of experiments, we showed that moving rats can keep a safe distance from a moving robot (Telensky et al., 2009), an ability that depends on the intact hippocampus (Telensky et al., 2011) and intact anterior cingulate cortex (Svoboda et al., 2017). Our current work extends these previous findings by showing that the rat can assess not just the distance from a moving significant object, but also its relative position to the object. While navigation relative to a moving beacon is a variant of *taxon* navigation, our task presents a different and more demanding cognitive problem, which requires a more complex spatial strategy: *locale* navigation (Gothard et al., 1996).

While the neural representation of stationary objects has been studied systematically in the hippocampus (Gothard et al., 1996; Rivard et al., 2004), anterior cingulate cortex (Weible et al., 2009; Weible et al., 2012), perirhinal cortex (Deshmukh et al., 2012; Burke et al., 2012; Burke & Barnes, 2015) and medial (Høydal et al., 2019) and lateral entorhinal cortex (Deshmukh & Knierim, 2011; Wang et al., 2018), the neuronal substrate for representations of moving objects were previously assessed in only a few studies. Earlier studies reported that hippocampal neurons responded to the position of moving objects in allocentric space but they rarely assessed the responses to the position of a rat relative to moving objects (for such exception see Ho et al., 2008). In these studies, the position of moving objects (inanimate or animate) in space did not influence hippocampal place cells much (Zynyuk et al., 2012), modulated place cell firing a little (Ho et al., 2008), or was represented in the firing of hippocampal cells (Danjo et al., 2018; Omer et al., 2018). The likelihood of observing the influence of moving objects on neuronal firing increased when the object's position was more relevant for the rat in a particular experiment.

In our task, processing the rat's position relative to the robot is reinforced. In addition to this information, the rat could also process types of information defined in other frames of reference, i.e. information about the rat's position in the room, information about the robot's position in the room, and about the robot's position relative to the rat. Preliminary data from our electrophysiological recordings indeed show room-referenced spatial signal in addition to robot-related signal in hippocampal unit discharge in rats interacting with the moving robot (unpublished observations). Similarly, other previous studies provide behavioral and electrophysiological evidence that rats can process spatial information about their position in multiple reference frames (Gothard et al., 1996; Kelemen & Fenton, 2010; Kelemen & Fenton, 2016; Kelemen & Fenton, 2013). Theories of spatial navigation typically consider navigation in a single planar Cartesian reference frame with two dimensions (A. David Redish, 1999) (but see (Touretzky & Muller, 2006)). Navigation in dynamic environments, such as environments enriched with moving objects presented in

this paper, calls for the extension of classical spatial navigation theories to include multiple reference frames of navigation. There are two basic (not mutually exclusive) ways how spatial information about distinct concurrently present and relevant frames of reference can be processed in the brain: one approach assumes different spatial frames are processed independently, the competing view suggests a single integrated complex representation of multiple spatial aspects of complex experience. Experimental findings into this question remain so far inconclusive. In hippocampal recordings, neuronal ensembles representing distinct frames of reference were shown to be active at different times organized by a so-called functional grouping mechanism (Kelemen & Fenton, 2010; Kelemen & Fenton, 2013; Kelemen & Fenton, 2016; Jezek et al., 2011). There is also evidence for modulation of hippocampal spatial neuronal responses by additional parameters, such as an animal's vertical position, creating three dimensional representation (Hayman et al., 2011). Extension of this ability for multi-dimensional representations could provide an alternative means for the representation of moving objects in an environment.

Representation of moving objects

A number of studies from various labs have reported the representation of stationary objects in the CA1 region of the hippocampus (Deshmukh & Knierim, 2013; Burke & Barnes, 2015; Gothard et al., 1996). In many other studies, it has been reported that object present in the arena did not alter the firing pattern of cells in the hippocampus (Cressant et al., 1997; Zynyuk et al., 2012) and highlighted the importance of salience of the object for being encoded in the brain (Cressant et al., 1997; Gothard et al., 1996). It has now been shown in various studies that the hippocampus encodes stationary objects, and this is one of the many roles that the hippocampal neurons subserve. However, there is little understanding of how moving objects are represented in the hippocampus. Some of the studies which have tried to find out if the hippocampal firing is influenced by moving objects had provided conflicting evidence. For example, a study by Ho et al., 2008, which used a toy car as a moving object on the arena found that the hippocampal firing in the recorded animal is indeed influenced by various parameters of a moving object. In another study (Zynyuk et al., 2012) the hippocampal place cells were reported to be weakly influenced by the presence of another moving object (also see von Heimendahl et al., 2012). In the above study, the experimenters used a conspecific rat, as another moving object, along with the recorded rat. None of these studies directly focused on if there is any representation of the moving object. However, in the last few years, there has been exciting development in our understanding of this question about how hippocampal

neurons encode moving objects. These include two studies by Teruko Danjo (Danjo et al., 2018) and David Omer (Omer et al., 2018) and also other studies including the (Mou & Ji, 2016; Sutherland & Bilkey, 2020). Collectively, these studies found that the CA1 region of the hippocampus indeed encodes at least some information about another moving object or a conspecific. An important point highlighted by these studies (Danjo et al., 2018; Omer et al., 2018) is the issue of the salience of the object or conspecific to the recorded rat which appears to be necessary for observing electrophysiological changes in the hippocampal neurons. These studies also highlighted the salience of the object (conspecific) for representation in the brain, which appears to be important for representation in the brain. Our own novel task was based on this premise that for observing the representation of the animal with respect to a (moving) object, the other object should be salient to the animal.

In our data, we observed cells which only represented the animal's position in the room (figure 4.14) along with cells which had representation in various reference frames (figures 4.16 and 4.17). We also observed cells which did not seem to encode the position of the animal in the room but encoded its position relative to the object and of the object relative to the animal (unit 2, figures 4.16 and 4.17). The presence of these type of cells in the hippocampus is in line with the increasing evidence that the hippocampus is also involved in social information processing (Omer et al., 2018; Danjo et al., 2018; von Heimendahl et al., 2012; Sutherland & Bilkey, 2020; Mou & Ji, 2016; Leroy et al., 2018; Meira et al., 2018; Hitti & Siegelbaum, 2014). More specifically object representation has been observed in CA1 (Deshmukh & Knierim, 2013; Burke et al., 2011; Manns & Eichenbaum, 2009; Komorowski et al., 2009). To see whether the recorded cells clustered into different classes we constructed distribution for coherence and spatial information (figures 4.18, 4.19, 4.20 and 4.21). The coherence and spatial info distributions were continuous in all reference frames for CSCs. In spatial information distributions for theta cells there were few outliers, otherwise, the distributions were continuous as for coherence, pointing towards lack of different classes of cells. These responses can be explained if we think about the various combinations of inputs projecting onto the pyramidal cells in CA1. For example cells not changing with the robot might be receiving stronger input from space encoding cells in the upstream region, grid and border cells in the MEC, while those that changed and/or represented information in the reference frame of rat to robot or vice versa might receive relatively stronger inputs from cells in the LEC (Deshmukh & Knierim, 2013). It could be also that these responses (representations) are the result of the same brain computations on dynamic inputs, as the situation in the arena is dynamic with the moving robot. Further, the inputs among

individual cells are not expected to be the same as in nearby regions in the hippocampus (for example distal versus proximal CA1 (Henriksen et al., 2010)) and other brain areas (Hargreaves et al., 2005).

Although we observed various types of representations in both trained and untrained animals suggesting that these could be essential in general to navigate with an object on the arena. One of the important differences between groups was that spatial information for CSCs in all reference frames did not differ in untrained rats, suggesting they were encoding information equally in all the frames (figure 4.22B). However, in the case of the trained rat, there was a statistically significant difference in spatial information in all reference frames (figure 4.22B). Interestingly, the values of spatial information across reference frames differ. However, we also found a tendency for the spatial parameters like coherence, spatial information, etc., to follow a pattern. Coherence was higher for trained rats, however, spatial information and the related measure, information per spike, had the tendency to be comparatively lower in trained animals. Based on previous evidence (von Heimendahl et al., 2012; Zynyuk et al., 2012), it is expected that cells from untrained rats could show responsiveness to the robot in our experiment. However, the tendency to observe more spatial information in untrained versus trained rats seems contrary to what one would expect given the moving robot was more salient to the trained rat.

6. Conclusion

In conclusion, we behaviorally characterized and analyzed the rats' ability to navigate with respect to a moving object. In our experiments, the rats avoided specific positions defined in relation to a moving robot, either the front of the robot or one side of the robot. The avoidance did not depend on prominent visual patterns (drawings) on the robot, as the geometry of the all-white robot was sufficient to guide the avoidance behavior. Robot movement was not necessary as the avoidance behavior was preserved also in the presence of a stationary robot. This important and cognitively challenging aspect of navigation deserves a further study on the level of behavior as well as underlying neuronal mechanisms required for coordination of own position and position of an object. We observed cells which encoded information not only about where the rat was in the room but also about the rat relative to the robot and vice versa. However, we did not found any evidence of different cell types in our recordings.

7. References

Ahuja, N., Lobellová, V., Stuchlík, A., & Kelemen, E. (2020). Navigation in a Space With Moving Objects: Rats Can Avoid Specific Locations Defined With Respect to a Moving Robot. *Frontiers in Behavioral Neuroscience*, *14*. https://doi.org/10.3389/fnbeh.2020.576350

Alexander, G. M., Farris, S., Pirone, J. R., Zheng, C., Colgin, L. L., & Dudek, S. M. (2016). Social and novel contexts modify hippocampal CA2 representations of space. *Nature Communications*, *7*(1), 10300. https://doi.org/10.1038/ncomms10300

Barker, G. R. I., Bird, F., Alexander, V., & Warburton, E. C. (2007). Recognition Memory for Objects, Place, and Temporal Order: A Disconnection Analysis of the Role of the Medial Prefrontal Cortex and Perirhinal Cortex. *Journal of Neuroscience*, *27*(11), 2948–2957. https://doi.org/10.1523/JNEUROSCI.5289-06.2007

Battaglia, F. P. (2004). Local Sensory Cues and Place Cell Directionality: Additional Evidence of Prospective Coding in the Hippocampus. *Journal of Neuroscience*, *24*(19), 4541–4550. https://doi.org/10.1523/JNEUROSCI.4896-03.2004

Boccara, C. N., Sargolini, F., Thoresen, V. H., Solstad, T., Witter, M. P., Moser, E. I., & Moser, M.-B. (2010). Grid cells in pre- and parasubiculum. *Nature Neuroscience*, *13*(8), 987–994. https://doi.org/10.1038/nn.2602

Bostock, E., Muller, R. U., & Kubie, J. L. (1991). Experience-dependent modifications of hippocampal place cell firing. *Hippocampus*, *1*(2), 193–205. https://doi.org/10.1002/hipo.450010207

Breese, C., Hampson, R., & Deadwyler, S. (1989). Hippocampal place cells: stereotypy and plasticity. *The Journal of Neuroscience*, *9*(4), 1097–1111. https://doi.org/10.1523/JNEUROSCI.09-04-01097.1989

Bures, J., Fenton, A. A., Kaminsky, Y., Rossier, J., Sacchetti, B., & Zinyuk, L. (1997). Dissociation of exteroceptive and idiothetic orientation cues： effect on hippocampal place cells and place navigation. *Philosophical Transactions of the Royal Society of London. Series B: Biological Sciences*, *352*(1360), 1515–1524. https://doi.org/10.1098/rstb.1997.0138

Burke, S.N., Maurer, A. P., Hartzell, A. L., Nematollahi, S., Uprety, A., Wallace, J. L., & Barnes, C. A. (2012). Representation of three-dimensional objects by the rat perirhinal cortex. *Hippocampus*, *22*(10), 2032–2044. https://doi.org/10.1002/hipo.22060

Burke, Sara N., & Barnes, C. A. (2015). The neural representation of 3-dimensional objects in rodent memory circuits. *Behavioural Brain Research*, *285*, 60–66. https://doi.org/10.1016/j.bbr.2014.09.001

Burke, Sara N., Maurer, A. P., Nematollahi, S., Uprety, A. R., Wallace, J. L., & Barnes, C. A. (2011). The influence of objects on place field expression and size in distal hippocampal CA1. *Hippocampus*, *21*(7), 783–801. https://doi.org/10.1002/hipo.20929

Burwell, R. D., & Amaral, D. G. (1998). Perirhinal and postrhinal cortices of the rat: Interconnectivity and connections with the entorhinal cortex. *The Journal of Comparative Neurology*, *391*(3), 293–321. https://doi.org/10.1002/(SICI)1096-9861(19980216)391:3<293::AID-CNE2>3.0.CO;2-X

Buzsáki, G. (1986). Hippocampal sharp waves: Their origin and significance. *Brain Research*, *398*(2), 242–252. https://doi.org/10.1016/0006-8993(86)91483-6

Canto, C. B., Wouterlood, F. G., & Witter, M. P. (2008). What Does the Anatomical Organization of the Entorhinal Cortex Tell Us? *Neural Plasticity*, *2008*, 1–18. https://doi.org/10.1155/2008/381243

Cembrowski, M. S., Bachman, J. L., Wang, L., Sugino, K., Shields, B. C., & Spruston, N. (2016). Spatial Gene-Expression Gradients Underlie Prominent Heterogeneity of CA1 Pyramidal Neurons. *Neuron*, *89*(2), 351–368. https://doi.org/10.1016/j.neuron.2015.12.013

Chafee, M. V., Crowe, D. A., Averbeck, B. B., & Georgopoulos, A. P. (2005). Neural Correlates of Spatial Judgement during Object Construction in Parietal Cortex. *Cerebral Cortex*, *15*(9), 1393–1413. https://doi.org/10.1093/cercor/bhi021

Chevaleyre, V., & Siegelbaum, S. A. (2010). Strong CA2 Pyramidal Neuron Synapses Define a Powerful Disynaptic Cortico-Hippocampal Loop. *Neuron*, *66*(4), 560–572. https://doi.org/10.1016/j.neuron.2010.04.013

Chiang, M.-C., Huang, A. J. Y., Wintzer, M. E., Ohshima, T., & McHugh, T. J. (2018). A role for CA3 in social recognition memory. *Behavioural Brain Research*, *354*, 22–30. https://doi.org/10.1016/j.bbr.2018.01.019

Colgin, L. L., Denninger, T., Fyhn, M., Hafting, T., Bonnevie, T., Jensen, O., Moser, M.-B., & Moser, E. I. (2009). Frequency of gamma oscillations routes flow of information in the hippocampus. *Nature*, *462*(7271), 353–357. https://doi.org/10.1038/nature08573

Colgin, L. L., Moser, E. I., & Moser, M.-B. (2008). Understanding memory through hippocampal remapping.

Trends in Neurosciences, *31*(9), 469–477. https://doi.org/10.1016/j.tins.2008.06.008

Collett, T. S., Cartwright, B. A., & Smith, B. A. (1986). Landmark learning and visuo-spatial memories in gerbils. *Journal of Comparative Physiology A Sensory, Neural, and Behavioral Physiology*, *158*(6), 835–851. https://doi.org/10.1007/BF01324825

Conway, B. R. (2018). The Organization and Operation of Inferior Temporal Cortex. *Annual Review of Vision Science*, *4*(1), 381–402. https://doi.org/10.1146/annurev-vision-091517-034202

Cressant, A., Muller, R. U., & Poucet, B. (1997). Failure of Centrally Placed Objects to Control the Firing Fields of Hippocampal Place Cells. *The Journal of Neuroscience*, *17*(7), 2531–2542. https://doi.org/10.1523/JNEUROSCI.17-07-02531.1997

Crowe, D. A., Averbeck, B. B., & Chafee, M. V. (2008). Neural Ensemble Decoding Reveals a Correlate of Viewer- to Object-Centered Spatial Transformation in Monkey Parietal Cortex. *Journal of Neuroscience*, *28*(20), 5218–5228. https://doi.org/10.1523/JNEUROSCI.5105-07.2008

Csicsvari, Jozsef, Hirase, H., Czurkó, A., Mamiya, A., & Buzsáki, G. (1999). tFast Network Oscillations in the Hippocampal CA1 Region of the Behaving Rat. *The Journal of Neuroscience*, *19*(16), RC20–RC20. https://doi.org/10.1523/JNEUROSCI.19-16-j0001.1999

Dabaghian, Y., Mémoli, F., Frank, L., & Carlsson, G. (2012). A Topological Paradigm for Hippocampal Spatial Map Formation Using Persistent Homology. *PLoS Computational Biology*, *8*(8), e1002581. https://doi.org/10.1371/journal.pcbi.1002581

Danjo, T., Toyoizumi, T., & Fujisawa, S. (2018). Spatial representations of self and other in the hippocampus. *Science*, *359*(6372), 213–218. https://doi.org/10.1126/science.aao3898

del Angel Ortiz, R., Contreras, C. M., Gutiérrez-Garcia, A. G., & González, M. F. M. (2016). Social Interaction Test between a Rat and a Robot: A Pilot Study. *International Journal of Advanced Robotic Systems*, *13*(1), 4. https://doi.org/10.5772/62015

Deshmukh, S. S. (2014). Spatial and Nonspatial Representations in the Lateral Entorhinal Cortex. In J. J. Derdikman, D., Knierim (Ed.), *Space,Time and Memory in the Hippocampal Formation* (pp. 127–152). Springer-Verlag. https://doi.org/DOI 10.1007/978-3-7091-1292-2

Deshmukh, S. S., Johnson, J. L., & Knierim, J. J. (2012). Perirhinal cortex represents nonspatial, but not spatial, information in rats foraging in the presence of objects: Comparison with lateral entorhinal

cortex. *Hippocampus*, *22*(10), 2045–2058. https://doi.org/10.1002/hipo.22046

Deshmukh, S. S., & Knierim, J. J. (2011). Representation of Non-Spatial and Spatial Information in the Lateral Entorhinal Cortex. *Frontiers in Behavioral Neuroscience*, *5*, 1–33. https://doi.org/10.3389/fnbeh.2011.00069

Deshmukh, S. S., & Knierim, J. J. (2012). Hippocampus. *Wiley Interdisciplinary Reviews: Cognitive Science*, *3*(2), 231–251. https://doi.org/10.1002/wcs.1164

Deshmukh, S. S., & Knierim, J. J. (2013). Influence of local objects on hippocampal representations: Landmark vectors and memory. *Hippocampus*, *23*(4), 253–267. https://doi.org/10.1002/hipo.22101

Dolorfo, C. L., & Amaral, D. G. (1998). Entorhinal cortex of the rat: Topographic organization of the cells of origin of the perforant path projection to the dentate gyrus. *The Journal of Comparative Neurology*, *398*(1), 25–48. https://doi.org/10.1002/(SICI)1096-9861(19980817)398:1<25::AID-CNE3>3.0.CO;2-B

Duvelle, É., & Jeffery, K. J. (2018). Social Spaces: Place Cells Represent the Locations of Others. *Current Biology*, *28*(6), R271–R273. https://doi.org/10.1016/j.cub.2018.02.017

Eichenbaum, H., Wiener, S., Shapiro, M., & Cohen, N. (1989). The organization of spatial coding in the hippocampus: a study of neural ensemble activity. *The Journal of Neuroscience*, *9*(8), 2764–2775. https://doi.org/10.1523/JNEUROSCI.09-08-02764.1989

Ekstrom, A. D., Kahana, M. J., Caplan, J. B., Fields, T. A., Isham, E. A., Newman, E. L., & Fried, I. (2003). Cellular networks underlying human spatial navigation. *Nature*, *425*(6954), 184–188. https://doi.org/10.1038/nature01964

Fahy, F. L., Riches, I. P., & Brown, M. W. (1993). Neuronal activity related to visual recognition memory: long-term memory and the encoding of recency and familiarity information in the primate anterior and medial inferior temporal and rhinal cortex. *Experimental Brain Research*, *96*(3), 457–472. https://doi.org/10.1007/BF00234113

Feinberg, L. M., Allen, T. A., Ly, D., & Fortin, N. J. (2012). Recognition memory for social and non-social odors: Differential effects of neurotoxic lesions to the hippocampus and perirhinal cortex. *Neurobiology of Learning and Memory*, *97*(1), 7–16. https://doi.org/10.1016/j.nlm.2011.08.008

Fenton, A. A., Wesierska, M., Kaminsky, Y., & Bures, J. (1998). Both here and there: Simultaneous expression of autonomous spatial memories in rats. *Proceedings of the National Academy of Sciences*,

95(19), 11493–11498. https://doi.org/10.1073/pnas.95.19.11493

Foster, T., Castro, C., & McNaughton, B. (1989). Spatial selectivity of rat hippocampal neurons: dependence on preparedness for movement. *Science*, *244*(4912), 1580–1582. https://doi.org/10.1126/science.2740902

França, T. F. A., & Monserrat, J. M. (2019). Hippocampal place cells are topographically organized, but physical space has nothing to do with it. *Brain Structure and Function*, *224*(9), 3019–3029. https://doi.org/10.1007/s00429-019-01968-9

Fyhn, M. (2004). Spatial Representation in the Entorhinal Cortex. *Science*, *305*(5688), 1258–1264. https://doi.org/10.1126/science.1099901

Gianelli, S., Harland, B., & Fellous, J.-M. (2018). A new rat-compatible robotic framework for spatial navigation behavioral experiments. *Journal of Neuroscience Methods*, *294*, 40–50. https://doi.org/10.1016/j.jneumeth.2017.10.021

Gothard, K., Skaggs, W., Moore, K., & McNaughton, B. (1996). Binding of hippocampal CA1 neural activity to multiple reference frames in a landmark-based navigation task. *The Journal of Neuroscience*, *16*(2), 823–835. https://doi.org/10.1523/JNEUROSCI.16-02-00823.1996

Hafting, T., Fyhn, M., Molden, S., Moser, M.-B., & Moser, E. I. (2005). Microstructure of a spatial map in the entorhinal cortex. *Nature*, *436*(7052), 801–806. https://doi.org/10.1038/nature03721

Hargreaves, Eric L., Rao. G., Lee, I., Knierim, J. (2005). Major Dissociation Between Medial and Lateral Entorhinal Input to Dorsal Hippocampus. *Science*, *308*(5729), 1792–1794. https://doi.org/10.1126/science.1110449

Hasselmo, M. E., Rolls, E. T., Baylis, G. C., & Nalwa, V. (1989). Object-centered encoding by face-selective neurons in the cortex in the superior temporal sulcus of the monkey. *Experimental Brain Research*, *75*(2), 417–429. https://doi.org/10.1007/BF00247948

Hayman, R., Verriotis, M. A., Jovalekic, A., Fenton, A. A., & Jeffery, K. J. (2011). Anisotropic encoding of three-dimensional space by place cells and grid cells. *Nature Neuroscience*, *14*(9), 1182–1188. https://doi.org/10.1038/nn.2892

Henriksen, E. J., Colgin, L. L., Barnes, C. A., Witter, M. P., Moser, M.-B., & Moser, E. I. (2010). Spatial Representation along the Proximodistal Axis of CA1. *Neuron*, *68*(1), 127–137.

https://doi.org/10.1016/j.neuron.2010.08.042

Hensler, J. G. (2006). Serotonergic modulation of the limbic system. *Neuroscience & Biobehavioral Reviews*, *30*(2), 203–214. https://doi.org/10.1016/j.neubiorev.2005.06.007

Hetherington, P. A., & Shapiro, M. L. (1997). Hippocampal place fields are altered by the removal of single visual cues in a distance-dependent manner. *Behavioral Neuroscience*, *111*(1), 20–34. https://doi.org/10.1037/0735-7044.111.1.20

Hitti, F. L., & Siegelbaum, S. A. (2014). The hippocampal CA2 region is essential for social memory. *Nature*, *508*(7494), 88–92. https://doi.org/10.1038/nature13028

Ho, S. A., Hori, E., Kobayashi, T., Umeno, K., Tran, A. H., Ono, T., & Nishijo, H. (2008). Hippocampal place cell activity during chasing of a moving object associated with reward in rats. *Neuroscience*, *157*(1), 254–270. https://doi.org/10.1016/j.neuroscience.2008.09.004

Høydal, Ø. A., Skytøen, E. R., Andersson, S. O., Moser, M.-B., & Moser, E. I. (2019). Object-vector coding in the medial entorhinal cortex. *Nature*, *568*(7752), 400–404. https://doi.org/10.1038/s41586-019-1077-7

Igarashi, K. M., Ito, H. T., Moser, E. I., & Moser, M.-B. (2014). Functional diversity along the transverse axis of hippocampal area CA1. *FEBS Letters*, *588*(15), 2470–2476. https://doi.org/10.1016/j.febslet.2014.06.004

Jeffery, K. J. (1998). Learning of landmark stability and instability by hippocampal place cells. *Neuropharmacology*, *37*(4–5), 677–687. https://doi.org/10.1016/S0028-3908(98)00053-7

Jezek, K., Henriksen, E. J., Treves, A., Moser, E. I., & Moser, M.-B. (2011). Theta-paced flickering between place-cell maps in the hippocampus. *Nature*, *478*(7368), 246–249. https://doi.org/10.1038/nature10439

John, O. (2006). Hippocampal Neurophysiology in the Behaving Animal. In *The Hippocampus Book* (pp. 475–548). Oxford University Press. https://doi.org/10.1093/acprof:oso/9780195100273.003.0011

Johnson, A., & Redish, A. D. (2007). Neural ensembles in CA3 transiently encode paths forward of the animal at a decision point. *Journal of Neuroscience*, *27*(45), 12176–12189. https://doi.org/10.1523/JNEUROSCI.3761-07.2007

Jung, M., Wiener, S., & McNaughton, B. (1994). Comparison of spatial firing characteristics of units in dorsal and ventral hippocampus of the rat. *The Journal of Neuroscience*, *14*(12), 7347–7356.

https://doi.org/10.1523/JNEUROSCI.14-12-07347.1994

Karlsson, M. P., & Frank, L. M. (2009). Awake replay of remote experiences in the hippocampus. *Nature Neuroscience*, *12*(7), 913–918. https://doi.org/10.1038/nn.2344

Kelemen, E., & Fenton, A. A. (2010). Dynamic Grouping of Hippocampal Neural Activity During Cognitive Control of Two Spatial Frames. *PLoS Biology*, *8*(6), e1000403. https://doi.org/10.1371/journal.pbio.1000403

Kelemen, E., & Fenton, A. A. (2013). Key Features of Human Episodic Recollection in the Cross-Episode Retrieval of Rat Hippocampus Representations of Space. *PLoS Biology*, *11*(7), e1001607. https://doi.org/10.1371/journal.pbio.1001607

Kelemen, E., & Fenton, A. A. (2016). Coordinating different representations in the hippocampus. *Neurobiology of Learning and Memory*, *129*, 50–59. https://doi.org/10.1016/j.nlm.2015.12.011

Kim, E. J., Park, M., Kong, M.-S., Park, S. G., Cho, J., & Kim, J. J. (2015). Alterations of Hippocampal Place Cells in Foraging Rats Facing a “Predatory” Threat. *Current Biology*, *25*(10), 1362–1367. https://doi.org/10.1016/j.cub.2015.03.048

Klausberger, T., Magill, P. J., Márton, L. F., Roberts, J. D. B., Cobden, P. M., Buzsáki, G., & Somogyi, P. (2003). Brain-state- and cell-type-specific firing of hippocampal interneurons in vivo. *Nature*, *421*(6925), 844–848. https://doi.org/10.1038/nature01374

Knierim, J. J. (2002). Dynamic Interactions between Local Surface Cues, Distal Landmarks, and Intrinsic Circuitry in Hippocampal Place Cells. *The Journal of Neuroscience*, *22*(14), 6254–6264. https://doi.org/10.1523/JNEUROSCI.22-14-06254.2002

Knierim, J. J., Kudrimoti, H. S., & McNaughton, B. L. (1998). Interactions Between Idiothetic Cues and External Landmarks in the Control of Place Cells and Head Direction Cells. *Journal of Neurophysiology*, *80*(1), 425–446. https://doi.org/10.1152/jn.1998.80.1.425

Knierim, J., Kudrimoti, H., & McNaughton, B. (1995). Place cells, head direction cells, and the learning of landmark stability. *The Journal of Neuroscience*, *15*(3), 1648–1659. https://doi.org/10.1523/JNEUROSCI.15-03-01648.1995

Komorowski, R. W., Manns, J. R., & Eichenbaum, H. (2009). Robust Conjunctive Item-Place Coding by Hippocampal Neurons Parallels Learning What Happens Where. *Journal of Neuroscience*, *29*(31),

9918–9929. https://doi.org/10.1523/JNEUROSCI.1378-09.2009

Kubie, J., Muller, R., & Bostock, E. (1990). Spatial firing properties of hippocampal theta cells. *The Journal of Neuroscience*, *10*(4), 1110–1123. https://doi.org/10.1523/JNEUROSCI.10-04-01110.1990

Lai, H. K., Moorhouse, A., & Gibbs, B. (2016). Experimental round-robin evaluation of structure-borne sound source force-power test methods. *Noise Control Engineering Journal*, *64*(2), 170–180. https://doi.org/10.3397/1/376369

Leroy, F., Park, J., Asok, A., Brann, D. H., Meira, T., Boyle, L. M., Buss, E. W., Kandel, E. R., & Siegelbaum, S. A. (2018). A circuit from hippocampal CA2 to lateral septum disinhibits social aggression. *Nature*, *564*(7735), 213–218. https://doi.org/10.1038/s41586-018-0772-0

Leutgeb S, Leutgeb JK, Barnes CA, Moser EI, McNaughton BL, M. M. (2005). Independent Codes for Spatial and Episodic Memory in Hippocampal Neuronal Ensembles. *Science*, *309*(619), 619–623. https://doi.org/10.1126/science.1114037

Leutgeb, S. (2004). Distinct Ensemble Codes in Hippocampal Areas CA3 and CA1. *Science*, *305*(5688), 1295–1298. https://doi.org/10.1126/science.1100265

Leutgeb, S., & Leutgeb, J. K. (2007). Pattern separation, pattern completion, and new neuronal codes within a continuous CA3 map. *Learning & Memory*, *14*(11), 745–757. https://doi.org/10.1101/lm.703907

Lever, C., Burton, S., Jeewajee, A., O'Keefe, J., & Burgess, N. (2009). Boundary Vector Cells in the Subiculum of the Hippocampal Formation. *Journal of Neuroscience*, *29*(31), 9771–9777. https://doi.org/10.1523/JNEUROSCI.1319-09.2009

Lu, L., Igarashi, K. M., Witter, M. P., Moser, E. I., & Moser, M.-B. (2015). Topography of Place Maps along the CA3-to-CA2 Axis of the Hippocampus. *Neuron*, *87*(5), 1078–1092. https://doi.org/10.1016/j.neuron.2015.07.007

MacDonald, C. J., Lepage, K. Q., Eden, U. T., & Eichenbaum, H. (2011). Hippocampal "Time Cells" Bridge the Gap in Memory for Discontiguous Events. *Neuron*, *71*(4), 737–749. https://doi.org/10.1016/j.neuron.2011.07.012

Manns, J. R., & Eichenbaum, H. (2009). A cognitive map for object memory in the hippocampus. *Learning & Memory*, *16*(10), 616–624. https://doi.org/10.1101/lm.1484509

Markus, E., Qin, Y., Leonard, B., Skaggs, W., McNaughton, B., & Barnes, C. (1995). Interactions between location and task affect the spatial and directional firing of hippocampal neurons. *The Journal of Neuroscience*, *15*(11), 7079–7094. https://doi.org/10.1523/JNEUROSCI.15-11-07079.1995

Maurer, A. P., VanRhoads, S. R., Sutherland, G. R., Lipa, P., & McNaughton, B. L. (2005). Self-motion and the origin of differential spatial scaling along the septo-temporal axis of the hippocampus. *Hippocampus*, *15*(7), 841–852. https://doi.org/10.1002/hipo.20114

McHugh, T. J., Blum, K. I., Tsien, J. Z., Tonegawa, S., & Wilson, M. A. (1996). Impaired Hippocampal Representation of Space in CA1-Specific NMDAR1 Knockout Mice. *Cell*, *87*(7), 1339–1349. https://doi.org/10.1016/S0092-8674(00)81828-0

McNaughton, B., Knierim, J., & Wilson, M. (1995). Vector Encoding and the Vestibular Foundations of Spatial Cognition: Neurophysiological and Computational Mechanisms. In *THE COGNITIVE NEUROSCIENCES*.

McNaughton, B. L., Barnes, C. A., Gerrard, J. L., Gothard, K., Jung, M. W., Knierim, J. J., Kudrimoti, H., Qin, Y., Skaggs, W. E., Suster, M., & Weaver, K. L. (1996). Deciphering the hippocampal polyglot: the hippocampus as a path integration system. *The Journal of Experimental Biology*, *199*(Pt 1), 173–185. http://www.ncbi.nlm.nih.gov/pubmed/8576689

McNaughton, B. L., Barnes, C. A., & O'Keefe, J. (1983). The contributions of position, direction, and velocity to single unit activity in the hippocampus of freely-moving rats. *Experimental Brain Research*, *52*(1), 41–49. https://doi.org/10.1007/BF00237147

Meira, T., Leroy, F., Buss, E. W., Oliva, A., Park, J., & Siegelbaum, S. A. (2018). A hippocampal circuit linking dorsal CA2 to ventral CA1 critical for social memory dynamics. *Nature Communications*, *9*(1), 4163. https://doi.org/10.1038/s41467-018-06501-w

Mou, X., & Ji, D. (2016). Social observation enhances cross-environment activation of hippocampal place cell patterns. *ELife*, *5*, e18022. https://doi.org/10.7554/eLife.18022

Muller, R., & Kubie, J. (1987). The effects of changes in the environment on the spatial firing of hippocampal complex-spike cells. *The Journal of Neuroscience*, *7*(7), 1951–1968. https://doi.org/10.1523/JNEUROSCI.07-07-01951.1987

Muller, R., & Kubie, J. (1989). The firing of hippocampal place cells predicts the future position of freely moving rats. *The Journal of Neuroscience*, *9*(12), 4101–4110. https://doi.org/10.1523/JNEUROSCI.09-

12-04101.1989

Naber, P. A., Caballero-Bleda, M., Jorritsma-Byham, B., & Witter, M. P. (1997). Parallel input to the hippocampal memory system through peri- and postrhinal cortices. *NeuroReport*, *8*(11), 2617–2621. https://doi.org/10.1097/00001756-199707280-00039

Navratilova, Z. and McNaughton, B. L. (2014). *Space,Time and Memory in the Hippocampal Formation* (D. Derdikman & J. J. Knierim (eds.)). Springer Vienna. https://doi.org/10.1007/978-3-7091-1292-2

O'Keefe, J., Nadel, L. (1978). *The Hippocampus as a Cognitive Map*.

O'Keefe, J. (2007). Hippocampal Neurophysiology in the Behaving Animal. In *The Hippocampus Book* (pp. 475–548).

O'Keefe, J., & Conway, D. H. (1978). Hippocampal place units in the freely moving rat: Why they fire where they fire. *Experimental Brain Research*, *31*(4), 573–590. https://doi.org/10.1007/BF00239813

O'Keefe, J., & Dostrovsky, J. (1971). The hippocampus as a spatial map. Preliminary evidence from unit activity in the freely-moving rat. *Brain Research*, *34*(1), 171–175. https://doi.org/10.1016/0006-8993(71)90358-1

O'Keefe, John. (1976). Place units in the hippocampus of the freely moving rat. *Experimental Neurology*, *51*(1), 78–109. https://doi.org/10.1016/0014-4886(76)90055-8

O'Keefe, John, & Burgess, N. (1996). Geometric determinants of the place fields of hippocampal neurons. *Nature*, *381*(6581), 425–428. https://doi.org/10.1038/381425a0

O'Keefe, John, Nadel, L., Keightley, S., & Kill, D. (1975). Fornix lesions selectively abolish place learning in the rat. *Experimental Neurology*, *48*(1), 152–166. https://doi.org/10.1016/0014-4886(75)90230-7

O'Keefe, John, & Recce, M. L. (1993). Phase relationship between hippocampal place units and the EEG theta rhythm. *Hippocampus*, *3*(3), 317–330. https://doi.org/10.1002/hipo.450030307

Okuyama, T., Kitamura, T., Roy, D. S., Itohara, S., & Tonegawa, S. (2016). Ventral CA1 neurons store social memory. *Science*, *353*(6307), 1536–1541. https://doi.org/10.1126/science.aaf7003

Omer, D. B., Maimon, S. R., Las, L., & Ulanovsky, N. (2018). Social place-cells in the bat hippocampus. *Science*, *359*(6372), 218–224. https://doi.org/10.1126/science.aao3474

Ono, T., Nakamura, K., Nishijo, H., & Eifuku, S. (1993). Monkey hippocampal neurons related to spatial and nonspatial functions. *Journal of Neurophysiology*, *70*(4), 1516–1529. https://doi.org/10.1152/jn.1993.70.4.1516

Pan, W.-X., & McNaughton, N. (2004). The supramammillary area: its organization, functions and relationship to the hippocampus. *Progress in Neurobiology*, *74*(3), 127–166. https://doi.org/10.1016/j.pneurobio.2004.09.003

Pastalkova, E., Kelemen, E., & Bures, J. (2003). Operant behavior can be triggered by the position of the rat relative to objects rotating on an inaccessible platform. *Proceedings of the National Academy of Sciences*, *100*(4), 2094–2099. https://doi.org/10.1073/pnas.0438002100

Quirk, G., Muller, R., & Kubie, J. (1990). The firing of hippocampal place cells in the dark depends on the rat's recent experience. *The Journal of Neuroscience*, *10*(6), 2008–2017. https://doi.org/10.1523/JNEUROSCI.10-06-02008.1990

Rainer, G., & Ranganath, C. (2002). Coding of Objects in the Prefrontal Cortex in Monkeys and Humans. *The Neuroscientist*, *8*(1), 6–11. https://doi.org/10.1177/107385840200800104

Rainer, G., Rao, S. C., & Miller, E. K. (1999). Prospective Coding for Objects in Primate Prefrontal Cortex. *The Journal of Neuroscience*, *19*(13), 5493–5505. https://doi.org/10.1523/JNEUROSCI.19-13-05493.1999

Ranck, J. B. (1973). Studies on single neurons in dorsal hippocampal formation and septum in unrestrained rats. *Experimental Neurology*, *41*(2), 462–531. https://doi.org/10.1016/0014-4886(73)90290-2

Redish, A. D., Battaglia, F. P., Chawla, M. K., Ekstrom, A. D., Gerrard, J. L., Lipa, P., Rosenzweig, E. S., Worley, P. F., Guzowski, J. F., McNaughton, B. L., & Barnes, C. A. (2001). Independence of Firing Correlates of Anatomically Proximate Hippocampal Pyramidal Cells. *The Journal of Neuroscience*, *21*(5), RC134–RC134. https://doi.org/10.1523/JNEUROSCI.21-05-j0004.2001

Redish, A. David. (1999). *Beyond the Cognitive Map*. The MIT Press. https://doi.org/10.7551/mitpress/1571.001.0001

Renaudineau, S., Poucet, B., & Save, E. (2007). Flexible use of proximal objects and distal cues by hippocampal place cells. *Hippocampus*, *17*(5), 381–395. https://doi.org/10.1002/hipo.20277

Ringnér, M. (2008). What is principal component analysis? *Nature Biotechnology*, *26*(3), 303–304.

https://doi.org/10.1038/nbt0308-303

Risold, P. Y., & Swanson, L. W. (1996). Structural Evidence for Functional Domains in the Rat Hippocampus. *Science*, *272*(5267), 1484–1486. https://doi.org/10.1126/science.272.5267.1484

Rivard, B., Li, Y., Lenck-Santini, P.-P., Poucet, B., & Muller, R. U. (2004). Representation of Objects in Space by Two Classes of Hippocampal Pyramidal Cells. *Journal of General Physiology*, *124*(1), 9–25. https://doi.org/10.1085/jgp.200409015

Sargolini, F. (2006). Conjunctive Representation of Position, Direction, and Velocity in Entorhinal Cortex. *Science*, *312*(5774), 758–762. https://doi.org/10.1126/science.1125572

Save, E., Cressant, A., Thinus-Blanc, C., & Poucet, B. (1998). Spatial Firing of Hippocampal Place Cells in Blind Rats. *The Journal of Neuroscience*, *18*(5), 1818–1826. https://doi.org/10.1523/JNEUROSCI.18-05-01818.1998

Savelli, F., Yoganarasimha, D., & Knierim, J. J. (2008). Influence of boundary removal on the spatial representations of the medial entorhinal cortex. *Hippocampus*, *18*(12), 1270–1282. https://doi.org/10.1002/hipo.20511

Shapiro, M. L., Tanila, H., & Eichenbaum, H. (1997). Cues that hippocampal place cells encode: Dynamic and hierarchical representation of local and distal stimuli. *Hippocampus*, *7*(6), 624–642. https://doi.org/10.1002/(SICI)1098-1063(1997)7:6<624::AID-HIPO5>3.0.CO;2-E

Shi, Q., Ishii, H., Kinoshita, S., Takanishi, A., Okabayashi, S., Iida, N., Kimura, H., & Shibata, S. (2013). Modulation of rat behaviour by using a rat-like robot. *Bioinspiration & Biomimetics*, *8*(4), 046002. https://doi.org/10.1088/1748-3182/8/4/046002

Siegel, J. J., Nitz, D., & Bingman, V. P. (2006). Lateralized functional components of spatial cognition in the avian hippocampal formation: Evidence from single-unit recordings in freely moving homing pigeons. *Hippocampus*, *16*(2), 125–140. https://doi.org/10.1002/hipo.20139

Siegel, M., Warden, M. R., & Miller, E. K. (2009). Phase-dependent neuronal coding of objects in short-term memory. *Proceedings of the National Academy of Sciences*, *106*(50), 21341–21346. https://doi.org/10.1073/pnas.0908193106

Skaggs, W E, & McNaughton, B. L. (1992). Computational approaches to hippocampal function. *Current Opinion in Neurobiology*, *2*(2), 209–211. https://doi.org/10.1016/0959-4388(92)90014-c

Skaggs, William E., & McNaughton, B. L. (1998). Spatial Firing Properties of Hippocampal CA1 Populations in an Environment Containing Two Visually Identical Regions. *The Journal of Neuroscience*, *18*(20), 8455–8466. https://doi.org/10.1523/JNEUROSCI.18-20-08455.1998

Solstad, T., Boccara, C. N., Kropff, E., Moser, M.-B., & Moser, E. I. (2008). Representation of Geometric Borders in the Entorhinal Cortex. *Science*, *322*(5909), 1865–1868. https://doi.org/10.1126/science.1166466

Speakman, A., & O'Keefe, J. (1990). Hippocampal Complex Spike Cells do not Change Their Place Fields if the Goal is Moved Within a Cue Controlled Environment. *European Journal of Neuroscience*, *2*(6), 544–555. https://doi.org/10.1111/j.1460-9568.1990.tb00445.x

Stackman, R. W., & Taube, J. S. (1997). Firing Properties of Head Direction Cells in the Rat Anterior Thalamic Nucleus: Dependence on Vestibular Input. *The Journal of Neuroscience*, *17*(11), 4349–4358. https://doi.org/10.1523/JNEUROSCI.17-11-04349.1997

Sutherland, C. J., & Bilkey, D. K. (2020). Hippocampal coding of conspecific position. *Brain Research*, *1745*, 146920. https://doi.org/10.1016/j.brainres.2020.146920

Suzuki, W. A. (1996). The anatomy, physiology and functions of the perirhinal cortex. *Current Opinion in Neurobiology*, *6*(2), 179–186. https://doi.org/10.1016/S0959-4388(96)80071-7

Svoboda, J., Lobellová, V., Popelíková, A., Ahuja, N., Kelemen, E., & Stuchlík, A. (2017). Transient inactivation of the anterior cingulate cortex in rats disrupts avoidance of a dynamic object. *Neurobiology of Learning and Memory*, *139*, 144–148. https://doi.org/10.1016/j.nlm.2017.01.003

SVOBODA, J., TELENSKÝ, P., BLAHNA, K., BUREŠ, J., & STUCHLÍK, A. (2012). Comparison of Male and Female Rats in Avoidance of a Moving Object: More Thigmotaxis, Hypolocomotion and Fear-Like Reactions in Females. *Physiological Research*, *61*, 659–663. https://doi.org/10.33549/physiolres.932406

Taube, J., Muller, R., & Ranck, J. (1990). Head-direction cells recorded from the postsubiculum in freely moving rats. II. Effects of environmental manipulations. *The Journal of Neuroscience*, *10*(2), 436–447. https://doi.org/10.1523/JNEUROSCI.10-02-00436.1990

Taube, J. S. (2007). The Head Direction Signal: Origins and Sensory-Motor Integration. *Annual Review of Neuroscience*, *30*(1), 181–207. https://doi.org/10.1146/annurev.neuro.29.051605.112854

Telensky, P., Svoboda, J., Blahna, K., Bures, J., Kubik, S., & Stuchlik, A. (2011). Functional inactivation of the rat hippocampus disrupts avoidance of a moving object. *Proceedings of the National Academy of Sciences*, *108*(13), 5414–5418. https://doi.org/10.1073/pnas.1102525108

Telensky, P., Svoboda, J., Pastalkova, E., Blahna, K., Bures, J., & Stuchlik, A. (2009). Enemy avoidance task: A novel behavioral paradigm for assessing spatial avoidance of a moving subject. *Journal of Neuroscience Methods*, *180*(1), 29–33. https://doi.org/10.1016/j.jneumeth.2009.02.010

Terrazas, A. (2005). Self-Motion and the Hippocampal Spatial Metric. *Journal of Neuroscience*, *25*(35), 8085–8096. https://doi.org/10.1523/JNEUROSCI.0693-05.2005

Tolman, E. C. (1948). Cognitive maps in rats and men. *Psychological Review*, *55*(4), 189–208. https://doi.org/10.1037/h0061626

Touretzky, D. S., & Muller, R. U. (2006). Place field dissociation and multiple maps in hippocampus. *Neurocomputing*, *69*(10–12), 1260–1263. https://doi.org/10.1016/j.neucom.2005.12.088

Tsao, A., Moser, M.-B., & Moser, E. I. (2013). Traces of Experience in the Lateral Entorhinal Cortex. *Current Biology*, *23*(5), 399–405. https://doi.org/10.1016/j.cub.2013.01.036

Tzakis, N., & Holahan, M. R. (2019). Social Memory and the Role of the Hippocampal CA2 Region. *Frontiers in Behavioral Neuroscience*, *13*, 1–15. https://doi.org/10.3389/fnbeh.2019.00233

Ulanovsky, N., & Moss, C. F. (2007). Hippocampal cellular and network activity in freely moving echolocating bats. *Nature Neuroscience*, *10*(2), 224–233. https://doi.org/10.1038/nn1829

Vanderwolf, C. . (1969). Hippocampal electrical activity and voluntary movement in the rat. *Electroencephalography and Clinical Neurophysiology*, *26*(4), 407–418. https://doi.org/10.1016/0013-4694(69)90092-3

von Heimendahl, M., Rao, R. P., & Brecht, M. (2012). Weak and Nondiscriminative Responses to Conspecifics in the Rat Hippocampus. *Journal of Neuroscience*, *32*(6), 2129–2141. https://doi.org/10.1523/JNEUROSCI.3812-11.2012

Wan, H., Aggleton, J. P., & Brown, M. W. (1999). Different Contributions of the Hippocampus and Perirhinal Cortex to Recognition Memory. *The Journal of Neuroscience*, *19*(3), 1142–1148. https://doi.org/10.1523/JNEUROSCI.19-03-01142.1999

Wang, C., Chen, X., Lee, H., Deshmukh, S. S., Yoganarasimha, D., Savelli, F., & Knierim, J. J. (2018). Egocentric coding of external items in the lateral entorhinal cortex. *Science*, *362*(6417), 945–949. https://doi.org/10.1126/science.aau4940

Weible, A. P., Rowland, D. C., Monaghan, C. K., Wolfgang, N. T., & Kentros, C. G. (2012). Neural Correlates of Long-Term Object Memory in the Mouse Anterior Cingulate Cortex. *Journal of Neuroscience*, *32*(16), 5598–5608. https://doi.org/10.1523/JNEUROSCI.5265-11.2012

Weible, A. P., Rowland, D. C., Pang, R., & Kentros, C. (2009). Neural Correlates of Novel Object and Novel Location Recognition Behavior in the Mouse Anterior Cingulate Cortex. *Journal of Neurophysiology*, *102*(4), 2055–2068. https://doi.org/10.1152/jn.00214.2009

Widloski, J., Fiete, I. (2014). *Space,Time and Memory in the Hippocampal Formation* (D. Derdikman & J. J. Knierim (eds.)). Springer Vienna. https://doi.org/10.1007/978-3-7091-1292-2

Wiener, S. I., Korshunov, V. A., Garcia, R., & Berthoz, A. (1995). Inertial, Substratal and Landmark Cue Control of Hippocampal CA1 Place Cell Activity. *European Journal of Neuroscience*, *7*(11), 2206–2219. https://doi.org/10.1111/j.1460-9568.1995.tb00642.x

Wiener, S., Paul, C., & Eichenbaum, H. (1989). Spatial and behavioral correlates of hippocampal neuronal activity. *The Journal of Neuroscience*, *9*(8), 2737–2763. https://doi.org/10.1523/JNEUROSCI.09-08-02737.1989

Winters, B. D., Forwood, S. E., Cowell, R. A., Saksida, L. M., Bussey, T. J. (2004). Double Dissociation between the Effects of Peri-Postrhinal Cortex and Hippocampal Lesions on Tests of Object Recognition and Spatial Memory: Heterogeneity of Function within the Temporal Lobe. *Journal of Neuroscience*, *24*(26), 5901–5908. https://doi.org/10.1523/JNEUROSCI.1346-04.2004

Winters, B. D., & Reid, J. M. (2010). A distributed cortical representation underlies crossmodal object recognition in rats. *Journal of Neuroscience*. https://doi.org/10.1523/JNEUROSCI.6073-09.2010

WITTER, M. P., WOUTERLOOD, F. G., NABER, P. A., & VAN HAEFTEN, T. (2006). Anatomical Organization of the Parahippocampal-Hippocampal Network. *Annals of the New York Academy of Sciences*, *911*(1), 1–24. https://doi.org/10.1111/j.1749-6632.2000.tb06716.x

Young, B., Fox, G., & Eichenbaum, H. (1994). Correlates of hippocampal complex-spike cell activity in rats performing a nonspatial radial maze task. *The Journal of Neuroscience*, *14*(11), 6553–6563. https://doi.org/10.1523/JNEUROSCI.14-11-06553.1994

Young, B. J., Otto, T., Fox, G. D., & Eichenbaum, H. (1997). Memory Representation within the Parahippocampal Region. *The Journal of Neuroscience*, *17*(13), 5183–5195. https://doi.org/10.1523/JNEUROSCI.17-13-05183.1997

Young, W. S., Li, J., Wersinger, S. R., & Palkovits, M. (2006). The vasopressin 1b receptor is prominent in the hippocampal area CA2 where it is unaffected by restraint stress or adrenalectomy. *Neuroscience*, *143*(4), 1031–1039. https://doi.org/10.1016/j.neuroscience.2006.08.040

Zhu, X. O., Brown, M. W., McCabe, B. J., & Aggleton, J. P. (1995). Effects of the novelty or familiarity of visual stimuli on the expression of the immediate early gene c-fos in rat brain. *Neuroscience*, *69*(3), 821–829. https://doi.org/10.1016/0306-4522(95)00320-I

Zinyuk, L., Kubik, S., Kaminsky, Y., Fenton, A. A., & Bures, J. (2000). Understanding hippocampal activity by using purposeful behavior: Place navigation induces place cell discharge in both task-relevant and task-irrelevant spatial reference frames. *Proceedings of the National Academy of Sciences*, *97*(7), 3771–3776. https://doi.org/10.1073/pnas.97.7.3771

Zynyuk, L., Huxter, J., Muller, R. U., & Fox, S. E. (2012). The presence of a second rat has only subtle effects on the location-specific firing of hippocampal place cells. *Hippocampus*, *22*(6), 1405–1416. https://doi.org/10.1002/hipo.20977